bioRxiv preprint doi: https://doi.org/10.1101/2022.11.22.517350; this version posted November 23, 2022. The copyright holder for this preprint (which was not certified by peer review) is the author/funder, who has granted bioRxiv a license to display the preprint in perpetuity. It is made available under aCC-BY-NC-ND 4.0 International license.

Integrated Multi-omics Analyses of NFKB1 patients B cells points towards an up regulation of NF-κB network inhibitors

Nadezhda Camacho-Ordonez[1,2,3], Neftali Ramirez[1,2*], Sara Posadas-Cantera[1,2*], Andrés Caballero-Oyteza[1,2], Manfred Fliegauf[1,2,4], Fangwen Zhao[5], Maria Guarini [5], Victoria Gernedl [5], Mateo Pecoroaro[6], Klaus Warnatz[1,2,7], Christoph Bock[5,8,9], Esteban Ballestar[10], Roger Geiger[6,11], Michele Proietti[1,2,12,13], and Bodo Grimbacher[1,2,4,7,13,14].

Affiliations
[1] Institute for Immunodeficiency, University Medical Center Freiburg, Freiburg, Germany
[2] Center for Chronic Immunodeficiency, University Medical Center Freiburg, Freiburg, Germany
[3] Faculty of Biology, University of Freiburg, Freiburg, Germany
[4] Center for Integrative Biological signaling Studies (CIBSS), University of Freiburg, Freiburg, Germany
[5] CeMM Research Center for Molecular Medicine of the Austrian Academy of Sciences, Vienna, Austria
[6] Institute for Research in Biomedicine, Università della Svizzera Italiana, Bellinzona, Switzerland
[7] Department of Rheumatology and Clinical Immunology, University Medical Center Freiburg, Freiburg, Germany
[8]Medical University of Vienna, Center for Medical Statistics, Informatics and Intelligent Systems (CeMSIIS), Institute of Artificial Intelligence, Vienna, Austria
[9]Ludwig Boltzmann Institute for Rare and Undiagnosed Diseases, Vienna, Austria
[10]Epigenetics and Immune Disease Group, Josep Carreras Research Institute (IJC), 08916 Badalona, Barcelona, Spain
[11]Institute of Oncology Research, Università della Svizzera Italiana, Bellinzona, Switzerland
[12]Department of Rheumatology and Clinical Immunology, Hannover Medical University, Hannover, Germany
[13] Resolving Infection Susceptibility (RESIST) - Cluster of Excellence 2155 to Hannover Medical School, Satellite Center Freiburg, Freiburg, Germany
[14]German Center for Infection Research (DZFI), Satellite Center Freiburg, Freiburg, Germany.
*These authors have contributed equally to this work

Corresponding author: Bodo Grimbacher, MD, Institute for Immunodeficiency, Center for Chronic Immunodeficiency, Medical Center, Faculty of Medicine, Albert-Ludwigs-University of Freiburg. Breisacher Straβe 115, 79106 Freiburg, Germany. E-mail: bodo.grimbacher@uniklinik-freiburg.de

Authors e-mails:
Nadezhda Camacho-Ordonez < nadezhda.camacho@uniklinik-freiburg.de>
Sara Posadas Cantera <sara.posadas.cantera@uniklinik-freiburg.de>
Neftali Jose Ramirez <neftali.ramirez@uniklinik-freiburg.de>
Andrés Caballero-Oyteza <andres.caballero@uniklinik-freiburg.de>
Manfred Fliegauf <manfred.fliegauf@uniklinik-freiburg.de>
Fangwen Zhao <fzhao@cemm.oeaw.ac.at>
Maria Guarini < mguarini@cemm.oeaw.ac.at>
Victoria Gernedl <vgernedl@gmail.com>
Matteo Pecoroaro <matteo.pecoraro@irb.usi.ch>
Klaus Warnatz <klaus.warnatz@uniklinik-freiburg.de>
Christoph Bock <CBock@cemm.oeaw.ac.at>
Esteban Ballestar <eballestar@carrerasresearch.org>
Roger Geiger <roger.geiger@irb.usi.ch>
Michele Proietti <michele.proietti@uniklinik-freiburg.de>
Bodo Grimbacher <bodo.grimbacher@uniklinik-freiburg.de>

Abbreviations
ATAC-seq: assay for Transposase-Accessible Chromatin using sequencing
CSR: class switch recombination
CVID: Common Variable Immunodeficiency
FACS: fluorescence activated cell sorting
NFKB1: Nuclear Factor kappa B subunit 1
PBMCs: Peripheral Blood Mononuclear Cells
RRBS: Reduced represented bisulfite sequencing
SE: Superenhancers
TFBM: transcription factor binding motifs
TNF: Tumor Necrosis factor
WES: whole exome sequencing
WT: wild type

bioRxiv preprint doi: https://doi.org/10.1101/2022.11.22.517350; this version posted November 23, 2022. The copyright holder for this preprint (which was not certified by peer review) is the author/funder, who has granted bioRxiv a license to display the preprint in perpetuity. It is made available under aCC-BY-NC-ND 4.0 International license.

Abstract

The transcription factor NF-κB plays a pivotal role in the adaptive immune response. Pathogenic variants in *NFKB1* are the most common genetic etiology of common variable immunodeficiency (CVID). Patients frequently present with impaired terminal B cell differentiation, autoimmunity, and hyperinflammatory immune dysregulation. NF-κB signaling and target gene expression are expected to be dysregulated in *NFKB1*-mutated patients. Here, we performed a multi-omics characterization of B cells from a cohort of clinically affected and unaffected *NFKB1* mutation carriers. Our analysis identified specific epigenetic dysregulation and gene expression differences on B cells from *NFKB1*-mutated patients. We observed an aberrant expression of negative regulators of NF-κB signaling in *NFKB1* mutation carriers, which may be a key factor for the autoinflammatory phenotype of these patients. Moreover, our analysis points towards a dysregulation of *XBP1* and *BCL3*, key players of B cell activation and proliferation at different stages of B cell differentiation. The reduced expression of negative regulators of the NF-κB network is likely to be one of several mechanisms responsible for the aberrant NF-κB signaling, which impairs the maintenance of a normal humoral immune response. In summary, our findings highlight epigenetic and gene expression changes in B cells associated with *NFKB1* mutations. Our data give insight into future therapeutic opportunities for patients with *NFKB1* (haplo)insufficiency.

Key words: NFKB1 haploinsufficiency, immune dysregulation, B cells, RNA-seq, ATAC-seq, DNA methylation, proteomics

Introduction

Heterozygous damaging variants in *NFKB1* constitute the most common genetic cause of common variable immunodeficiency (CVID)[1–8]. The NF-κB signaling pathway plays a central role in multiple biological processes, including the adaptive immune response[9,10]. NF-κB comprises five family members: p65 (RelA), RelB, c-Rel, p105/p50 (*NFKB1*, activated by the canonical pathway), and p100/p52 (*NFKB2*, activated by the non-canonical pathway)[11]. *NFKB1* encodes the precursor p105, which undergoes proteasomal processing of its C-terminal half to generate the mature p50. In the cytoplasm, p50 predominantly assembles with p65 (RelA) but remains inactive while forming a complex with the inhibitor of NF-κB-alpha (IκBα). Upon pathway stimulation, IκBα becomes phosphorylated, ubiquitinated and subsequently degraded by the proteasome. The de-inhibited p50:p65 heterodimers then enter the nucleus and regulate the expression of NF-κB target genes[12,13]. However, p50 and p52 may also form homodimers, presumably functioning as transcriptional repressors, as these homodimers lack a transactivation domain which is only provided by the Rel proteins.

NFKB1 mutations are associated with a broad phenotype ranging from clinically unaffected to antibody deficiency and immune dysregulation within members of the same family[1,7,14]. Affected mutation carriers have a high frequency of autoimmunity, lymphoproliferation, noninfectious enteropathy, opportunistic infections, autoinflammation and malignancy[2,3,7]. Many patients have reduced numbers of class-switch memory B cells with an accumulation of CD21low B cells while maintaining an overall normal T-cell phenotype[15–17].

The observation of *NFKB1* haploinsufficiency mutations suggests that *NFKB1*-related diseases result in *decreased* NF-κB signaling[18] due to insufficient availability of signaling components. This observation is supported by reports of RelA haploinsufficiency[19,20]. Nevertheless, as shown by the existence of A20 deficiency, a negative regulator of the NF-κB signaling pathway, immune dysregulation can also be a result of an *increased* NF-κB activation[21–23]. We previously demonstrated that *NFKB1* mutations cluster into at least four different groups: N-terminal truncating mutations causing p50 haploinsufficiency, truncating mutations in the central part that predict immediate expression of p50-like proteins (precursor skipping), missense mutation affecting only the p105 precursor, and missense mutations affecting both, p105 and the active p50 (N-terminal half)[7,24]. An increase of p50 molecules by e.g. precursor-skipping mutations may support the formation of p50 homodimers, which would in turn repress gene transcription (as they lack the TAD domain of the Rel proteins) and therefore block NF-κB signaling. Clinical observations, however, taught us that *inhibition* of proinflammatory NF-κB signaling e.g. by anti-TNFα or anti–IL1 therapy ameliorated disease activity (Franxman et.al.[25], Toh et.al.[26], Dieli-Crimi et.al.[16], and unpublished observation B. Grimbacher).

bioRxiv preprint doi: https://doi.org/10.1101/2022.11.22.517350; this version posted November 23, 2022. The copyright holder for this preprint (which was not certified by peer review) is the author/funder, who has granted bioRxiv a license to display the preprint in perpetuity. It is made available under aCC-BY-NC-ND 4.0 International license.

Thus, for a research evidence-based treatment of the patient, it is crucial to understand the detailed impact of the identified *NFKB1* variants on the NF-κB signaling processes, its chromatin regulation, the role of posttranscriptional modifications, and crosstalk between NF-κB and other signaling pathways, in the context of disease. Because of the nature of the genetic mutations in *NFKB1*, downstream effects on NF-κB target genes are expected. These NF-κB target genes, however, may lead to the expected pro-inflammatory response and regulate differentiation and effector function in lymphocytes[27,28]. Yet, there is also a substantial number of NF-κB target genes which are involved in autoregulatory negative feedback loops to limit NF-κB signaling[29]. Therefore, the assessment of expression profiles of these genes may provide us with a more complete and quantitative measure of the biological processes involved in disease expressivity and penetrance caused by the heterozygous mutations in *NFKB1*. Moreover, deeper mechanistic insights into the pathogenesis of NF-κB immune dysregulation are urgently needed to facilitate the identification of specific targets for therapy.

Recent progress in genomic and transcriptomic sequencing analysis elucidated the genetic landscape of several immune diseases[30–32]. These multi-omics strategies have already revealed new mechanisms and potential targets to develop novel therapies. Here, we performed an integrative genomic, epigenomic, transcriptomic, and proteomic analysis in B cells of *NFKB1* mutation carriers compared to individuals with wild-type *NFKB1* (WT). The resulting data serve as an important resource for future biological, diagnostic, and drug discovery efforts.

Materials and methods

Study Participants

In this study we included 13 individuals with heterozygous pathogenic mutations in *NFKB1* from six different families (six affected and seven unaffected *NFKB1* mutation carriers) and 23 unrelated control individuals tested WT for *NFKB1*. Written consent was obtained from all individuals. This study was approved by the institutional review board and conducted according to the ethical standards of the Helsinki Declaration. Approved ethics protocols are iPAD EC No.76/19, and for the NFKB Study protocol No. 295/13_200149 and 93/18_191111, from the University Hospital of the Albert-Ludwigs-University, Freiburg, Germany.

Whole-exome sequencing

Genomic DNA was purified from human peripheral blood mononuclear cells (PBMCs) using QIAamp kits (Qiagen, Hilden, Germany) according to the manufacturer's protocol. Whole-exome sequencing (WES) was performed using the custom SureSelect exome sequencing protocol from Agilent (Waldbronn, Germany). Exomes were enriched by using SureSelect exome v5 probes. Libraries were sequenced twice (two flow cells) on a HiSeq 2500 v4 with a 2 × 76 bp protocol generating four raw sequence data files (FASTQ) per sample. Data preprocessing was performed according to the GATK best practices and involved the following steps: (1) conversion of FASTQ files into an unmapped BAM file (PICARD tool FastqToSam), (2) addition of tags to the Illumina adapter sequences of the unmapped BAM file (PICARD tool MarkIlluminaAdapters), (3) conversion of the unmapped tagged BAM file into a FASTQ file (PICARD tool SamToFastq), (4) alignment to the reference genome build UCSC hg38 (BWA MEM), (5) identification of duplicated reads (MarkDuplicates PICARD), (6) BAM recalibration, and (7) indel realignment. Variant calling was performed with three different variant callers: GATK Haplotype caller, FreeBayes, and SAMtools. BASH and R scripts were subsequently used to (1) merge the VCF files, (2) identify and unify dinucleotide changes, and (3) format the data sets for importation into an in-house specialized SQL database (GemmaDB) at the Center for Chronic Immunodeficiency in Freiburg. Variant annotation was performed using Ensembl's Variant Effect Predictor tool (ensemble.org), and allele frequency (AF) data were extracted from the gnomAD exome (v2.1.1) and genome (v3) data sets (GnomAD browser). Individual frequencies were obtained by transforming the gnomAD AF data. Variant filtering was performed by selecting variants with (1) an individual frequency below 1% in both our internal cohort and the gnomAD (exomes or genomes) populations, which included control cohorts, such as those in the NHLBI-GO Exome Sequencing Project or the 1000 Genomes project, (2) a "high" or "moderate" predicted impact, (3) an alternative AF larger than 0.3 and read depth larger than 20, and (4) a zygosity matching an autosomal recessive or X-linked recessive mode of inheritance.

Confirmation of Identified Sequence Variants by Sanger-Sequencing

DNA isolation was performed from blood samples treated with EDTA according to our local protocol using QIAamp kits (Qiagen, Hilden, Germany). *NFKB1* exons were amplified by PCR from gDNA and processed for Sanger sequencing according to standard protocols. Primer sequences are available in Supp.Table S1.

bioRxiv preprint doi: https://doi.org/10.1101/2022.11.22.517350; this version posted November 23, 2022. The copyright holder for this preprint (which was not certified by peer review) is the author/funder, who has granted bioRxiv a license to display the preprint in perpetuity. It is made available under aCC-BY-NC-ND 4.0 International license.

Peripheral Blood Mononuclear Cells isolation and FACS sorting from isolated cells

Peripheral Blood Mononuclear Cells (PBMCs) were isolated from EDTA blood by Ficoll density centrifugation following standard protocols. Cells were centrifugated for 5 minutes, 300g at RT, and the supernatant was discarded. The cell pellet was resuspended with 100µl of the corresponding master mix containing optimized dilutions of antibodies, for 30 minutes at 4°C. Next, cells were washed with FACS buffer and centrifuged for 5 minutes, 300g at RT. The supernatant was discarded and the cell pellet was resuspended in 200µl of FACS buffer for sorting.

In a first approach, 10 patient and 19 WT PBMC samples were sorted into naïve B cells (CD19+IgD, CD27-) and stimulated for 24 hours. B cell sorting was conducted with: CD19 APC-Cy7, CD20 APC, CD21 PE-Cy7, CD27 Brilliant Violet 421, CD38 PerCP-Cy5.5, IgM Alexa Fluor 488, IgD PE. Cells were sorted on a MoFlo Astrios Cell sorter (Beckman Coulter, Brea, CA, USA). Naïve B lymphocytes (250.000 cells/ml) were seeded on a 96 well round bottom plate in RPMI medium supplemented with 10% FCS and 1% Penicillin-Streptomycin. These cells were stimulated with 1µg/ml CD40L (provided by Pascal Schneider, Lausanne, Switzerland) and 50ng/ml IL21 (Miltenyi) and incubated for 24 hours at 37ºC, 5% CO2. After stimulation, cell numbers were determined with a Neubauer chamber. A total of 5,000-50,000 cells were used for DNA and RNA extraction, 5,000-50,000 were used for ATAC-sequencing and 74,000-200,000 for proteome analysis. B cell activation (CD69 APC, CD80 Brilliant Violet 421, CD86 PerCP-Cy5.5, CD95 Brilliant Violet 650, HLA-DR PE-Cy7) was measured on a B LSR Fortessa from Becton Dickinson (BD Biosciences, San Jose,CA).

On a second approach, PBMCs from three patients with pathogenic *NFKB1* variants and four WT control individuals were sorted into four different B cell subtypes: naïve (CD19+, CD21+, IgM+, IgD+, CD27, CD38-), IgM+ memory (CD19+, CD21+, IgM+, IgD, CD27+, CD38-), switched memory (CD19+, CD21+, IgM-, IgD-,CD27+,CD38-) and CD21low (CD19+,CD21-, IgM+/-, IgD+/-, CD27+/-, CD38-). B cell sort: IgM Alexa Flour 488, IgD PE, CD38 PerCP-Cy5.5, CD21 PE-Cy7, CD19 APC, CD27 BV450. Cells were sorted with the Cell sorter (Beckman Coulter, Brea, CA, USA). The cell pellets were subjected to DNA and RNA isolation.

RNA / DNA isolation and sequencing

DNA and RNA were extracted from isolated cells using a Qiagen AllPrep DNA/RNA Micro Kit. DNA concentration was determined using a Qubit fluorometer (Termo Fisher Scientific). Library preparation and sequencing by Reduced Represented Bisulfite Sequencing (RRBS) was performed at the CeMM Research Center for Molecular Medicine of the Austrian Academy of Sciences in Vienna, Austria, according to an established and extensively validated protocol[33–35].

The RNA library preparation and the sequencing was performed by Novogene (Cambridge, UK). The NEBNext RNA First Strand Synthesis Module and NEBNext Ultra Directional Second Strand Synthesis Module were used for low input RNA samples. The low input RNA concentrations from different healthy controls were sequenced using different library preparations and they were tested for the best sequencing outcome. The tested library preparations were the above mentioned low-input protocol, an rRNA depletion protocol and a SMARTer amplification protocol. After quality control, it was decided to process all samples from patients with the SMARTer amplification protocol, due to the higher number of unique reads. Samples were sequenced using the NovaSeq 6000 (Illumina) in paired-end mode. Generated reads had a length of 150 bp.

DNA methylation analysis

DNA was isolated from 5,000-50,000 FACS purified cells using the Qiagen DNA/RNA Micro Kit. RnBeads v2.12.2 was used for the analysis with standard settings[36]. Except for the addition of a set annotation for regulatory elements taken from Ensembl Regulatory Bild from BLUEPRINT data, hg38 assembly. Specifically, transcription factor binding sites, CTCF-binding sites, proximal and distal enhancers were used to study their overlap with differentially methylated regions using a custom RnBeads workflow. DNA Methylation values were calculated across 500bp regions. Only windows that contained ≥5 CpG sites were considered. The single nearest gene option was used for the association between the different genomic regions and genes.

RNA data analysis

RNA was isolated from 5,000-50,000 FACS-purified cells using Qiagen AllPrep DNA/RNA Micro Kit. The fastq files were uploaded to the Galaxy web platform and the public server usegalaxy.eu was used for the first part of the analysis [37]. Quality control of raw reads was done using FastQC. Quality Trimming was performed with TrimGalore, 10bp were removed from the 5' end of each read. Sequences were aligned to the reference genome (GRCh38/hg38) using RNA-STAR. Default parameters for paired-end

bioRxiv preprint doi: https://doi.org/10.1101/2022.11.22.517350; this version posted November 23, 2022. The copyright holder for this preprint (which was not certified by peer review) is the author/funder, who has granted bioRxiv a license to display the preprint in perpetuity. It is made available under aCC-BY-NC-ND 4.0 International license.

were used, except for the modification of the length of the genomic sequence around annotated junctions to 149 and the maximum number of alignments to output a read's alignment results to 3. Duplicates were not removed. The gene expression was measured with FeatureCounts using built-in gene annotations, unstranded specification and default parameters. Further analysis was performed in R v4.2.0 with an R custom script. Genes with read counts lower than 100 were excluded from the analysis. Differentially expressed gene analysis was done using R Bioconductor package DESeq2 v.3.15. Batch effect was corrected. Variance stabilizing transformation was applied to DESeq2 results. Differential expressed genes were filtered according to their adjusted p-value (<0.05) and absolute value of log2 fold change (>0.5). Principal component analysis was carried out after batch correction using Bioconductor limma package. Heatmaps and volcano plots were generated using the R package pheatmap, and the Bioconductor package EnhancedVolcano, respectively. Gene set enrichment analysis (GSEA) was performed using the R Bioconductor package fgsea together with the Hallmark, and KEGG pathways from the M SigDb. All differentially expressed genes were used for GSEA. Ggplot2 package was used to create dot plots of pathway analysis.

Protein extraction and enzymatic digestion

Between 74.000-200.000 FACS-sorted cells were washed twice in phosphate-buffered saline (PBS), and dry pellets were flash frozen and stored at -80°C. Further processing was performed in the Institute Biochemistry in Bellinzona., Switzerland. Cell pellets were lysed in 50 µl of 8M urea in 50 mM ammonium bicarbonate (ABC) followed by sonication (15 minutes at 4°C), with a Bioruptor (Diagenode). Up to 100µg of protein extract per sample was reduced with 10 mM dithiothreitol (20 minutes at RT). Subsequently, proteins from each sample were alkylated with 50mM iodoacetamide (30 minutes at RT) and digested with 1 µg of LysC (FUJIFILM Wako) in 8M urea, 50 mM ABC (2 hours at RT). After digestion, the buffer was diluted with 50 mM ABC to a final of 2M urea and digested overnight at RT with 1 µg trypsin (Promega, Walldorf, Germany). On the next day, the addition of acetonitrile (ACN) to 2% and trifluoroacetic acid (TFA) to 0.3% terminated the trypsin digestion. The samples were centrifuged 5 minutes at maximum speed, and the supernatants were desalted using C18 StageTips. Peptide elution was achieved with 80% ACN, 0.5% acetic acid. To evaporate the solution, vacuum centrifugation was performed followed by resuspension of the purified peptides with 2% ACN, 0.5% acetic acid, 0.1% TFA. Up to 1 µg of purified peptides per sample were injected in a liquid chromatograph- tandem mass spectrometer, as single-shot measurements.

Liquid chromatography– with tandem mass spectrometry (LC-MS/MS) analysis

Peptide separation in buffer A (0.1% formic acid) was achieved using an EASY-nLC 1200 HPLC system (Thermo Fisher Scientific) and a column (75 µm inner diameter, 50 cm length, ReproSil-Pur C18-AQ 1.9 µm). Elution was carried out in a 5-30% buffer B (80% ACN, 0.1% formic acid) linear gradient for 150 minutes and a flow rate of 250 nl/min. Ions were produced by a nanoelectrospray source (Thermo Fisher Scientific) and fragments feed into a Q Exactive HF mass spectrometer (Thermo Fisher Scientific). Measurements were performed in a data-dependent mode. Parameter settings in Xcalibur software (Thermo Scientific) comprised a survey scan range of 300-1,650 m/z, resolution of 60,000 at 200 m/z, maximum injection time of 20 ms and AGC target of 3e6. In a 1.7 m/z isolation window, up to ten ions with high frequency and a charge of 2-5 were isolated. Next, the ions underwent higher-energy collisional dissociation (HCD) fragmentation with a normalized collision energy of 27 to acquire MS/MS scans. Repeated sequencing was excluded by setting dynamic exclusion to 30 s. Measurement parameters comprised a resolution of 15,000 at 200 m/z, maximum injection time of 55 ms and AGC target of 1e5.

ATAC-seq processing

Accessible chromatin mapping was performed using the ATAC-seq method as previously described[38] with parameters reported in Ramirez et al[39]. In brief, 5,000-50.000 cells per experiment were centrifuged 5 minutes at 8°C, and resuspended in 25 µl transposase mixture (12.5 µl Tagmentation DNA buffer, 1 µl Tn5 transposase (Illumina), 10.75 µl nuclease-free water, 0.25 µl 1% digitonin (Promega) and 0.5 µl 50x Protease Inhibitor cocktail (Roche)). After incubation of the solution, 30 minutes at 37°C, and DNA purification, the DNA was eluted in 13.5 µl 10mM Tris-HCI, pH 8.5. Further library preparation (NEBNext Ultra II kit) and sequencing, 50bp single-end on a HiSeq 4000 was performed at the CeMM Research Center for Molecular Medicine of the Austrian Academy of Sciences in Vienna, Austria.

ATAC-seq analysis

Unaligned reads were quality controlled using FastQC. Reads were then trimmed, aligned to hg38, and filtered using Skewer, Bowtie2[40], and Sambamba[41] respectively. As previously described, all downstream analyses were performed on the filtered reads[42] (>100 million). Reads mapping to mitochondrial DNA were excluded before peak calling was performed using HOMER[43]. The parameters '-style factor

bioRxiv preprint doi: https://doi.org/10.1101/2022.11.22.517350; this version posted November 23, 2022. The copyright holder for this preprint (which was not certified by peer review) is the author/funder, who has granted bioRxiv a license to display the preprint in perpetuity. It is made available under aCC-BY-NC-ND 4.0 International license.

and -L 20' were used to analyze transcription factors (20-fold greater tag density than in the surrounding 10kb region) and '-style super' was used to analyze super enhancers with default settings. With 'getDifferentialPeaksreplicates.pl -balanced –edgeR -L 10' parameters (10- fold greater tag density than background), differential transcription factor peaks were identified. Peaks were merged for the same cell type using mergePeaks and annotated with annotatePeaks.pl. To perform principal component analysis, a non-annotated file generated with the 'noann' option was uploaded to Rstudio and visualized with ggplot2 (version 3.3.5). Transcription factor binding motifs were identified with HOMER function findMotifsGenome.pl and '-size 200 (peak size) and -len 8,10,12,15 (motif length)' settings. Next, a matrix file was generated using HOMER with '-size 200 -hist 400 (bin size in bp) -ghist (outputs gene profiles for each gene) parameters. The matrix file was used for unsupervised hierarchical clustering using Cluster 3.0 (parameters: normalize genes, cluster genes and array, similarity metric: correlated uncentered) and visualized with Java Tree View.

Proteome data analysis

Using the MaxQuant software, v.1.6.7.0[44] and the integrated Andromeda search engine[45], peptides and proteins with a false discovery rate of < 1% were determined from the Xcalibur raw files. The Human UniProt database (June 2019) and a common contaminants database were used for peptide and protein identification with "Trypsin/P" enzyme specificity, a maximum of 2 missed cleavages and minimum length of 7. Variable modifications included N-terminal protein acetylation and methionine oxidation, whereas cysteine carbamidomethylation was selected as fixed modification. To compare runs among each other, mass and normalized retention time (time window of 0.7 minutes and an alignment time window of 20 minutes) were used. The MaxLFQ algorithm[46] was used to quantify label-free proteins (LFQ) with a minimum peptide ratio count of 1 and LFQ intensities were log2 transformed. Proteins only identified by site, reverse peptides, and potential contaminants were removed. In Rstudio, the R Bioconductor package DEP (version 1.12.0) was used for normalization and imputation with a left-censored method (0.3 width and 1.8 downshift). The t-test from the R package limma (version 3.46.0) was used to determine differently expressed proteins (alpha = 0.05, absolute log2 fold change = 1.5). All visualizations were performed as described for the transcriptome analysis.

Association between DNA methylation, open chromatin and Gene Expression

For association analysis, samples that had DNA methylation, ATAC-seq and/or gene expression data were examined. The Bioconductor package Complex Heatmap (v2.10.0) with a custom R script were used for the association analysis between gene expression, DNA methylation, and ATAC-seq. For methylation and ATAC-seq data, methylation and preferentially open chromatin regions from *NFKB1* mutation carriers were used for the analysis. For RNA-seq and proteome data, differential gene or protein expression between *NFKB1* mutation carriers and WT controls were used. The median methylation is represented as a beta-value from 0 to 1 (0 to 100% methylation). For ATAC-seq data, position adjusted reads from initial peak regions were used. For differentially expressed genes in the RNA-seq, data log2-fold changes values were used, as were for differentially expressed proteins. Venn diagrams were drawn using the R package ggVennDiagram. We performed a supervised analysis of NF-κB target genes on B cells in all the data sets. The list of NFκB -target genes was adapted from https://www.bu.edu/nf-kb/gene-resources/target-genes/, and an additional search with PubMed.

Results

Clinical and genetic characterization of patients

In this study, we included a total of 13 *NFKB1* mutation carriers from six different families and 23 individuals WT for *NFKB1* (Table 1). Among the mutation carriers, six were classified as affected and seven were unaffected. All affected individuals presented with hypogammaglobulinemia and a history of recurrent respiratory infections. The median age of mutation carriers was 55.5 (±21.28) years. The clinical phenotype was characterized by lymphoproliferation, particularly splenomegaly and lymphadenopathy. Autoimmunity and inflammatory gastrointestinal involvement were present in all affected individuals. At the time of analysis, all but one affected mutation carrier (FR097.2) received immunomodulatory treatment (Table 2).

All *NFKB1* mutation carriers underwent WES for mutation detection and Sanger sequencing to verify the presence of the variant. All variants with a frequency of less than 1% in gnomAD (https://gnomad.broadinstitute.org) which were detected in our patients by WES are displayed in the supplementary

bioRxiv preprint doi: https://doi.org/10.1101/2022.11.22.517350; this version posted November 23, 2022. The copyright holder for this preprint (which was not certified by peer review) is the author/funder, who has granted bioRxiv a license to display the preprint in perpetuity. It is made available under aCC-BY-NC-ND 4.0 International license.

Table S2. Eleven individuals carried N-terminal truncating mutations, predicted to cause haploinsufficiency of the p105 precursor protein, and the mature p50. Patient FR005 carried the mutation c.295C>T; p.Gln99*, it was previously described [5]. The single base pair deletion (c.872delA; p.Asn291Metfs*141) was present in eight patients (from two different families). Patients FR095 and FR097.2 are affected and members of the same family as patients FR098 and FR099. In the other family, all patients (FR100, FR101, FR102 and FR103) were unaffected. All individuals were previously reported[78]. Patients FR023 and FR302 carry the haploinsufficiency mutations c.835+2T>G (p.Ser338Leufs*94) and c.589delA (p.Ile197Serfs*55), respectively. The mutation of patient FR023 was previously reported[7]. In addition, two patients, including one affected (FR036), and one unaffected (FR113) member from the same family carried a precursor skipping mutation c.1365delT (p.Val456*). These types of mutations affect the central part of p105 and predict the immediate expression of a p50-like protein thereby skipping the precursor stage. However, all eleven patients with pathogenic mutations in *NFKB1* also carried rare variants (<1% in gnomAD) in NF-κB downstream target genes (Table 3).

Abnormal expression of NF-κB target genes in unstimulated and stimulated B cell subsets indicates reduced expression of negative regulators

Heterodimeric NF-κB transcription factors (composed of p50 and one of the Rel proteins) act as inducers of gene expression[47,48]. We determined the gene expression profiles of both sorted unstimulated naïve B cells, and CD40L/IL21-stimulated naïve B cells derived from *NFKB1* mutation carriers by RNA seq. We obtained RNA sequencing data of stimulated naïve B cells from ten *NFKB1* mutation carriers (three affected and seven unaffected), and 18 age- and gender-matched healthy donors, WT for *NFKB1*. In addition, we performed RNA sequencing on four unstimulated B cell subtypes (naïve-, IgM memory, switched memory, and CD21low- B cells) from three affected *NFKB1* mutation carriers (FR095, FR103, and FR302) and 4 WT. A list of sequencing data available per sample is listed in Supp. Table S3.

Since IL21 and CD40L stimulation induce a strong activation of NF-κB signaling, leading B cells to a proliferative burst and later plasma cell differentiation[49], we inspected the transcriptome of 24h activated naïve B cells on ten *NFKB1* mutation carriers (three affected and seven unaffected) and 18 NFKB1 WT individuals. In comparison to wildtype controls, stimulated naïve B cells from NFKB1 mutation carriers displayed profound changes in NF-κB target gene expression. This observation suggests that the pathogenic effect of these variants is evident at the transcriptional level (column 1, Figure 1a). Particularly, the increased expression of *NR4A2* and *GZMB*, in combination with the decreased mRNA expression of *TNFAIP3, TRAF1, TRAF6, TNIP1 and CYLD*, points towards an induction of B cell proliferation and dysregulation of NF-κB inhibitors[18]. Interestingly, some B cells secrete granzyme B (codified by *GZMB*) when recognizing viral antigens, in the setting of infection, in autoimmune diseases, in chronic lymphocytic B cell leukemia, and when infiltrating solid tumors [50–52]. Therefore, *NFKB1* haploinsufficiency seems to mimic this state of a chronic stimulus such as present in chronic virally infected B cells.

We then asked whether the disease status of each patient might influence NF-κB target gene expression i.e. whether affected and unaffected mutation carriers display unique NF-κB target gene expression profiles. Thus, we split the analysis of the ten stimulated naïve B cells *NFKB1*-mutated samples into two groups. The first group comprised three patients, who were clinically affected at the time of blood drawing. The second group contained seven unaffected mutation carriers. Data analysis presented in columns 2 and 3 in Figure 1a shows that the affected *NFKB1* mutation carriers accounted for the strong NF-κB target gene dysregulation when compared to matched healthy controls, while the seven unaffected *NFKB1* mutation carriers remained with almost normal levels of NF-κB target gene expression. When comparing affected *versus* unaffected *NFKB1* mutation carriers, *SOCS1* had lower expression levels (column 4, Fig 1a.). *SOCS1* is one component of the ubiquitin ligase complex that mediates NF-κB degradation[53], suggesting that the ubiquitination process of NF-κB subunits in the control of transcription is impaired.

In summary, columns 1-4 in Figure 1a show that stimulated naïve B cells of *NFKB1* mutation carriers have a significantly different gene expression pattern when compared to WT. To investigate which biological processes are most affected, we performed pathway analysis utilizing hallmark gene sets. In *NFKB1* mutation carriers, we found TNF-α signaling *via* NF-κB, and the interferon gamma (IFN-γ) response to be under-expressed.

Next, we compared the data sets of unstimulated naïve B cells from three NFKB1 mutation carriers (FR095, FR103, and FR302) to four matching healthy control samples. We observed that unstimulated

bioRxiv preprint doi: https://doi.org/10.1101/2022.11.22.517350; this version posted November 23, 2022. The copyright holder for this preprint (which was not certified by peer review) is the author/funder, who has granted bioRxiv a license to display the preprint in perpetuity. It is made available under aCC-BY-NC-ND 4.0 International license.

naïve B cells from *NFKB1* mutation carriers showed changes of NF-κB target gene expression (column 5, Figure 1a) with overall lower expression levels compared to WT. As expected, under resting conditions, the haploinsufficiency mutation leads to a reduced production of p105, hence also a reduced amount of its processed form p50, and therefore to disturbances of the baseline expression of NF-κB target genes[1].

We were also interested whether other unstimulated B cell subsets such as IgM memory-, switched memory-, or CD21-low B cells showed a dysregulation of NF-κB target genes. Whereas CD21-low B cells showed only minor variation when compared to healthy donors, we found clearly reduced expression levels for a distinguished set of NF-κB target genes in IgM memory- and switched memory B cell compartments. For instance, genes codifying for NF-κB inhibitors *NFKBIA, NFKBID, NFKBIE*, and transcription factors essential during B cell development (*BCL3* and *XBP1*) were strongly dysregulated (columns 6-8, Figure 1a). This observation goes along with the observation that NFKB1 patients present with impaired terminal B cell differentiation.

To test how *NFKB1* mutations affect downstream pathways, we performed a KEGG enrichment analysis on differentially expressed NF-κB- target genes. We compared stimulated naïve B cells from affected mutation carriers (three affected) to the WT control group. In patient samples, we found reduced expression levels of genes of the NF-κB signaling pathway such as *ATM, BCL2, BIRC2 (c-IAP1), BTK, CD40, CYLD, LYN, NFKBIA(I*κBα*), PLAU (uPA), PLCG2, RELB, SYK, TAB, TIRAP, TRAF2, TRAF3,* and *TRAF6*. Importantly, expression of several negative regulators of the NF-κB signaling pathway was found to be reduced including *CYLD, TNP1, TRAF1, TNFAIP2 and TNFAIP3* (A20) (Figure 1b). Moreover, increased expression of core and regulatory components of the proteasome (20S and PA700) was observed (Figure 1c). The proteasome has an important role in the strict control of NF-κB activity. On one side, the ubiquitination and proteasomal degradation of IκB promotes NF-κB activity. On the other side, ubiquitination leads to degradation of NF-κB subunits and culminates its transcriptional activity[54].

Next, we compared stimulated B cells derived from the entire group of *NFKB1* mutation carriers (n=10) with the WT control group. Consistent with the previous observations, we found a decreased expression of genes encoding for components of the NF-κB signaling pathway, like *BIRC2 (c-IAP1), BTK, CD40, CYLD, LYN, PLAU (uPA), PLCG2, RELB, TIRAP, TRAF3,* and *TRAF6* (Supp. Fig. S2), while regulatory components of the proteasome showed increased expression (Supp. Figure S3). In stimulated naïve B cells from unaffected *NFKB1* mutation carriers, we found reduced expression of both, genes of the NF-κB signaling pathway (*NFKB1* itself*, BCL2L1,* and *TNFAIP3*), and genes related to the TNF-α signaling pathway (*NOD2,* and again *NFKB1* and *TNFAIP3*). Some genes on the TNF-α signaling pathway had increased expression (AP-1, FOS, and BCL3), data shown in Supplementary Fig.S4-S6. From these results, we conclude that NF-κB signaling is active in mutated B cells, with reduced expression of several negative regulators of the pathway.

To achieve the termination of the NF-κB response the cell employs several mechanisms, including a negative feedback loop[24,29,55]. In the stimulated data set we observed a low expression of negative regulators of NF-κB in NFKB1 mutation carriers (Figure 1d). Remarkably, we also found lower expression of negative regulators of NF-κB in unstimulated naïve-, IgM memory-, and switched memory- B cells from *NFKB1* patients, but not in CD21low B cells (Fig. 1e). This was not surprising, given that CD21low B cells usually show a divergent RNA-seq profile[56]. This population has been associated with autoimmunity and chronic parasitic or viral infections[17].

Our findings demonstrate that the transcriptional program of stimulated and unstimulated B cells across different subtypes is compromised in *NFKB1*-mutated cells. The lack of negative regulation may lead to chronic inflammation as observed in our patients, and in patients with rheumatoid arthritis[57]. Consistent with the transcriptional profile of stimulated naïve B cells, the limited expression of negative regulators of NF-κB signaling might explain the inflammatory phenotype of *NFKB1*-mutated individuals as well as the immune dysregulation. From these observations, we conclude that transcriptional changes are associated with clinical manifestations of immune dysregulation.

bioRxiv preprint doi: https://doi.org/10.1101/2022.11.22.517350; this version posted November 23, 2022. The copyright holder for this preprint (which was not certified by peer review) is the author/funder, who has granted bioRxiv a license to display the preprint in perpetuity. It is made available under aCC-BY-NC-ND 4.0 International license.

Defective B cell differentiation and proliferation is caused by impairment of Chromatin accessibility in NFKB1-mutated cells

To study the enhancer landscapes in *NFKB1* mutation carriers, isolated B cells from three affected (FR005, FR023, and FR036) and five unaffected (FR099, FR100, FR101, FR102 and, FR103) *NFKB1* mutation carriers, and 17 wildtype control individuals were stimulated with CD40L/IL21 for 24h and analyzed for chromatin accessibility by ATAC-seq. 549 differentially accessible regions (DARs) were detected comparing *NFKB1* mutation carriers to WT. The majority of DARs were accessible in WT (381), while 168 DARs were accessible in mutation carriers (Figure 2a). To identify transcription factors associated with differential chromatin accessibility, we performed *de novo* transcription factor binding motif (TFBM) analyses. The *CTCF* motif was identified as the most enriched TFBM in *NFKB1* mutation carriers compared to WT, suggesting that the chromatin architecture is impaired. Furthermore, binding motifs for *NFAT, NKX2, NR1A2* and *STAT5* were found enriched, influencing B cell differentiation and proliferation. Enrichment in DNA-binding factors involved in cell activation and survival, such as *REL, SPIB, MZF1, ETV6* and *IRF-BATF,* were found enriched in WT individuals (Figure 2b). In order to identify a dysregulated chromatin landscape related to affected disease status, affected *NFKB1* mutation carriers were compared to WT. Consistent with the previous findings, one third of DARs (479) were accessible in affected *NFKB1* mutation carriers and two third of DARs (917) were accessible in WT (Fig. 2c). Similar TFBM were detected in WT, such as *SPIB*, *REL, IRF and BATF*. For *NFKB1* mutation carriers, *CTCF* was the motif with the highest enrichment, as in the previous analyses. CCCTC-binding factor (CTCF) is a chromatin architectural protein, which facilitates the interaction of different chromatin regions. It can thereby function as a repressor, transcriptional activator or insulator protein, and it can also recruit other transcription factors while bound to chromatin domain boundaries[58]. Furthermore, motifs for TFs involved in germinal center (GC) response were enriched such as *SP1*, *SOX4, IRF1*, and *PAX5* (Fig. 2d). In contrast to the affected *NFKB1* mutation carriers, the unaffected carriers presented with two third of DARs (248), while the WT had 129 DARs accessible (Fig. 2e). CTCF was the most enriched TFBM, as in previous analyses. The binding motif for STAT5 was detected, which was similarly enriched in the combined analysis of *NFKB1* mutation carriers. Transcription factors influencing B cell activation and development, such as *IKZF1* and *FRA1*, showed enriched motif accessibility. As observed in the previous analyses, *REL* and *SPIB* were enriched in WT (Fig. 2f). In addition, enrichment of the *NFKB2* binding motif was detected. Due to opposing results from affected and unaffected *NFKB1* mutation carriers, the two groups were compared to identify disease-specific signatures. Similar as in the comparison of unaffected *NFKB1* mutation carriers *vs* WT, two thirds of DARs (242) were accessible in the unaffected individuals, while one third of DARs (150) were accessible in affected *NFKB1* mutation carriers (Fig. 2g). *SIX2, PRDM4, OSR2*, Pu.1-IRF and *IRF5* were the most enriched TFBM in affected *NFKB1* mutation carriers. For unaffected *NFKB1* mutation carriers *SPI1, REL, AP-1, SOX10* and *SPIC* were most enriched TFBMs (Fig. 2h). With our identification of accessible chromatin and TFBM, our data reveal dysregulation of key players of B cell differentiation and proliferation. NF-κB (*REL*) and ETS family members (*SPIB, SPI1, SPIC*) seem most affected, as they were observed in all comparisons.

Super-enhancers (SE) are regulatory elements characterized by high levels of chromatin modification[59]. These non-coding elements distribute regulatory information within the 3D nuclear chromatin architecture creating SE-promoter contacts that modulate a cell-specific gene expression[60]. NF-κB has a role in the activation of SE[61,62]. To study the super-enhancer landscape of NF-κB target genes, we looked for chromatin accessible regions on *NFKB1* mutation carriers compared to WT (Fig 3). The majority of preferentially accessible regions were on the unaffected group (n=15), followed by WT (n=10) and affected (n=4). In the unaffected group, key regions for B cell proliferation and differentiation were preferentially open (*BCL2, BCL3, CD83, FOSB, NR4A2* and *IRF1*), but we also found open regions for NF-κB negative regulators, *TRAF1* and *TNIP1*. In the WT group, we identified *BCL3, FOSB, IRF1*, and *NR4A2* being preferentially open. These factors act synergistically with NF-κB to activate transcription upon BCR stimulation. The negative regulator *NFKBIA* was also open in this group. Finally, in the affected group, *FOSB, IRF1,* and *NR4A2* were preferentially open, as well as the negative regulator *NFKBIA*. Previous studies have associated SE with NF-κB target genes *in vitro* and in mouse models[61,63,64]. Our analysis indicates that in NF-κB mutated cells chromatin opening at SE is disturbed. This might be an additional factor influencing the TF-DNA binding that causes variation in NF-κB target gene expression.

Taken together, our data suggest that a network of unique chromatin accessibility profiles result in differences on NFKB1 mutated cells, affecting B cell function and differentiation upon activation.

bioRxiv preprint doi: https://doi.org/10.1101/2022.11.22.517350; this version posted November 23, 2022. The copyright holder for this preprint (which was not certified by peer review) is the author/funder, who has granted bioRxiv a license to display the preprint in perpetuity. It is made available under aCC-BY-NC-ND 4.0 International license.

Aberrant expression of NF-κB target genes is independent from changes of the methylation pattern in four distinct B cell subsets from *NFKB1* patients

To further explore underlying mechanisms of *NFKB1*-disease in our cohort, we performed in parallel DNA methylation analysis by RRBS and transcriptional profiling by bulk RNA-seq in four distinct unstimulated B cell subsets (unstimulated naïve-, IgM memory-, switched memory-, and CD21low-B cells) derived from three *NFKB1* mutation carriers (FR95, FR103 and FR302), and four *NFKB1* wild-type individuals (C1, C2, C3 and C4). All mutation carriers harboured a pathogenic variant leading to haploinsufficiency (Tables 1 and 2).

We performed transcriptome analysis with a cut-off p-value of <0.05, and an absolute log2-fold change of >0.5. Comparison of WT to *NFKB1* mutation carriers revealed significant expression changes in the unstimulated B cell subsets. In naïve B cells, 1193 genes were differentially expressed (727 downregulated and 466 upregulated), while 33 genes were downregulated in IgM memory-B cells. In addition, 1230 differentially expressed genes were found in switched memory-B cells (869 downregulated and 361 upregulated), and 227 differentially expressed genes in CD21 low-B cells (192 downregulated and 35 upregulated). In *NFKB1* mutation carriers, hallmark gene pathway analysis revealed a predominantly negative enrichment of TGF-beta signaling in all but the CD21low B cell compartment. In naïve B cells, the mTOR signaling pathway, often activated in tumors[65], was positively enriched, while inflammatory response, hypoxia, and the UV response were negatively enriched (Fig 4a). The role of NF-κB in these processes has been associated with the disruption of cell homeostasis in the disease context[66,67]. In IgM memory- and switched memory- B cells, we found the interferon gamma (IFN-γ) response negatively enriched (Fig 4b and c). Zumakero et al.[68] demonstrated that IFN-γ induces an epigenetic reprograming of B cells, which results in increased chromatin accessibility of transcription binding motifs for NF-κB, IRF4 and BLIMP1 and thus promotes the formation of antibody secreting cells. However, in CD21low B cells we found merely positive enrichment (Fig 4d). These data are consistent with enriched CD21low populations in patients with chronic immune activation[17]. Moreover, KEGG pathway analysis showed increased *BTK* expression in unstimulated naïve B cells and switched memory B cells. In depth analysis can be found in the supplementary material Figures S7-S12. Our findings highlight, how *NFKB1* mutations profoundly alter B cell biology through the activation or repression of NF-κB target genes.

Subsequently, we characterized the methylation profiles of all four unstimulated B cell subsets. Differences in methylation patterns between *NFKB1* mutation carriers and WT were considered relevant when loci (β-values) were 10% or more differentially methylated, with an FDR of <0.05. We observed gradual global demethylation on B cells from the naïve to the memory compartment in healthy individuals, as previously reported[69–72]. Differences in the global methylation pattern were evident at the transition from the naïve, to the IgM-, and switched memory compartments. Patients showed higher methylation levels when compared to WT (Fig 5a). In healthy controls, 14,349 DMRs were hypomethylated in the transition from naïve to IgM memory B cells and 5,028 DMRs in the transition from IgM to switched memory compartment. In contrast, *NFKB1* mutation carriers showed impaired demethylation. We observed 9,137 hypomethylated DMRs at the naïve to IgM memory stage, and 1,785 at the IgM memory to switched memory compartment (Supp.TableS4). These findings corroborate the important role of methylation during B cell differentiation and suggest a contribution of aberrant methylation events to B cell dysfunction.

We then focused on differential methylation distribution across various regions (Figure 5b). The majority of DMRs were located at gene regulatory regions, particularly at enhancers, CTCF-, and transcription factor binding sites. Enhancers are known for dynamic methylation patterns[73,74]. During B cell development, around 40% of genes with methylated enhancers are included in the regulatory process of gene expression [71,75,76]. Several papers suggest that DNA-methylation affects transcription factor binding, indicating that a removal of methylation allows transcription factors to bind within the landscape of hypomethylated regulatory regions[77–80]. Particularly, CTCF has been reported to have a highly specific response to low levels of methylation[81].

At CpG islands, we identified 470 DMRs (151 hypomethylated and 319 hypermethylated) in unstimulated naïve B cells, 346 DMRs (142 hypomethylated and 214 hypermethylated) in IgM memory B cells, 925 DMRs (346 hypomethylated and 579 hypermethylated) in switched memory B cells, and 963 DMRs (299 hypomethylated and 664 hypermethylated) in CD21-low B cells. When looking specifically at promoter regions, 78 DMRs were identified in unstimulated naïve B cells (43 hypomethylated and 35 hypermethylated), 58 DMRs in IgM memory B cells (25 hypomethylated and 33 hypermethylated), 170 DMRs in switched memory B cells (89 hypomethylated and 81 hypermethylated), and 178 DMRs in

bioRxiv preprint doi: https://doi.org/10.1101/2022.11.22.517350; this version posted November 23, 2022. The copyright holder for this preprint (which was not certified by peer review) is the author/funder, who has granted bioRxiv a license to display the preprint in perpetuity. It is made available under aCC-BY-NC-ND 4.0 International license.

CD21-low B cells (82 hypomethylated and 96 hypermethylated). However, none of these DMRs were linked to NF-κB target genes, which was unexpected, since DNA methylation at promoter regions is generally linked to the maintenance of gene silencing[82] and various NF-κB target genes were found with reduced transcriptional activity.

During B cell differentiation and upon antigen encounter, peripheral mature B cells undergo somatic hypermutation (SHM) and class switch recombination (CSR), which are both associated with a high cellular replication rate and extensive demethylation[83,84]. NF-κB contributes to CSR by binding to the 3' enhancer, a locus control region located downstream of *IGHA1* [85,86]. However, methylation of *IGHA1* remained unchanged in *NFKB1* patients. Instead, we found hypermethylation at promoter regions of *IGHD* in unstimulated naïve B cells and of *IGHV4-28* and *IGLV9*-49 loci in IgM memory B cells (Table 4).

Plasma cell differentiation is a coordinated process that involves changes in gene expression, and hence gene regulation[87]. When looking at the nearest gene to the DMRs, we found several genes with a role in B cell development dysregulated. Among others, *NFKB1* patients compared to WT showed higher methylation levels of *MZB1* in naïve B cells and lower levels in the switched memory compartment. *MZB1* is expressed in marginal zone B cells and it is highly upregulated during plasma cell differentiation[88,89]. In addition, we found higher levels of methylation of *SLAMF1* in *NFKB1* patients in comparison with healthy individuals in IgM memory B cells. *SLAMF1* is part of the signaling lymphocytic activation molecule family and has a binding site for *NFκB.* In B cells it is upregulated following activation, and plays a role in T and B cell co-stimulation[90]. Increased expression has been reported in patients with autoimmune thyroiditis, lymphoid leukemias and lymphomas [91–93].Moreover, we found DMRs at the immunoglobulin chain locus of *NFKB1* patients when compared to WT (Table 4). Expression and rearrangement of immunoglobulin genes takes place during B cell differentiation[94]. The contribution of aberrant DNA methylation to antibody production has been suggested by increased methylation levels in patients with CVID and phenotypically discordant monozygotic twin studies [72,95]. Accordingly, our data supports the notion that dysregulated DNA methylation also contributes to B cell dysfunction in patients with *NFKB1* mutations. In line with the above findings, the limited expression of negative regulators of NF-κB signaling at the transcriptome level may be a key constituent for the observed hyperinflammatory immune dysregulation in *NFKB1*-mutated patients. Additionally, p105/p50 insufficient patients display altered methylation patterns in distinct B cell subsets, which might contribute to the defective B cell function.

Proteome analysis of stimulated naïve B cells from *NFKB1* mutation carriers also shows dysregulation in the B cell function

To elucidate effects of *NFKB1* mutations on the protein level, we examined the proteome of CD40L and IL21-stimulated naïve B cells from three affected and three unaffected *NFKB1* mutation carriers and five healthy donors. All individuals had also been included in the transcriptome analysis. 4,666 differentially expressed proteins were detected in the *NFKB1* mutation carriers with cutoffs at >0.5 absolute log2 fold change and <0.05 adjusted p-value (Supp. figure S13).In contrast to the transcriptome data, pathway analysis using Hallmark genes revealed IFN-α and -γ as most enriched in affected *NFKB1* mutation carriers. IFN-α lowers the threshold for B cell antibody responses[96], while IFN-γ inhibits B cell proliferation during maturation[97]. The pathways for epithelial-mesenchymal transition, coagulation, and UV-response were reduced (Figure 6a), all of which are pathways known to be activated by *NFKB1* [98,99]. The same pathways were observed to be decreased in unaffected *NFKB1* mutation carriers. However, in unaffected patients PI3K-Akt-mTOR signaling was most enriched (Figure 6b). The PI3K-Akt-mTOR axis is essential for normal B cell metabolism, proliferation and development [100].

When correlating log2-fold changes for differentially expressed genes with their corresponding differentially expressed proteins, we found a statically significant positive correlation (p=0.07, r=0.06) for affected and unaffected *NFKB1* mutation carriers compared to WT (Figure 7a). However, when we separating the groups according to disease status (affected or unaffected) and comparing them to WT, no correlation was observed (Figures 7b and 7c). A weak correlation between mRNA transcripts and proteins could be explained by translation regulation, and post-transcriptional protein modifications and degradation[101], which became evident only after we analyzed the groups according to disease status.

bioRxiv preprint doi: https://doi.org/10.1101/2022.11.22.517350; this version posted November 23, 2022. The copyright holder for this preprint (which was not certified by peer review) is the author/funder, who has granted bioRxiv a license to display the preprint in perpetuity. It is made available under aCC-BY-NC-ND 4.0 International license.

Multi-omics analysis of *NFKB1*-insufficient B cells reveals accessible chromatin regions with incomplete demethylation

Given the essential role of NF-κB signaling in various physiological processes and the severe consequences of potential dysregulation, NF-κB activity requires tightly adjustable control mechanisms. Since active transcription factors bind to chromatin in order to modulate target gene expression[102], chromatin accessibility and epigenetic modifications, such as DNA methylation, can determine the duration and strength of NF-κB binding and therefore the transcriptional output[103,104]. To explore the relationship between epigenetic changes and differential gene expression in *NFKB1* mutation carriers, we performed an association analysis of DNA methylation levels and preferentially open chromatin regions, with differentially expressed genes and differentially expressed proteins obtained by comparing affected *NFKB1* mutation carriers to WT control individuals (Figures 8a and 8b). While hypomethylation at promoters and preferentially open chromatin regions facilitates transcription, hypermethylation generally associates with lower accessibility. Inspecting our data for such conditions, we found two genes, *BAX* and *SERPINE2*, to have increased expression, open chromatin and hypomethylated promoters. *TRAF3, TRAF6, TP53BP2, STAT5A, RIPK2, NFKBIA, BCL2, ATM, TNFAIP3, NFKBIZ, CD83, and CD40* showed promoter hypomethylation and open chromatin, although transcription was reduced. In contrast, *CDKN1A* had promoter hypermethylation, closed chromatin and reduced expression, while *TNIP1* had promoter hypermethylation, open chromatin and reduced expression. *TRAF1, RELB, TNFAIP2, NFKBIE* and *REL,* had a reduced transcription, with hypomethylated promoters but closed chromatin. Interestingly, *NFKB1* itself had a preferentially open chromatin and a hypomethylated promoter region, although its transcripts were underrepresented. This observation indicates that the mutant transcripts might undergo accelerated decay, as previously suggested by Fliegauf et al.,[1] which, in addition to protein loss due to devastating defects, contribute to the p105/p50 haploinsufficient condition in patient-derived cells.

To integrate methylation and transcriptome data of unstimulated cells, we analyzed downstream genes of the NF-κB signaling pathway in all four B-cell subtypes (Figures 8c and d). We identified hypomethylation and lower expression levels of members of the IRF (*IRF1*) and AP-1 (JUNB, *JUND, FOS*, *and FOSB*) families of transcription factors in the naïve-, IgM memory-, and switched memory B cell compartments. Among the IRFs, IRF1 can associate with members of the NF-κB/Rel family, generating complexes that synergistically activate transcription[105]. It has been suggested that NF-κB and Fos/Jun have synergistic mechanisms of gene regulation[106]. *IRF2* was hypomethylated and showed increased expression in naïve B cells and switched memory B cells. IRF2 is an antagonistic transcriptional repressor of IRF1, and interferes with NF-κB activation[107]. Among the genes encoding negative regulators of NF-κB, we found hypomethylation and lower transcript levels for *NFKBIA, NFKBIE, NFKBID* and *TNFAIP3* in naïve B cells, for *NFKBIA* and *NFKBIE* in IgM memory B cells, and for *NFKBIA* and *TNFAIP3* in switched memory B cells. Other members of the NF-κB family (*REL*, *RELA* and *RELB*) were hypomethylated and their transcripts were reduced, which was observed for *NFKB1* in unstimulated naïve B cells and switched memory B cells. Moreover, *BCL3* was hypomethylated and lower expressed in naïve- and switched memory- B cells, respectively. *BCL3*, a nuclear member of the I-κB family, can enhance transcription of NF-κB target genes by binding to p50 homodimers[108].

In addition, *CD83,* an activation marker of B cells in the light zone of the GC reaction[109,110], was hypomethylated and had reduced expression in IgM memory B cells and switched memory B cells. *XBP1,* a transcription factor that enables high immunoglobulin expression and changes associated with terminal B cell differentiation into plasma cells, was hypomethylated and its transcripts were reduced in IgM memory- and switched memory B cells. In the CD21-low compartment we found increased expression and hypomethylation of *CITED4* (CBP/p300-interacting transactivator 4). NF-κB engages CBP/p300 and its histone acetyltransferase activity for transcriptional activation of the IL6 promoter[111]. Moreover, we identified transcripts of genes coding for regulators of the epigenetic machinery, such as methyltransferase *METTL23*, lysine demethylase *KDM5D*, and *PRDM11,* which enables chromatin binding, to be underrepresented in the CD21-low B cell compartment. Additionally, transcripts of *TAF1A* (TATA box binding protein associated factor), genes with a role in ubiquitylation (*DTX3, DTX3L, SUMO2, USP9Y*), and immunoglobulin genes (*IGKV3-15, IGKV3-20, IGKV1-12, IGHV3-33, IGLV2-11*) also showed decreased levels in CD21-low B cells. In-depth analysis of different comparisons can be found in the Supplementary Material Figures S14-17.

Our results demonstrate a compromised B cell function on *NFKB1*-mutated cells in different omics dimensions. First, we found a reduced expression of negative NF-κB pathway regulators. Second, we showed that regions encoding crucial factors for B cell proliferation and differentiation had changes in chromatin accessibility. In addition, our results indicate that *NFKB1*-mutated B cells have aberrant DNA

bioRxiv preprint doi: https://doi.org/10.1101/2022.11.22.517350; this version posted November 23, 2022. The copyright holder for this preprint (which was not certified by peer review) is the author/funder, who has granted bioRxiv a license to display the preprint in perpetuity. It is made available under aCC-BY-NC-ND 4.0 International license.

methylation patterns. We also detected changes in protein expression levels linked to B cell differentiation and maturation. Overall, our findings provide evidence for overlapping layers of dysregulation, which collectively dictate aberrant gene activation profiles and changes in the NF-κB network. Following these results, it is likely that direct perturbations within the NF-κB signaling pathway, added to a blurred cross-talk with other families of transcription factors, and changes in epigenetic regulation, explain the aberrant B cell differentiation, hypogammaglobulinemia, and autoimmunity, all observed in our patients. Moreover, the imbalance of the negative feedback loop embedded in the NF-κB system may perpetuate inflammation and autoimmunity.

Discussion

Pathogenic mutations in *NFKB1* have been associated with various phenotypes ranging from antibody deficiency to immune dysregulation[4,5,7,24]. Given that the NF-κB signaling network plays a central role in many cellular processes, impaired immune functions might originate not only from deleterious expression of the transcription factor, but also from delayed, accelerated or prolonged downstream effects. In this study, we present a multi-omics characterization of *NFKB1* (p105/p50) insufficiency in B cells, involving WES, RNA-sequencing, ATAC-sequencing, methylation, and proteomics. It demonstrates a direct relationship between affected patients and aberrant chromatin accessibility, epigenetic, and transcriptional alterations in NF-κB target genes, including members of the network of negative feedback loop that ensure the termination of the NF-κB response.

Based on WES data, we identified *NFKB1* mutation carriers harboring other variants with low allele frequency in NF-κB target genes and genes causing inborn errors of immunity. Due to the complexity of the NF-κB signaling pathway, we underscore the possibility that these variants additionally modify NF-κB signaling at various stages; hence, they might act synergistically or antagonistically, and therefore influence disease presentation and severity. This could potentially contribute to the very variable disease penetrance and expressivity observed in patients with *NFKB1* insufficiency. That this concept is a viable hypothesis has been demonstrated in selected publications such as in Sic et al.[112].

We showed that *NFKB1*-insufficient B cells display widespread transcriptome changes that are present in stimulated and non-stimulated naïve B cells, IgM memory B cells, switched memory B cells, and to a lower extent in CD21low B cells. The activation of NF-κB is tightly regulated and requires a cascade of post-translational modifications through phosphorylation and ubiquitination events that culminate in the activation of the signalling pathway[104]. Interestingly, the ubiquitination regulators TRAF2, TRAF6, cIAP1/2, and TAB proteins had reduced expression levels in mutation carriers. Moreover, both TNF-α and IL-1 proinflammatory responses are mediated by NF-κB signaling[18]. We found a repression of genes related to TNF-α signaling in *NFKB1* mutation carriers, however, we cannot say whether this is directly caused by the mutation in *NFKB1* or whether this is a regulatory effect by the B cells in order to limit NF-κB-mediated hyperinflammation.

The NF-κB signalling pathway contains homeostatic feedback mechanisms that limit and restore its inducible activation[55]. In mutation carriers, we found transcripts of genes encoding for negative regulators to be underrepresented[18]: *TNFAIP3* codes for the deubiquitinase A20 which removes polyubiquitin chains from TNF receptor-associated factor 6 (*TRAF6*); and *TRAF1* which interferes with the linear ubiquitination of NEMO. Also, *TNIP1,* which encodes a component of the A20-ubiquitin editing complex, and *CYLD* which deubiquitinates *TAK1* were found to be downregulated. *CYLD* is a regulatory enzyme with deubiquitylating activity. *CYLD* it is not a direct NF-κB target gene, but controls de deubiquitinylation of NF-κB target genes, including *TRAF2, TRAF6, TAK1, BCL3, IKKY, RIP1, RIGI,* and *TBK1*. Mutations in *CYLD* can be found in patients with familial cylindromatosis, hair-follicle keratinocytes, and nasopharyngeal tumors, suggesting its role as a tumor suppressor[113,114]. In keratinocytes, Massoumi et al.[115] demonstrated that CYLD inhibits cell proliferation and tumor growth through the block of BCL3-NF-κB dependent signaling. Non-Hodgkin B cell lymphoma and solid organ cancer have been reported in around 16% of *NFKB1* insufficient patients[7]. A reduced expression of *CYLD* could be a clue for the pathogenic mechanisms of malignancy in these individuals, but requires further investigation.

Aberrant inactivation of NF-κB activity is a common factor of autoimmunity, autoinflammation and cancer[116–118]. Germline frameshift mutations in *TNFAIP3*, resulting in A20 haploinsufficiency have also been identified in patients with an autoimmune lymphoproliferative syndrome-like phenotype (ALPS) and T cells from these patients exhibit increased NF-κB activation[119]. Germline loss-of-function in *TNFAIP3*

bioRxiv preprint doi: https://doi.org/10.1101/2022.11.22.517350; this version posted November 23, 2022. The copyright holder for this preprint (which was not certified by peer review) is the author/funder, who has granted bioRxiv a license to display the preprint in perpetuity. It is made available under aCC-BY-NC-ND 4.0 International license.

leading to A20 haploinsufficiency was shown to cause Behcet-like autoimmunity[120], a phenotype which has also been reported in *NFKB1*-mutated individuals. Actually, all affected mutation carriers from our cohort presented with autoimmunity and autoinflammation. Dysregulation of NF-κB downstream inhibition might prevent appropriate attenuation of proinflammatory signaling and could lead to increased inflammation in *NFKB1* haploinsufficiency. This observation is important for the development of potential new drug targets. The ubiquitin-proteasome system plays an important role in the activation of NF-κB. The use of proteasome inhibitors like Bortezomib was shown to be effective in autoimmune disorders such as systemic lupus and myasthenia gravis[121]. Nevertheless, positive feedback mechanisms within the signaling pathway might also contribute to human disease. As TNF-α and IL1 initiate the canonical pathway and also are an NF-κB target genes, it might create a positive feedback loop until signals perpetuating this cascade are eliminated. Thus, targeting TNF-α or IL1 signaling also constitutes a promising therapeutic approach especially in patients presenting with an inflammatory phenotype (anti-IL1) and gastrointestinal involvement (anti-TNF-α) [122].

Another group of anti-inflammatory proteins are the suppressors of cytokine signaling (SOCS), which interfere with proinflammatory signaling pathways, such as the JAK-STAT and NF-κB signaling network [123]. *SOCS1* codifies for a protein that functions as a ubiquitin ligase, leading to polyubiquitination and proteasomal degradation of p65 in the nucleus[124,125]. When we compared affected to unaffected *NFKB1* mutation carriers, we found *SOCS1* to be lower expressed in affected patients. This could add to the disease status of our patients, as less *SOCS1* means more p65 and hence more proinflammatory gene transcription. Especially in concert with the observed increased presence of interferons described above, seen in the proteome of our *NFKB1*-mutated individuals, inhibition of the JAK-STAT signaling pathway may also be beneficial for these patients.

The production of granzyme B in NF-κB1-deficient B cells seems also noteworthy to us: granzyme B is being produced by activated B cells[50] e.g. when detecting viral antigens[52]. Hence, its production in our patient's B cells may either point towards undiagnosed chronic viral infection(s) (in this case it would be secondary to the genetic defect), or the *NFKB1*-mutation itself leads to an activated state of B cells (the mutation would be the primary cause for granzyme B expression). This observation also raises the hypothesis that in CVID patients without underlying genetic defect, possibly chronic viral infections may be the underlying culprit?

The expression of *SERPINE2* in CD21-low B cells could indicate that these cells may be the consequence of an insufficient germinal center reaction not only in NF-κB1-insufficient patients, but possibly also in other patients with increased levels of CD21-low B cells, such as in patients with systemic lupus or HIV infection [126,127]. *SERPINE2* is known to be expressed in cells undergoing homologous recombination DNA repair [128]. The hypothesis is that during a defective or incomplete GC reaction, in which double strand breaks occur at the human IgG locus on chromosome 14 for class switch recombination, DNA repair seems to be insufficient, giving rise to a constant pool of *SERPINE2*-expressing CD21-low B cells.

At the chromatin level, we detected an enrichment of binding motifs of transcription factors associated with B-cell function in stimulated naïve B cells. For example, CTCF is required to sustain the germinal center transcriptional program to avoid premature plasma cell differentiation[129]. Moreover, BATF and Fra1, a member of the AP-1 family of transcription factors, were enriched. Fra1 is involved in the regulation of follicular B-cell differentiation into plasma cells[130]. BATF controls activation-induced cytidine deaminase (AID) and germline transcripts of the intervening heavy-chain region and constant heavy-chain region[131]. These findings are in agreement with a recent report on CVID and epigenetic dysregulation in B cells[72]. Epigenetic alterations affecting genes and regulatory elements in memory B cells impair plasma cell differentiation[87,132] While we did not find DNA methylation changes in naïve B cells, we found demethylation defects occurring from the transition from naïve, to IgM memory-, and to switch memory- B cells. These data are consistent with the observed hypermethylation in gene regions at immunoglobulin loci in IgM memory, switched memory- and CD21low- B cells in our datasets. This is an important observation, because DNA methylation changes are required for somatic hypermutation and class switch recombination[84,133].

bioRxiv preprint doi: https://doi.org/10.1101/2022.11.22.517350; this version posted November 23, 2022. The copyright holder for this preprint (which was not certified by peer review) is the author/funder, who has granted bioRxiv a license to display the preprint in perpetuity. It is made available under aCC-BY-NC-ND 4.0 International license.

Our omics approach confirmed that chromatin accessibility is a key regulatory mechanism to facilitate transcription factor binding[103]. NF-κB is able to influence the chromatin state through a variety of mechanisms, including the recruitment of components of the general transcription machinery. Frequently, the selective interaction with these co-activators is dependent on specific post-translational modification of NF-κB subunits[134]. We observed that methylation defects may compromise the functionality of the transcriptional machinery, and that aberrant regulation at different layers might be the cause of hypogammaglobulinemia and autoimmunity in these patients. More detailed proteomic data may provide deeper insights into the downstream signaling consequences of *NFKB1* insufficiency. As shown in previous reports[135,136] the correlation between RNA and protein analysis was low also in our study. NF-κB controls numerous signaling cascades in the immune system. Therefore, it is conceivable that haploinsufficiency mutations affecting also the function of negative regulators of the NF-κB pathway, are leading to autoimmune or inflammatory conditions.

One limitation of this study is that we did not perform experiments in cell lines or in a murine system, and these experiments need to be conducted to move from the descriptive state of associations, as presented here, to the causality and proven NF-κB network dependencies and interactions. Moreover, during the course of this project we learned that single cell analysis, although more expensive, would most likely have been superior to our approach of bulk sequencing of sorted B lymphocyte subsets.

Here, we described the implications of pathogenic *NFKB1*-mutations on B cells on different levels. Our study highlights the additional insights that can be gained by integrating omics data sources. Our analysis provides evidence of hyperinflammation in *NFKB1*-mutated cells caused by the reduced expression of negative regulators. This may open new pathways for the development of personalized targeted therapy. We consider that the observations described here, and the data underlying them, will be a key resource for future in-depth studies of the immune dysregulation associated with defects of the NF-κB signaling network.

Supplemental information

Acknowledgements
We thank all affected individuals, their family members and healthy volunteers who participated in this study. We thank Pavla Mrovecova, Katrin Hübscher, Anastasja Maks, and Hanna Haberstroh for excellent technical assistance. We acknowledge the Lighthouse Core Facility for their excellent assistance with cell sorting and flow cytometry. Some samples have been taken from the CCI-biobank, a partner of the Freeze Biobank Freiburg. We thank the Biomedical Sequencing Facility at CeMM for assistance with next-generation Sequencing .The authors acknowledge the support of the Freiburg Galaxy Team: Beatriz Serrano-Solano and Björn Grüning, Bioinformatics, University of Freiburg (Germany) funded by the Collaborative Research Centre 992 Medical Epigenetics (DFG grant SFB 992/1 2012) and the German Federal Ministry of Education and Research BMBF grant 031 A538A de.NBI-RBC.We are grateful to Pascal Schneider for providing CD40L.

Funding
B.G. receives support by the Deutsche Forschungsgemeinschaft (DFG) SFB1160/2_B5, under Germany's Excellence Strategy (CIBSS – EXC-2189 – Project ID 390939984, and RESIST – EXC 2155 – Project ID 390874280); by the E-rare program of the EU, managed by the DFG, grant code GR1617/14-1/iPAD; and by the German Federal Ministry of Education and Research (BMBF) through a grant to the German Auto-Immunity Network (GAIN), grant code 01GM1910A. This work was supported in part by the Center for Chronic Immunodeficiency (CCI), Freiburg Center for Rare Diseases (FZSE), and by the Deutsche Forschungsgemeinschaft (DFG, German Research Foundation) – 450392965**.** M.P. is funded by the Deutsche Forschungsgemeinschaft (DFG, German Research Foundation) under Germany's Excellence Strategy - EXC 2155 - project number 390874280. E.B. is funded by Carlos III Health Institute (ISCII), Ref. AC18/00057, associated with i-PAD project (E-RARE). The article processing charge was funded by the Baden-Wuerttemberg Ministry of Science, Research and Art and the University of Freiburg in the funding programme Open Access Publishing. KW has received grants by the German Federal Ministry of Education and Research (BMBF) through a grant to the German Auto-Immunity Network (GAIN), grant code 01GM1910A and by the DFG TRR130. M.F was funded partly by an NF-κB research grant from a collaborative research grant between Merck KGaA and UKL-FR (grant number ZVK2018073002) in the years 2019 to 2020.

bioRxiv preprint doi: https://doi.org/10.1101/2022.11.22.517350; this version posted November 23, 2022. The copyright holder for this preprint (which was not certified by peer review) is the author/funder, who has granted bioRxiv a license to display the preprint in perpetuity. It is made available under aCC-BY-NC-ND 4.0 International license.

Online resources

Ensembl Genome browser: https://www.ensembl.org/
Boston University Biology: https://www.bu.edu/nf-kb/gene-resources/target-genes/
UCSC Genome browser: https://genome.ucsc.edu/
Galaxy Europe: https://usegalaxy.eu/
GnomAD browser: https://gnomad.broadinstitute.org/downloads
R studio: https://www.rstudio.com/

Data availability

The exome data sets presented in this article are not publicly available because uploading the data is not part of the participants consent according to Art. 7 GDPR. All other omics data sets (RNA-seq, ATAC-seq, RRBS, and proteomics) have been deposited on SRA database (RRBS, RNA-, ATAC-seq) and ProteomeXchange Consortium via the PRIDE[137] partner repository.

Ethics statement

The ethics committee Freiburg approved this project with an effective date of 06.06.2019. In July 2019 the consent form under which patient samples had been collected, was approved under ETK-Nr_354/19. The i-PAD ethics vote carries the number EK-Freiburg_76/19 and the NFKB Study protocol has the approval No. 295/13_200149 and 93/18_191111. Written informed consent to participate in this study was provided by the participants themselves.

Author contributions

NC-O processed and collected samples, performed methylation, RNA-seq and association analysis, collected clinical data, wrote case reports, designed layout, figures and tables, and wrote the manuscript. NR processed and collected samples, analyzed ATAC and proteome data, designed ATAC data figures and wrote the manuscript. SP-C designed RNA-seq script, summarized data, processed and collected samples, wrote the manuscript. AC-O analyzed and interpreted WES data. MF performed functional testing of the variants and revised the work critically for intellectual content. FZ organized and coordinated ATAC and RRBS sample preparation, and performed preliminary quality control. MG processed ATAC sequence in patient samples. VG processed ATAC and RRBS sequencing on samples. MP measured proteome samples and revised analysis. KW cared for patients, provided clinical and immunological information. MP analyzed and interpreted WES, designed sorting strategy, revised the work critically for intellectual content. EB performed conception and designing of the study, revised the work critically for intellectual content. CB performed conception and designing of the study, revised the work critically for intellectual content. GR performed conception and designing of the study, processed proteome sequencing n samples. BG performed conception and designing of the study, provided and cared for study patients and revised the work critically for intellectual content. All authors contributed to manuscript revision, read, and approved the submitted version.

Declaration of interests

B.G. is employed by the University Hospital Freiburg, Germany. During the course of this study, he received funding for research from following third parties: Deutsche Forschungsgemeinschaft (DFG); the E-rare program of the EU, managed by the DFG; the „Netzwerk Seltener Erkrankungen“of the German Ministry of Education and Research (BMBF); Merck KGaA; Takeda Pharma Vertrieb GmbH & Co. KG; Bristol-Myers Squibb GmbH & Co. KGaA; Novartis Pharma AG, and CSL Behring GmbH. This work was supported in part by the Center for Chronic Immunodeficiency (CCI), Freiburg Center for Rare Diseases (FZSE). During the last 3 years B.G. was an advisor to following companies receiving fees less than 1,000€: Bristol-Myers Squibb Company, Adivo Associates Germany, Pharming Group NV, Epimune GmbH, GigaGen Inc., Atheneum Partners GmbH, and less than 5,000€: UCB Pharma S.A., Roche Pharma AG.

References

1. Fliegauf M, L. Bryant V, Frede N, Slade C, Woon S-T, Lehnert K, et al. Haploinsufficiency of the NF-κB1 Subunit p50 in Common Variable Immunodeficiency. Am J Hum Genet. 2015;97:389–403.
2. Boztug H, Hirschmugl T, Holter W, Lakatos K, Kager L, Trapin D, et al. NF-κB1 Haploinsufficiency Causing Immunodeficiency and EBV-Driven Lymphoproliferation. J Clin Immunol. 2016;36:533–40.

bioRxiv preprint doi: https://doi.org/10.1101/2022.11.22.517350; this version posted November 23, 2022. The copyright holder for this preprint (which was not certified by peer review) is the author/funder, who has granted bioRxiv a license to display the preprint in perpetuity. It is made available under aCC-BY-NC-ND 4.0 International license.

3. Schipp C, Nabhani S, Bienemann K, Simanovsky N, Kfir-Erenfeld S, Assayag-Asherie N, et al. Specific antibody deficiency and autoinflammatory disease extend the clinical and immunological spectrum of heterozygous NFKB1 loss-of-function mutations in humans. Haematologica. 2016;101:e392–6.
4. Kaustio M, Haapaniemi E, Göös H, Hautala T, Park G, Syrjänen J, et al. Damaging heterozygous mutations in NFKB1 lead to diverse immunologic phenotypes. J Allergy Clin Immunol. 2017;140:782–96.
5. Tuijnenburg P, Lango Allen H, Burns SO, Greene D, Jansen MH, Staples E, et al. Loss-of-function nuclear factor κB subunit 1 (NFKB1) variants are the most common monogenic cause of common variable immunodeficiency in Europeans. J Allergy Clin Immunol. 2018;142:1285–96.
6. Abolhassani H, Hammarström L, Cunningham-Rundles C. Current genetic landscape in common variable immune deficiency. Blood. 2020;135:656–67.
7. Lorenzini T, Fliegauf M, Klammer N, Frede N, Proietti M, Bulashevska A, et al. Characterization of the clinical and immunologic phenotype and management of 157 individuals with 56 distinct heterozygous NFKB1 mutations. J Allergy Clin Immunol. 2020;146:901–11.
8. Rojas-Restrepo J, Caballero-Oteyza A, Huebscher K, Haberstroh H, Fliegauf M, Keller B, et al. Establishing the Molecular Diagnoses in a Cohort of 291 Patients With Predominantly Antibody Deficiency by Targeted Next-Generation Sequencing: Experience From a Monocentric Study. Front Immunol. 2021;12.
9. Hayden MS, Ghosh S. NF-κB in immunobiology. Cell Res. 2011;21:223–44.
10. Ghosh S, Hayden MS. New regulators of NF-κB in inflammation. Nat Rev Immunol. 2008;8:837–48.
11. Oeckinghaus A, Ghosh S. The NF-κB Family of Transcription Factors and. Cold Spring Harb Perspect Biol. 2009;1–15.
12. Hoffmann A, Baltimore D. Circuitry of nuclear factor κB signaling. Immunol Rev. 2006;210:171–86.
13. O'Dea E, Hoffmann A. The regulatory logic of the NF-kappaB signaling system. Cold Spring Harb Perspect Biol. 2010;2:1–13.
14. Schröder C, Sogkas G, Fliegauf M, Dörk T, Liu D, Hanitsch LG, et al. Late-Onset Antibody Deficiency Due to Monoallelic Alterations in NFKB1. Front Immunol. 2019;10:1–12.
15. Keller B, Cseresnyes Z, Stumpf I, Wehr C, Fliegauf M, Bulashevska A, et al. Disturbed canonical nuclear factor of κ light chain signaling in B cells of patients with common variable immunodeficiency. J Allergy Clin Immunol. 2017;139:220-231.e8.
16. Dieli-Crimi R, Martínez-Gallo M, Franco-Jarava C, Antolin M, Blasco L, Paramonov I, et al. Th1-skewed profile and excessive production of proinflammatory cytokines in a NFKB1-deficient patient with CVID and severe gastrointestinal manifestations. Clin Immunol. 2018;195:49–58.
17. Keller B, Strohmeier V, Harder I, Unger S, Payne KJ, Andrieux G, et al. The expansion of human T-bet high CD21 low B cells is T cell dependent. Sci Immunol. 2021;6:eabh0891.
18. Barnabei L, Laplantine E, Mbongo W, Rieux-Laucat F, Weil R. NF-κB: At the Borders of Autoimmunity and Inflammation. Front Immunol. 2021;12:1–27.
19. Comrie WA, Faruqi AJ, Price S, Zhang Y, Rao VK, Su HC, et al. RELA haploinsufficiency in CD4 lymphoproliferative disease with autoimmune cytopenias. J Allergy Clin Immunol. 2018;141:1507-1510.e8.
20. Badran YR, Dedeoglu F, Leyva Castillo JM, Bainter W, Ohsumi TK, Bousvaros A, et al. Human RELA haploinsufficiency results in autosomal-dominant chronic mucocutaneous ulceration. J Exp Med. 2017;214:1937–47.
21. Low JT, Hughes P, Lin A, Siebenlist U, Jain R, Yaprianto K, et al. Impact of loss of NF-κB1, NF-κB2 or c-REL on SLE-like autoimmune disease and lymphadenopathy in Faslpr/lpr mutant mice. Immunol Cell Biol. 2016;94:66–78.
22. Etzioni A, Ciechanover A, Pikarsky E. Immune defects caused by mutations in the ubiquitin system. J Allergy Clin Immunol. 2017;139:743–53.
23. O'Reilly LA, Putoczki TL, Mielke LA, Low JT, Lin A, Preaudet A, et al. Loss of NF-κB1 Causes Gastric Cancer with Aberrant Inflammation and Expression of Immune Checkpoint Regulators in a STAT-1-Dependent Manner. Immunity. 2018;48:570-583.e8.
24. Fliegauf M, Grimbacher B. Nuclear factor κB mutations in human subjects: The devil is in the details. J Allergy Clin Immunol. 2018;142:1062–5.
25. Franxman TJ, Howe LE, Baker JR. Infliximab for Treatment of Granulomatous Disease in Patients with Common Variable Immunodeficiency. J Clin Immunol. 2014;34:820–7.
26. Toh J, Gavrilova T, Rubinstein A. Three Cases of Elevated IL-1beta in Common Variable Immunodeficiency (CVID) with Autoimmune Complications. J Allergy Clin Immunol.

bioRxiv preprint doi: https://doi.org/10.1101/2022.11.22.517350; this version posted November 23, 2022. The copyright holder for this preprint (which was not certified by peer review) is the author/funder, who has granted bioRxiv a license to display the preprint in perpetuity. It is made available under aCC-BY-NC-ND 4.0 International license.

2016;137:AB19.
27. Lawrence T. The nuclear factor NF-kappaB pathway in inflammation. Cold Spring Harb Perspect Biol. 2009;1:1–11.
28. Tak PP, Firestein GS. NF-κB a key role in inflammatory diseases. J Clin Invest. 2001;107:7–11.
29. Renner F, Schmitz ML. Autoregulatory feedback loops terminating the NF-κB response. Trends Biochem Sci. 2009;34:128–35.
30. Barturen G, Babaei S, Català-Moll F, Martínez-Bueno M, Makowska Z, Martorell-Marugán J, et al. Integrative Analysis Reveals a Molecular Stratification of Systemic Autoimmune Diseases. Arthritis Rheumatol. 2021;73:1073–85.
31. Teruel M, Barturen G, Martínez-Bueno M, Castellini-Pérez O, Barroso-Gil M, Povedano E, et al. Integrative epigenomics in Sjögren´s syndrome reveals novel pathways and a strong interaction between the HLA, autoantibodies and the interferon signature. Sci Rep. 2021;11:1–18.
32. Delhalle S, Bode SFN, Balling R, Ollert M, He FQ. A roadmap towards personalized immunology. npj Syst Biol Appl. 2018;4.
33. Klughammer J, Kiesel B, Roetzer T, Fortelny N, Nemc A, Nenning KH, Furtner J, Sheffield NC, Datlinger P, Peter N, Nowosielski M, Augustin M, Mischkulnig M, Ströbel T, Alpar D, Ergüner B, Senekowitsch M, Moser P, Freyschlag CF, Kerschbaumer J, Thomé C, Gra BC. The DNA methylation landscape of glioblastoma disease progression shows extensive heterogeneity in time and space. Nat Med. 2018;24:1611–24.
34. Sheffield NC, Pierron G, Klughammer J, Datlinger P, Schönegger A, Schuster M, Hadler J, Surdez D, Guillemot D, Lapouble E, Freneaux P, Champigneulle J, Bouvier R, Walder D, Ambros IM, Hutter C, Sorz E, Amaral AT, de Álava E, Schallmoser K, Strunk D, Rinne TE. DNA methylation heterogeneity defines a disease spectrum in Ewing sarcoma. Nat Med. 2017;23:386–95.
35. Koelsche C, Schrimpf D, Stichel D, Sill M, Sahm F, Reuss DE, et al. Sarcoma classification by DNA methylation profiling. Nat Commun. 2021;12.
36. Lafta MH, Gangadhar L. RNBeads 2.0: Comprehensive analysis of DNA methylation data. Ann Trop Med Public Heal. 2019;19:2003–19.
37. Afgan E, Baker D, van den Beek M, Blankenberg D, Bouvier D, Čech M, et al. The Galaxy platform for accessible, reproducible and collaborative biomedical analyses: 2016 update. Nucleic Acids Res. 2016;44:W3–10.
38. Corces MR, Buenrostro JD, Wu B, Greenside PG, Chan SM, Koenig JL, et al. Lineage-specific and single-cell chromatin accessibility charts human hematopoiesis and leukemia evolution. Nat Genet. 2016;48:1193–203.
39. Ramirez N, Posadas-cantera S, Langer N, Caballero A, Oteyza G De, Proietti M, et al. Multi-omics analysis of naïve B cells of patients harboring the C104R mutation in TACI. 2022;1–18.
40. Langmead B, Trapnell C, Pop M, Salzberg SL. Ultrafast and memory-efficient alignment of short DNA sequences to the human genome. Genome Biol. 2009;10.
41. Tarasov A, Vilella AJ, Cuppen E, Nijman IJ, Prins P. Sambamba: Fast processing of NGS alignment formats. Bioinformatics. 2015;31:2032–4.
42. Rendeiro AF, Schmidl C, Strefford JC, Walewska R, Davis Z, Farlik M, et al. Chromatin accessibility maps of chronic lymphocytic leukaemia identify subtype-specific epigenome signatures and transcription regulatory networks. Nat Commun. 2016;7.
43. Heinz S, Benner C, Spann N, Bertolino E, Lin YC, Laslo P, et al. Simple Combinations of Lineage-Determining Transcription Factors Prime cis-Regulatory Elements Required for Macrophage and B Cell Identities. Mol Cell. 2010;38:576–89.
44. Cox J, Mann M. MaxQuant enables high peptide identification rates, individualized p.p.b.-range mass accuracies and proteome-wide protein quantification. Nat Biotechnol. 2008;26:1367–72.
45. Cox J, Neuhauser N, Michalski A, Scheltema RA, Olsen J V., Mann M. Andromeda: A peptide search engine integrated into the MaxQuant environment. J Proteome Res. 2011;10:1794–805.
46. Cox J, Hein MY, Luber CA, Paron I, Nagaraj N, Mann M. Accurate proteome-wide label-free quantification by delayed normalization and maximal peptide ratio extraction, termed MaxLFQ. Mol Cell Proteomics. 2014;13:2513–26.
47. Weiterer S, Meier-Soelch J, Georgomanolis T, Mizi A, Beyerlein A, Weiser H, et al. Distinct IL-1α-responsive enhancers promote acute and coordinated changes in chromatin topology in a hierarchical manner. EMBO J. 2020;39:1–22.
48. Jurida L, Soelch J, Bartkuhn M, Handschick K, Müller H, Newel D, et al. The Activation of IL-1-induced enhancers depends on TAK1 kinase activity and NF-κB p65. Cell Rep. 2015;10:726–39.
49. Luo W, Weisel F, Shlomchik MJ. B Cell Receptor and CD40 Signaling Are Rewired for

bioRxiv preprint doi: https://doi.org/10.1101/2022.11.22.517350; this version posted November 23, 2022. The copyright holder for this preprint (which was not certified by peer review) is the author/funder, who has granted bioRxiv a license to display the preprint in perpetuity. It is made available under aCC-BY-NC-ND 4.0 International license.

Synergistic Induction of the c-Myc Transcription Factor in Germinal Center B Cells. Immunity. 2018;48:313-326.e5.
50. Hagn M, Jahrsdörfer B. Why do human B cells secrete granzyme B? Insights into a novel B-cell differentiation pathway. Oncoimmunology. 2012;1:1368–75.
51. Chesneau M, Mai H Le, Danger R, Le Bot S, Nguyen T-V-H, Bernard J, et al. Efficient Expansion of Human Granzyme B–Expressing B Cells with Potent Regulatory Properties. J Immunol. 2020;205:2391–401.
52. Hagn M, Schwesinger E, Ebel V, Sontheimer K, Maier J, Beyer T, et al. Human B Cells Secrete Granzyme B When Recognizing Viral Antigens in the Context of the Acute Phase Cytokine IL-21. J Immunol. 2009;183:1838–45.
53. Xu H, You M, Shi H, Hou Y. Ubiquitin-mediated NFκB degradation pathway. Cell Mol Immunol. 2015;12:653–5.
54. Collins PE, Mitxitorena I, Carmody RJ. The ubiquitination of NF-κB subunits in the control of transcription. Cells. 2016;5.
55. Prescott JA, Mitchell JP, Cook SJ. Inhibitory feedback control of NF-kB signalling in health and disease. Biochem J. 2021;478:2619–64.
56. Lau D, Lan LYL, Andrews SF, Henry C, Rojas KT, Neu KE, et al. Low CD21 expression defines a population of recent germinal center graduates primed for plasma cell differentiation. Sci Immunol. 2017;2:1–14.
57. van Loo G, Bekaert R. Negative Regulation of NF-kB and its involvement in RA. Arthritis Res Ther. 2011;13:1–11.
58. Kim S, Yu NK, Kaang BK. CTCF as a multifunctional protein in genome regulation and gene expression. Exp Mol Med. 2015;47:e166.
59. Whyte WA, Orlando DA, Hnisz D, Abraham BJ, Lin CY, Kagey MH, et al. Master transcription factors and mediator establish super-enhancers at key cell identity genes. Cell. 2013;153:307–19.
60. Pott S, Lieb JD. What are super-enhancers? Nat Genet. 2015;47:8–12.
61. Michida H, Imoto H, Shinohara H, Yumoto N, Seki M, Umeda M, et al. The Number of Transcription Factors at an Enhancer Determines Switch-like Gene Expression. Cell Rep. 2020;31:107724.
62. Brown JD, Lin CY, Duan Q, Griffin G, Federation AJ, Paranal RM, et al. NF-κB Directs Dynamic Super Enhancer Formation in Inflammation and Atherogenesis. Mol Cell. 2014;56:219–31.
63. Inoue F, Kircher M, Martin B, Cooper GM, Witten DM, McManus MT, et al. A systematic comparison reveals substantial differences in chromosomal versus episomal encoding of enhancer activity. Genome Res. 2017;27:38–52.
64. Shinohara H, Inoue K, Yumoto N, Nagashima T, Okada-Hatakeyama M. Stimulus-Dependent Inhibitor of Apoptosis Protein Expression Prolongs the Duration of B Cell Signalling. Sci Rep. 2016;6:1–12.
65. Zou Z, Tao T, Li H, Zhu X. MTOR signaling pathway and mTOR inhibitors in cancer: Progress and challenges. Cell Biosci. 2020;10:1–11.
66. O'Dea EL, Kearns JD, Hoffmann A. UV as an Amplifier Rather Than Inducer of NF-κB Activity. Mol Cell. 2008;30:632–41.
67. Oliver KM, Taylor CT, Cummins EP. Hypoxia. Regulation of NFκB signalling during inflammation: The role of hydroxylases. Arthritis Res Ther. 2009;11.
68. Zumaquero E, Stone SL, Scharer CD, Jenks SA, Nellore A, Mousseau B, et al. IFNγ induces epigenetic programming of human T-bethi B cells and promotes TLR7/8 and IL-21 induced differentiation. Elife. 2019;8:1–36.
69. Català-Moll F, Ferreté-Bonastre AG, Li T, Weichenhan D, Lutsik P, Ciudad L, et al. Activation-induced deaminase is critical for the establishment of DNA methylation patterns prior to the germinal center reaction. Nucleic Acids Res. 2021;49:5057–73.
70. Oakes CC, Seifert M, Assenov Y, Gu L, Przekopowitz M, Ruppert AS, et al. DNA methylation dynamics during B cell maturation underlie a continuum of disease phenotypes in chronic lymphocytic leukemia. Nat Genet. 2016;48:253–64.
71. Kulis M, Merkel A, Heath S, Queirós AC, Schuyler RP, Castellano G, et al. Whole-genome fingerprint of the DNA methylome during human B cell differentiation. Nat Genet. 2015;47:746–56.
72. Rodríguez-Ubreva J, Arutyunyan A, Bonder MJ, Pino-Molina L Del, Clark SJ, Calle-Fabregat C de la, et al. Single-Cell Atlas of Common Variable Immunodeficiency reveals germinal center-associated epigenetic dysregulation in B cell responses. Nat Commun. 2022;13:2021.12.20.473453.
73. Fleischer T, Tekpli X, Mathelier A, Wang S, Nebdal D, Dhakal HP, et al. DNA methylation at

bioRxiv preprint doi: https://doi.org/10.1101/2022.11.22.517350; this version posted November 23, 2022. The copyright holder for this preprint (which was not certified by peer review) is the author/funder, who has granted bioRxiv a license to display the preprint in perpetuity. It is made available under aCC-BY-NC-ND 4.0 International license.

enhancers identifies distinct breast cancer lineages. Nat Commun. 2017;8.
74. Lin X, Li L, Liu X, Tian J, Zheng W, Li J, et al. Genome-wide analysis of aberrant methylation of enhancer DNA in human osteoarthritis. BMC Med Genomics. 2020;13:1–10.
75. Ziller MJ, Gu H, Müller F, Donaghey J, Tsai LTY, Kohlbacher O, et al. Charting a dynamic DNA methylation landscape of the human genome. Nature. 2013;500:477–81.
76. Schlesinger F, Smith AD, Gingeras TR, Hannon GJ, Hodges E. De novo DNA demethylation and noncoding transcription define active intergenic regulatory elements. Genome Res. 2013;23:1601–14.
77. Domcke S, Bardet AF, Adrian Ginno P, Hartl D, Burger L, Schübeler D. Competition between DNA methylation and transcription factors determines binding of NRF1. Nature. 2015;528:575–9.
78. Hu S, Wan J, Su Y, Song Q, Zeng Y, Nguyen HN, et al. DNA methylation presents distinct binding sites for human transcription factors. Elife. 2013;2013:1–16.
79. Kribelbauer JF, Lu XJ, Rohs R, Mann RS, Bussemaker HJ. Toward a Mechanistic Understanding of DNA Methylation Readout by Transcription Factors. J Mol Biol. 2020;432:1801–15.
80. Medvedeva YA, Khamis AM, Kulakovskiy I V, Ba-Alawi W, Bhuyan MSI, Kawaji H, et al. Effects of cytosine methylation on transcription factor binding sites. BMC Genomics. 2014;15:119.
81. Maurano MT, Wang H, John S, Shafer A, Canfield T, Lee K, et al. Role of DNA Methylation in Modulating Transcription Factor Occupancy. Cell Rep. 2015;12:1184–95.
82. Jones PA. Functions of DNA methylation: islands, start sites, gene bodies and beyond. Nat Rev Genet. 2012;13:484–92.
83. Rodríguez-Cortez VC, del Pino-Molina L, Rodríguez-Ubreva J, Ciudad L, Gómez-Cabrero D, Company C, et al. Monozygotic twins discordant for common variable immunodeficiency reveal impaired DNA demethylation during naïve-to-memory B-cell transition. Nat Commun. 2015;6:7335.
84. Li G, Zan H, Xu Z, Casali P. Epigenetics of the antibody response. Trends Immunol. 2013;34:460–70.
85. Zelazowski P, Shen Y, Snapper CM. NF-κB/p50 and NF-κB/c-Rel differentially regulate the activity of the 3'αE-hsl,2 enhancer in normal murine B cells in an activation-dependent manner. Int Immunol. 2000;12:1167–72.
86. Laurencikiene J, Deveikaite V, Severinson E. HS1,2 Enhancer Regulation of Germline ε and γ2b Promoters in Murine B Lymphocytes: Evidence for Specific Promoter-Enhancer Interactions. J Immunol. 2001;167:3257–65.
87. Scharer CD, Barwick BG, Guo M, Bally APR, Boss JM. Plasma cell differentiation is controlled by multiple cell division-coupled epigenetic programs. Nat Commun. 2018;9.
88. Van Anken E, Pena F, Hafkemeijer N, Christis C, Romijn EP, Grauschopf U, et al. Efficient IgM assembly and secretion require the plasma cell induced endoplasmic reticulum protein pERp1. Proc Natl Acad Sci U S A. 2009;106:17019–24.
89. Shimizu Y, Meunier L, Hendershot LM. pERp1 is significantly up-regulated during plasma cell differentiation and contributes to the oxidative folding of immunoglobulin. Proc Natl Acad Sci U S A. 2009;106:17013–8.
90. Schwartz AM, Putlyaeva L V., Covich M, Klepikova A V., Akulich KA, Vorontsov IE, et al. Early B-cell factor 1 (EBF1) is critical for transcriptional control of SLAMF1 gene in human B cells. Biochim Biophys Acta - Gene Regul Mech. 2016;1859:1259–68.
91. Vitales-Noyola M, Ramos-Levi AM, Serrano-Somavilla A, Martinez-Herna Ndez R, Sampedro-Nuñez M, Di Pasquale C, et al. Expression and function of the costimulatory receptor SLAMF1 is altered in lymphocytes from patients with autoimmune thyroiditis. J Clin Endocrinol Metab. 2017;102:672–80.
92. Mikhalap S V., Shlapatska LM, Yurchenko O V., Yurchenko MY, Berdova GG, Nichols KE, et al. The adaptor protein SH2D1A regulates signaling through CD150 (SLAM) in B cells. Blood. 2004;104:4063–70.
93. Yurchenko MY, Kovalevska LM, Shlapatska LM, Berdova GG, Clark EA, Sidorenko SP. CD150 regulates JNK1/2 activation in normal and Hodgkin's lymphoma B cells. Immunol Cell Biol. 2010;88:565–74.
94. Oudinet C, Braikia FZ, Dauba A, Khamlichi AA. Recombination may occur in the absence of transcription in the immunoglobulin heavy chain recombination centre. Nucleic Acids Res. 2020;48:3553–66.
95. Rodríguez-Cortez VC, Del Pino-Molina L, Rodríguez-Ubreva J, Ciudad L, Gómez-Cabrero D, Company C, et al. Monozygotic twins discordant for common variable immunodeficiency reveal impaired DNA demethylation during naïve-to-memory B-cell transition. Nat Commun. 2015;6.
96. Braun D, Caramalho I, Demengeot J. IFn-α/β enhances BCR-dependent B cell responses. Int

bioRxiv preprint doi: https://doi.org/10.1101/2022.11.22.517350; this version posted November 23, 2022. The copyright holder for this preprint (which was not certified by peer review) is the author/funder, who has granted bioRxiv a license to display the preprint in perpetuity. It is made available under aCC-BY-NC-ND 4.0 International license.

Immunol. 2002;14:411–9.
97. Abed NS, Chace JH, Fleming AL, Cowdery JS. Interferon-γ regulation of B lymphocyte differentiation: Activation of B cells is a prerequisite for IFN-γ-mediated inhibition of B cell differentiation. Vol. 153, Cellular Immunology. 1994. p. 356–66.
98. Pires BRB, Mencalha AL, Ferreira GM, De Souza WF, Morgado-Díaz JA, Maia AM, et al. NF-kappaB is involved in the regulation of EMT genes in breast cancer cells. PLoS One. 2017;12:1–20.
99. Mussbacher M, Salzmann M, Brostjan C, Hoesel B, Schoergenhofer C, Datler H, et al. Cell type specific roles of nf-kb linking inflamation and thrombosis. Front Immunol. 2019;10:1–31.
100. Omori SA, Cato MH, Anzelon-Mills A, Puri KD, Shapiro-Shelef M, Calame K, et al. Regulation of Class-Switch Recombination and Plasma Cell Differentiation by Phosphatidylinositol 3-Kinase Signaling. Immunity. 2006;25:545–57.
101. Franks A, Airoldi E, Slavov N. Post-transcriptional regulation across human tissues. PLoS Comput Biol. 2017;13:1–20.
102. Weidemüller P, Kholmatov M, Petsalaki E, Zaugg JB. Transcription factors: Bridge between cell signaling and gene regulation. Proteomics. 2021;21:1–14.
103. Klemm SL, Shipony Z, Greenleaf WJ. Chromatin accessibility and the regulatory epigenome. Nat Rev Genet. 2019;20:207–20.
104. Huang B, Yang XD, Lamb A, Chen LF. Posttranslational modifications of NF-κB: Another layer of regulation for NF-κB signaling pathway. Cell Signal. 2010;22:1282–90.
105. Sgarbanti M, Remoli AL, Marsili G, Ridolfi B, Borsetti A, Perrotti E, et al. IRF-1 Is Required for Full NF-κB Transcriptional Activity at the Human Immunodeficiency Virus Type 1 Long Terminal Repeat Enhancer. J Virol. 2008;82:3632–41.
106. Stein B, Baldwin AS, Ballard DW, Greene WC, Angel P, Herrlich P. Cross-coupling of the NF-κB p65 and Fos/Jun transcription factors produces potentiated biological function. EMBO J. 1993;12:3879–91.
107. Chae M, Kim K, Park SM, Jang IS, Seo T, Kim DM, et al. IRF-2 regulates NF-κB activity by modulating the subcellular localization of NF-κB. Biochem Biophys Res Commun. 2008;370:519–24.
108. Nagel D, Vincendeau M, Eitelhuber AC, Krappmann D. Mechanisms and consequences of constitutive NF-κB activation in B-cell lymphoid malignancies. Oncogene. 2014;33:5655–65.
109. Li Z, Ju X, Silveira PA, Abadir E, Hsu WH, Hart DNJ, et al. CD83: Activation marker for antigen presenting cells and its therapeutic potential. Front Immunol. 2019;10:1–9.
110. Krzyzak L, Seitz C, Urbat A, Hutzler S, Ostalecki C, Gläsner J, et al. CD83 Modulates B Cell Activation and Germinal Center Responses. J Immunol. 2016;196:3581–94.
111. Berghe W Vanden, De Bosscher K, Boone E, Plaisance S, Haegeman G. The nuclear factor-κB engages CBP/p300 and histone acetyltransferase activity for transcriptional activation of the interleukin-6 gene promoter. J Biol Chem. 1999;274:32091–8.
112. Sic H, Speletas M, Cornacchione V, Seidl M, Beibel M, Linghu B, et al. An Activating Janus kinase-3 mutation is associated with cytotoxic T lymphocyte antigen-4-dependent Immune dysregulation syndrome. Front Immunol. 2017;8:1–14.
113. Verhoeft KR, Ngan HL, Lui VWY. The cylindromatosis (CYLD) gene and head and neck tumorigenesis. Cancers Head Neck. 2016;1.
114. Deng M, Dai W, Yu VZ, Tao L, Lung ML. Cylindromatosis lysine 63 deubiquitinase (CYLD) regulates NF-KB signaling pathway and modulates fibroblast and endothelial cells recruitment in nasopharyngeal carcinoma. Cancers (Basel). 2020;12:1–18.
115. Massoumi R, Chmielarska K, Hennecke K, Pfeifer A, Fässler R. Cyld Inhibits Tumor Cell Proliferation by Blocking Bcl-3-Dependent NF-κB Signaling. Cell. 2006;125:665–77.
116. Compagno M, Lim WK, Grunn A, Nandula S V., Brahmachary M, Shen Q, et al. Mutations of multiple genes cause deregulation of NF-B in diffuse large B-cell lymphoma. Nature. 2009;459:717–21.
117. Kato M, Sanada M, Kato I, Sato Y, Takita J, Takeuchi K, et al. Frequent inactivation of A20 in B-cell lymphomas. Nature. 2009;459:712–6.
118. Lisi S, Sisto M, Lofrumento DD, D'Amore M. Altered IκBα expression promotes NF-κB activation in monocytes from primary Sjo gren's syndrome patients. Pathology. 2012;44:557–61.
119. Takagi M, Ogata S, Ueno H, Yoshida K, Yeh T, Hoshino A, et al. Haploinsufficiency of TNFAIP3 (A20) by germline mutation is involved in autoimmune lymphoproliferative syndrome. J Allergy Clin Immunol. 2017;139:1914–22.
120. Zhou Q, Wang H, Schwartz DM, Stoffels M, Hwan Park Y, Zhang Y, et al. Loss-of-function mutations in TNFAIP3 leading to A20 haploinsufficiency cause an early-onset autoinflammatory disease. Nat Genet. 2015;48:67–73.

bioRxiv preprint doi: https://doi.org/10.1101/2022.11.22.517350; this version posted November 23, 2022. The copyright holder for this preprint (which was not certified by peer review) is the author/funder, who has granted bioRxiv a license to display the preprint in perpetuity. It is made available under aCC-BY-NC-ND 4.0 International license.

121. Schneider-Gold C , Reinacher-Schick A, Ellrichmann G GR. Bortezomib in severe MuSK-antibody positive myasthenia gravis: first clinical experience. Ther Adv Neurol Disord. 2017;10:339–41.
122. Betzler AC, Theodoraki MN, Schuler PJ, Döscher J, Laban S, Hoffmann TK, et al. NF-κB and its role in checkpoint control. Int J Mol Sci. 2020;21.
123. Starr R, Willson TA, Viney EM, Murray LJ, Rayner JR, Jenkins BJ, Gonda TJ, Alexander WS, Metcalf D, Nicola NA HD. A family of cytokine-inducible inhibitors of signalling. Nature. 1997;387:917–21.
124. Strebovsky J, Walker P, Lang R, Dalpke AH. Suppressor of cytokine signaling 1 (SOCS1) limits NFκB signaling by decreasing p65 stability within the cell nucleus . FASEB J. 2011;25:863–74.
125. Zhou X, Liu Z, Cheng X, Zheng Y, Zeng F, He Y. Socs1 and Socs3 degrades Traf6 via polyubiquitination in LPS-induced acute necrotizing pancreatitis. Cell Death Dis. 2015;6:1–9.
126. Moir S, Malaspina A, Ogwaro KM, Donoghue ET, Hallahan CW, Ehler LA, et al. HIV-1 induces phenotypic and functional perturbations of B cells in chronically infected individuals. Proc Natl Acad Sci U S A. 2001;98:10362–7.
127. Horisberger A, Humbel M, Fluder N, Bellanger F, Fenwick C, Ribi C, et al. Measurement of circulating CD21-CD27- B lymphocytes in SLE patients is associated with disease activity independently of conventional serological biomarkers. Sci Rep. 2022;12:9189.
128. Zhang J, Wu Q, Zhu L, Xie S, Tu L, Yang Y, et al. SERPINE2/PN-1 regulates the DNA damage response and radioresistance by activating ATM in lung cancer. Cancer Lett. 2022;524:268–83.
129. Wang H, Maurano MT, Qu H, Varley KE, Gertz J, Pauli F, et al. Widespread plasticity in CTCF occupancy linked to DNA methylation. Genome Res. 2012;22:1680–8.
130. Grötsch B, Brachs S, Lang C, Luther J, Derer A, Schlötzer-Schrehardt U, et al. The AP-1 transcription factor Fra1 inhibits follicular B cell differentiation into plasma cells. J Exp Med. 2014;211:2199–212.
131. Ise W, Kohyama M, Schraml BU, Zhang T, Schwer B, Basu U, et al. The transcription factor BATF controls the global regulators of class-switch recombination in both B cells and T cells. Nat Immunol. 2011;12:536–43.
132. Del Pino-Molina L, Rodríguez-Ubreva J, Canizales JT, Coronel-Díaz M, Kulis M, Martín-Subero JI, et al. Impaired CpG demethylation in common variable immunodeficiency associates with B cell phenotype and proliferation rate. Front Immunol. 2019;10:1–11.
133. Good-jacobson YZKL. Epigenetic regulation of B cell fate and function during an immune response. Immunol Rev. 2019;288:75–84.
134. Bhatt D, Ghosh S. Regulation of the NF-κB-mediated transcription of inflammatory genes. Front Immunol. 2014;5:1–9.
135. Grabowski P, Hesse S, Hollizeck S, Rohlfs M, Behrends U, Sherkat R, et al. Proteome analysis of human neutrophil granulocytes from patients with monogenic disease using data-independent acquisition. Mol Cell Proteomics. 2019;18:760–72.
136. Nusinow DP, Szpyt J, Ghandi M, Rose CM, McDonald ER, Kalocsay M, et al. Quantitative Proteomics of the Cancer Cell Line Encyclopedia. Cell. 2020;180:387-402.e16.
137. Perez-Riverol Y, Bai J, Bandla C, García-Seisdedos D, Hewapathirana S, Kamatchinathan S, et al. The PRIDE database resources in 2022: A hub for mass spectrometry-based proteomics evidences. Nucleic Acids Res. 2022;50:D543–52.

Figure Legends

Fig 1. Differential gene expression pattern in B cell subsets derived from NFKB1 mutation carriers indicates impairment of NFKB negative regulators and NFKB target genes.
a) Heatmap representation of differentially expressed NFKB target genes in WT and NFKB1 mutation carriers (log2 fold change ≥0.5, and adjusted p-value <0.5). Columns show the comparisons on unstimulated naïve-, stimulated naïve-, IgM memory-, and switched memory- B cells between NFKB1-mutated and WT. Color represents genes that are differentially expressed, where blue and red represent a decreased and an increased expression, respectively. **b)** Pathway overview of decreased expression of NFKB target genes comparing NFKB1 affected mutation carriers and WT. Differentially expressed genes are statically significant, with an adjusted p-value <0,05, and are highlighted in gray. Figure shows decrease expression of negative regulators of the NF-κB signaling pathway (*CYLD, TNP1, TRAF1, TNFAPI2 and TNFAIP3* (A20)) in affected NFKB1 mutation carriers on stimulated B cells. **c)** KEGG pathway representation of NFKB target genes with increased expression on stimulated naïve B cells in

bioRxiv preprint doi: https://doi.org/10.1101/2022.11.22.517350; this version posted November 23, 2022. The copyright holder for this preprint (which was not certified by peer review) is the author/funder, who has granted bioRxiv a license to display the preprint in perpetuity. It is made available under aCC-BY-NC-ND 4.0 International license.

affected NFKB1 mutation carriers compared to WT. Gray color indicates statically significant differentially expressed genes (adjusted p-value <0,05). Genes encoding proteasome subunits showed elevated mRNA expression. **d)** Volcano plot representation of the NFKB target genes transcriptomic comparison of affected plus unaffected-, affected- and unaffected- NFKB1 mutation carriers with WT. In blue, reduced expressed genes that negative regulate NF-kB signaling pathway on stimulated naïve B cells (log2 fold change ≤0.5, and adjusted p-value <0.5). **e)** Volcano plot representation of NFKB target genes at the transcriptomic level. NFKB1 mutation carriers were compared to WT across different unstimulated B cell subsets. Plots show data from unstimulated naïve-, IgM memory-, switched memory-, and CD21 low- B cells. Blue color dots represent reduced expressed genes with a role in the negative regulation of NF-kB signaling pathway (log2 fold change ≤0.5, and adjusted p-value <0.5). There were no differentially expressed negative regulator genes of the NFKB signaling pathway on CD21-lowB cells compared to WT.

Fig. 2 Chromatin accessibility defects in NFKB1 immune Dysregulation on stimulated naïve B cells. **a)** Clustered heatmap for the differentially accessible chromatin regions in NFKB1 mutation carriers compared to WT. Dots represent individuals included in the analysis, red indicates affected NFKB1 mutation carrier, blue unaffected NFKB1 mutation carrier, and black WT. Color on the heatmap indicates region with maximum (red) or minimum (blue) open chromatin. Preferentially open regions amounted to 168 in NFKB1 mutation carriers and 381 in WT. **b)** Cis-regulatory sequences associated with transcription factor binding motif (TFBM) regions of the NFKB1mutation carrier cluster or WT cluster. Letter size indicates nucleotide frequency. Numbers indicate significance of motif occurrence (binomial test). **c)** Heatmap including hierarchical clustering of 1396 differential accessible chromatin regions in affected NFKB1 mutation carriers compared to WT. Red dots indicate affected mutation carriers, and black dots WT. Preferentially open regions amounted to 479 in affected NFKB1 mutation carriers and 917 in WT. **d)** Cis-regulatory sequences associated with TFBM regions of the affected NFKB1 mutation carrier cluster or WT cluster. Letter size indicates nucleotide frequency. Numbers on the right indicate significance of motif occurrence (binomial test). **e)** Clustered heatmap for the 377 differentially accessible chromatin regions in unaffected NFKB1 mutation carriers compared to WT. Blue dots indicate unaffected NFKB1 mutation carrier and black dots WT. Blue color on the heatmap represents preferentially open regions, and red preferentially closed regions. Preferentially open regions amounted to 248 in unaffected NFKB1 mutation carriers, and 129 in WT. **f)** Cis-regulatory sequences associated with TFBM regions of the unaffected NFKB1 mutation carrier cluster or WT cluster. Letter size indicates nucleotide frequency. Numbers indicate significance of motif occurrence (binomial test). **g)** Heatmap including hierarchical clustering of 392 differential accessible chromatin regions in affected compared to unaffected NFKB1 mutation carriers. Red dots represent affected mutation carriers. Blue dots represent unaffected mutation carriers. Preferentially open regions amounted to 150 in affected and 242 in unaffected NFKB1 mutation carriers. **h)** Cis-regulatory sequences associated with TFMB regions of affected NFKB1 mutation carrier cluster or unaffected NFKB1 mutation carrier cluster. Sequence logos and P-values reflect the significance of motif occurrence are shown next to the corresponding motif.

Fig 3. Chromatin accessibility at superenhancers is disturbed on stimulated naïve B cells from NFKB1 patients. Venn diagram representing differentially accessible regions of NFKB target genes at super-enhancer regions. Differentially accessible regions from NFKB1 mutation carriers (affected and unaffected) and WT are represented. Associated gene names are listed in columns below the diagram

Fig 4. Gene set enrichment analyses show perturbations within the NFKB signaling network on unstimulated B cells across different subtypes. **a)** Dot plot pathway enrichment map showing significant up- and downregulated genes on unstimulated naïve B cells, **b)** Negative enrichment of pathways on IgM memory B cells when compared to WT **c)** Up- and downregulated gene pathways on switched memory B cells when compared to WT, **d)** Positive enrichment of pathways in CD21-low B cells. The GSEA analysis was performed using the fgsea package in R, where adjusted p-value <0.05 was considered significant. All differentially expressed genes were used for the analysis. Graphs include the gene count (number if DEG in pathway), and the adjusted p-value.

Fig 5. DNA methylation is impaired in the transition from naïve to memory compartments in unstimulated B cells from NFKB1 patients. a) Box plot depicting DNA methylation levels of DMRs on the different B cell subsets of NFKB1 mutation carriers(n=3) and WT (n=4). The lower and upper limits of the colored boxes represent the first(Q1) and third quartiles(Q3), respectively. The black horizontal line represents the media. Whiskers indicate the minimum and maximum values of the data set, and outliers are plotted as gray points. To test for significant differences Two-sided Wilcoxon test was used (* p-value ≤ 0.05, NS: not significant). **b)** Location proportion of DMRs across four different cell subtypes in the context of CpG islands, promoters and regulatory regions.

Fig. 6. The proteome of stimulated NFKB1 insufficient cells also reflects B cell dysfunction. Dot plots representing hallmark pathways. **a)** Hallmark pathways associated with increased (right) or decreased (left) differentially expressed proteins on affected mutation carriers when compared to WT. All categories are statically significantly enriched (adjusted p-value <0.5) **b)** Unaffected mutation carriers statistically significant enriched Hallmark

bioRxiv preprint doi: https://doi.org/10.1101/2022.11.22.517350; this version posted November 23, 2022. The copyright holder for this preprint (which was not certified by peer review) is the author/funder, who has granted bioRxiv a license to display the preprint in perpetuity. It is made available under aCC-BY-NC-ND 4.0 International license.

pathways (adjusted p-value <0.5) associated with increased (right) or decreased (left) differentially expressed proteins, when compared to WT, are depicted in the dot-plot. Graphs include the gene count (number of DEP in pathway), and the adjusted p-value.

Fig 7. Low correlation between differentially expressed genes and proteins on stimulated naïve B cells in NFKB1 mutation carriers. Scatter plots showing the correlation between **a)** NFKB1 mutation carriers compared to WT, **b)** Affected NFKB1 mutation carriers compared to WT, and **c)** Unaffected NFKB1 mutation carriers compared to WT. Scatterplot depicts the Pearson correlation coefficient (r) of differentially expressed genes (log2 fold change ≥0.5), and differentially expressed proteins (alpha = 0.05 and an absolute log2 fold change of 1.5) from the comparison between NFKB1 mutation carriers and WT.

Fig 8. Decrease expression of NFKB target genes in different omic levels on stimulated and unstimulated B cells from NFKB1 patients. a) Heatmap representation showing association between transcriptome, chromatin accessibility, methylome, and proteome from affected NFKB1 mutation carriers compared to WT in stimulated naïve B cells. For RNA-seq data, differentially expressed genes obtained from the comparison between NFKB1 mutation carriers to WT are shown. Color indicates log fold change were blue and red represent a decrease, and increased expression, respectively. The cutoff for differential expression was set at p<0.05 adjusted p-value and 0.5 for log2 fold change. For ATAC-seq, preferentially open or closed regions from *NFKB1* mutation carriers are shown. Blue bars represent preferentially closed and yellow bars preferentially open chromatin regions. Methylation data from NFKB1 mutation carriers are depicted. The median methylation is represented as a beta-value from 0 to 1 (0 to 100% methylation) at promoter regions. Color represents methylation values, where red is 100% and blue 0% methylation, respectively. For proteomic data, protein ratios were log-2 transformed. Differentially expressed proteins (alpha = 0.05 and an absolute log2 fold change of 1.5) from the comparison between NFKB1 mutation carriers and WT are represented. Color represents log fold change, where blue and red represent a decreased and increased expression, respectively. **b)** Venn diagram showing a supervised analysis of NFKB target genes in stimulated naïve B cells. Diagram represents the overlap between differentially expressed genes and differentially expressed proteins comparing affected mutation carriers to WT, plus preferentially open chromatin regions and methylation levels in affected NFKB1 mutation carriers. Associated gene names are shown in the columns below the diagram. **c)** Heatmap showing association between transcriptome and methylation levels on unstimulated B cells. A supervised analysis for NFKB target genes for naïve B-, IgM memory, switched memory-, and CD21low- B cells is represented. Additionally, for CD21-lowB cells, selected genes are shown. For differentially expressed genes data were obtained from the comparison of NFKB1 mutation carrier vs WT. Log2-fold changes values are indicated, cutoff for dysregulation was p-value <0.05. Blue and red color indicate decrease or increase expression, respectively. Methylation levels from NFKB1 mutation carriers are depicted. The median methylation is represented as a beta-value from 0 to 1 (0 to 100% methylation) at promoter regions. Blue color indicates 0% methylation, and red 100% methylation. **d)** Venn diagram representing a supervised analysis of NFKB target genes, between methylation levels and differentially expressed genes on unstimulated naïve-, IgM memory- and switched memory B cells. Additionally, for CD21-low B cells, selected genes are shown. Differentially expressed genes were obtained from the comparison between NFKB1 mutation carriers to WT (log2 fold change ≥0.5, and adjusted p-value <0.5). Methylation values from NFKB1 mutation carriers are represented. Associated gene names are listed in columns below the diagram.

bioRxiv preprint doi: https://doi.org/10.1101/2022.11.22.517350; this version posted November 23, 2022. The copyright holder for this preprint (which was not certified by peer review) is the author/funder, who has granted bioRxiv a license to display the preprint in perpetuity. It is made available under aCC-BY-NC-ND 4.0 International license.

Table 1. List of individuals included in this study

ID	Gender	Age	NFKB1 variant	Type of mutation	Phenotype
FR005	F	65	c.295C>T;p.Gln99*	Haploinsufficiency	affected
FR023	F	58	c.835+2T>G; p.Ser338Leufs*94	Haploinsufficiency	affected
FR036[#]	F	61	c.1365delT; p.Val456*	Precursor skipping	affected
FR095*	M	14	c.872delA;p.Asn291Metfs*141	Haploinsufficiency	affected
FR97.2*	F	25	c.872delA; p.Asn291Metfs*141	Haploinsufficiency	affected
FR302	F	53	c.589delA; p.Ile197Serfs*55	Haploinsufficiency	affected
FR098*	F	46	c.872delA; p.Asn291Metfs*141	Haploinsufficiency	unaffected
FR099*	M	27	c.872delA; p.Asn291Metfs*141	Haploinsufficiency	unaffected
FR100[+]	F	20	c.872delA; p.Asn291Metfs*141	Haploinsufficiency	unaffected
FR101[+]	F	52	c.872delA; p.Asn291Metfs*141	Haploinsufficiency	unaffected
FR102[+]	M	28	c.872delA; p.Asn291Metfs*141	Haploinsufficiency	unaffected
FR103[+]	F	27	c.872delA; p.Asn291Metfs*141	Haploinsufficiency	unaffected
FR113[#]	F	33	c.1365delT; p.Val456*	Precursor skipping	unaffected
FR040	M	55	WT	n.a.	WT
FR045	M	32	WT	n.a.	WT
FR046	F	37	WT	n.a.	WT
FR047	F	33	WT	n.a.	WT
FR048	F	56	WT	n.a.	WT
FR049	F	42	WT	n.a.	WT
FR050	M	28	WT	n.a.	WT
FR051	M	21	WT	n.a.	WT
FR052	F	28	WT	n.a.	WT
FR058	M	35	WT	n.a.	WT
FR061	F	43	WT	n.a.	WT
FR062	M	46	WT	n.a.	WT
FR063	F	30	WT	n.a	WT
FR064	F	36	WT	n.a.	WT
FR069	M	36	WT	n.a.	WT
FR075	F	50	WT	n.a.	WT
FR079	M	68	WT	n.a.	WT
FR081	F	59	WT	n.a.	WT
FR086	F	29	WT	n.a.	WT
C1	F	59	WT	n.a.	WT
C2	F	28	WT	n.a.	WT
C3	M	20	WT	n.a.	WT
C4	F	48	WT	n.a.	WT

WT: wild-type, n.a.: not applicable, (*) members of the same family, ([+]) members of the same family, ([#])members of the same family

Table 2. Clinical characteristics of affected mutation carriers

ID	Gender	Age	NFKB1 mutation	Category	Respiratory involvement	Gastrointestinal involvement	Lymphoproliferation	Autoimmunity	Others	Immunomodulation
FR005	F	65	c.295C>T;p.Gln99*	Haploinsufficiency	URTI, asthma	Celiac like diasease, hepatopathy	Splenomegaly, lymphadenopathy	Enteropathy	Osteoporosis, Norovirus infection, cold thyroid nodules	Glucocorticoids
FR023	F	58	c.835+2T>G;p.Ser338Leufs*94	Haploinsufficiency	URTI, GLILD	Liver cirrhosis	Splenomegaly	AITP, AIHA, Arthritis, CNS vasculitis	Osteopenia	Glucocorticoids, Upadacitinib
FR036	F	61	c.1365delT; p.Val456*	Precursor skipping	URTI, GLILD	CMV infection, hepatitis	Splenomegaly, lymphadenopathy	AITP, AIHA, enteropathy, arthritis	no	Glucocorticoids, Abatacept
FR095*	M	14	c.872delA; p.Asn291Metfs*141	Haploinsufficiency	URTI, pneumonia	IBD-like disease	no	Autoimmune thyroiditis, arthritis	Apthous ulcerations	Glucocorticoids, Abatacept
FR97.2*	F	25	c.872delA; p.Asn291Metfs*141	Haploinsufficiency	URTI	IBD-like disease	no	Arthritis	no	no
FR302	F	53	c.589delA; p.Ile197Serfs*55	Haploinsufficiency	URTI, pneumonia	Chronic diarrhea	Splenomegaly, lymphadenopathy	Enteropathy	no	Glucocorticoids

URTI: upper respiratory infections, GLILD: Granulomatous lymphocytic interstitial lung disease, CMV: cytomegalovirus, AITP: autoimmune thrombocytopenia, AIHA: autoimmune hemolytic anemia, CNS: central nervous system, IBD: inflammatory bowel disease, HCV, (*****) members of the same family

Table 3. List of Rare variants (<1% in gnomAD) in NF-κB downstream target genes of *NFKB1* mutation carriers

Subject_ID	Zygosity	AF	Gene	Transcript	CDS_change	Codon_change	Protein	Prot_change	Var_type	Impact	Published
FR005	HET	0,4571	TNFRSF4	ENST00000379236.4	c.619G>A	Gtg>Atg	ENSP00000368538.3	p.Val207Met	missense_variant	MODERATE	No
FR005	?	0,6923	IRF2	ENST00000393593.8	c.88-4del	NA	ENSP00000377218.3	NA	splice_region_variant	MODERATE	No
FR023	HET	0,4795	NOD2	ENST00000647318.1	c.2641G>C	Ggc>Cgc	ENSP00000495993.1	p.Gly881Arg	missense_variant	MODERATE	Yes
FR036	HET	0,4848	NFKBID	ENST00000606253.5	c.361C>T	Ccc>Tcc	ENSP00000475712.2	p.Pro121Ser	missense_variant	MODERATE	No
FR97.2	?	0,375	TERT	ENST00000310581.10	c.2130+5G>A	NA	ENSP00000309572.5	NA	splice_region_variant	MODERATE	No
FR97.2	HET	0,6471	NOD2	ENST00000647318.1	c.2828A>G	gAa>gGa	ENSP00000495993.1	p.Glu943Gly	missense_variant	MODERATE	No
FR098	HET	0,4324	DPYD	ENST00000370192.8	c.329A>G	tAt>tGt	ENSP00000359211.3	p.Tyr110Cys	missense_variant	MODERATE	No
FR098	HET	0,4792	SENP2	ENST00000296257.10	c.1576C>A	Ctt>Att	ENSP00000296257.5	p.Leu526Ile	missense_variant	MODERATE	No
FR100	?	0,52	ERBB2	ENST00000269571.9	c.1157C>A	gCc>gAc	ENSP00000269571.4	p.Ala386Asp	missense_variant	MODERATE	No
FR100	HET	0,396	NOD2	ENST00000647318.1	c.403G>A	Gtc>Atc	ENSP00000495993.1	p.Val135Ile	missense_variant	MODERATE	No
FR101	?	0,3636	ERBB2	ENST00000269571.9	c.1157C>A	gCc>gAc	ENSP00000269571.4	p.Ala386Asp	missense_variant	MODERATE	No
FR101	HET	0,5	DPYD	ENST00000370192.8	c.329A>G	tAt>tGt	ENSP00000359211.3	p.Tyr110Cys	missense_variant	MODERATE	No
FR101	HET	0,6098	SENP2	ENST00000296257.10	c.1576C>A	Ctt>Att	ENSP00000296257.5	p.Leu526Ile	missense_variant	MODERATE	No
FR102	HET	0,4894	DPYD	ENST00000370192.8	c.329A>G	tAt>tGt	ENSP00000359211.3	p.Tyr110Cys	missense_variant	MODERATE	No
FR103	HET	0,5741	DPYD	ENST00000370192.8	c.329A>G	tAt>tGt	ENSP00000359211.3	p.Tyr110Cys	missense_variant	MODERATE	No
FR103	HET	0,377	NOD2	ENST00000647318.1	c.403G>A	Gtc>Atc	ENSP00000495993.1	p.Val135Ile	missense_variant	MODERATE	No
FR113	HET	0,6122	ICAM1	ENST00000264832.8	c.1432C>T	Cgg>Tgg	ENSP00000264832.2	p.Arg478Trp	missense_variant	MODERATE	No
FR103	HET	0,4659	ABCA1	ENST00000374736.8	c.2328G>C	aaG>aaC	ENSP00000363868.3	p.Lys776Asn	missense_variant	MODERATE	No
FR103	?	0,8462	RIPK2	ENST00000220751.5	c.1029+4_1029+6del	NA	ENSP00000220751.4	NA	splice_region_variant	MODERATE	No
FR103	HET	0,5056	NFKBID	ENST00000606253.5	c.361C>T	Ccc>Tcc	ENSP00000475712.2	p.Pro121Ser	missense_variant	MODERATE	No
FR103	HET	0,5847	CASP4	ENST00000444739.7	c.560C>T	gCg>gTg	ENSP00000388566.2	p.Ala187Val	missense_variant	MODERATE	No

Table 4. Selected DMR among different B cell subtypes

Cell type	Region	Name	Mean WT	Mean NFKB1	p.value	Description
Unstimulated naive	*Promoter*	*IGHD*	0.74	0.96	1.05E-04	immunoglobulin heavy constant delta
	Gene	*MZB1*	0.38	0.52	0.045	marginal zone B and B1 cell specific protein
		IGKV1-13	1	0.81	5.42E-07	immunoglobulin kappa variable 1-13
		IGKV1D-13	1	0.88	2.06E-04	immunoglobulin kappa variable 1D-13
IgM memory	*Promoter*	*IGHV4-28*	0	1	2.59E-07	immunoglobulin heavy variable 4-28
		IGLV9-49	0.45	0.93	2.22E-04	immunoglobulin heavy variable 9-49
	Gene	*SLAMF1*	0.52	0.64	0.022	signaling lymphocytic activation molecule family member 1
		IGHV4-28	0	1	2.59E-07	immunoglobulin heavy variable 4-28
		IGLV9-49	0.45	0.93	2.22E-04	immunoglobulin lambda variable 9-49
Switched Memory	*Gene*	*IGKV2-24*	0.16	0.75	0.003	immunoglobulin kappa variable 2-24
		IGKV2-28	0	1	4.07E-05	immunoglobulin kappa variable 2-28
		IGKV2D-28	0.5	0.77	0.001	immunoglobulin kappa variable 2D-28
		MZB1	0.51	0.33	0.009	marginal zone B and B1 cell specific protein
CD21-low B cells	*Gene*	*IGKV2-24*	0	0.6	0.043	immunoglobulin kappa variable 2-24
		IGKV3D-11	0.83	0.95	0.048	immunoglobulin kappa variable 3D-11

a Target genes NFKB1 B cells

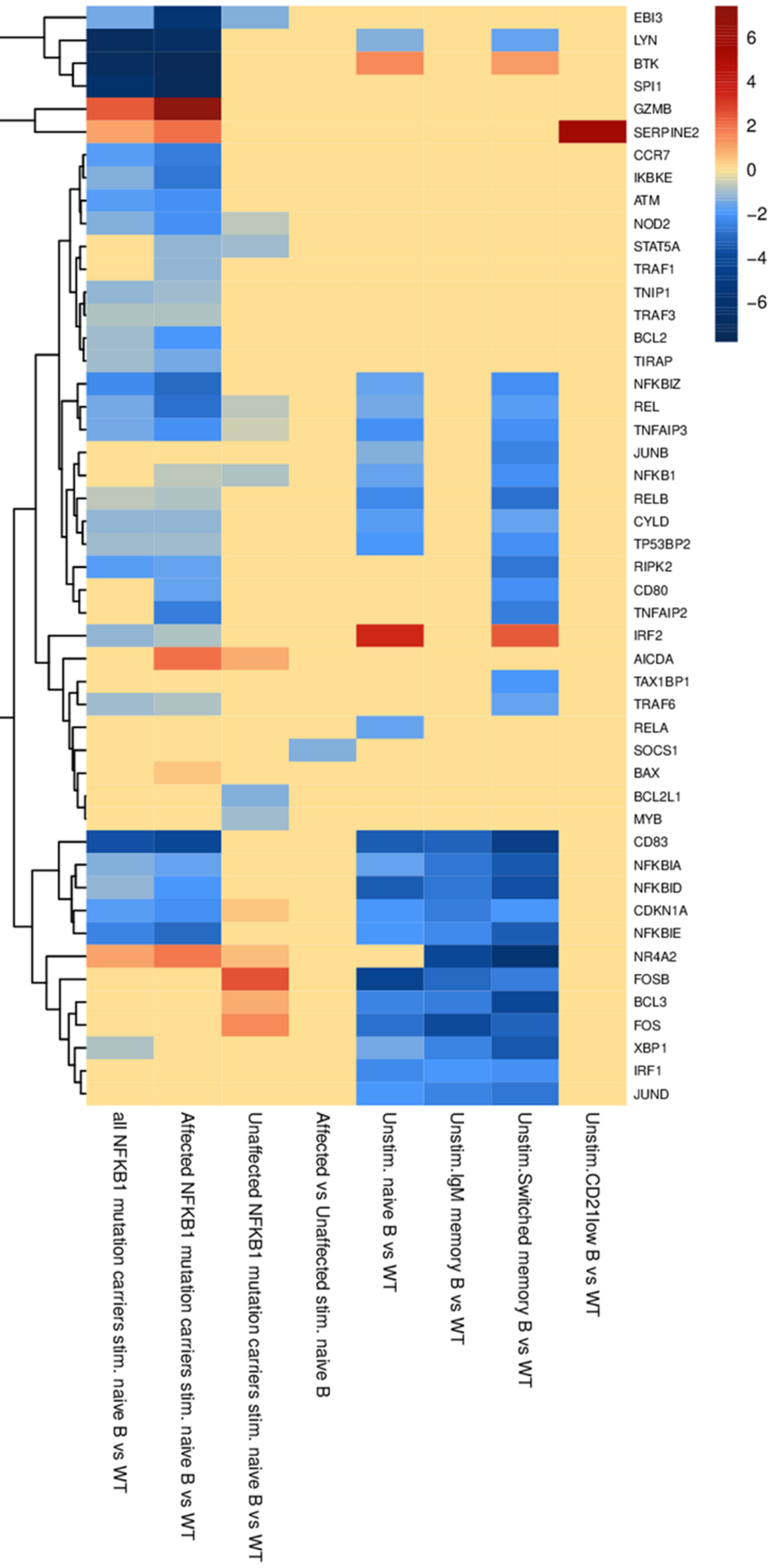

b Downregulated transcripts

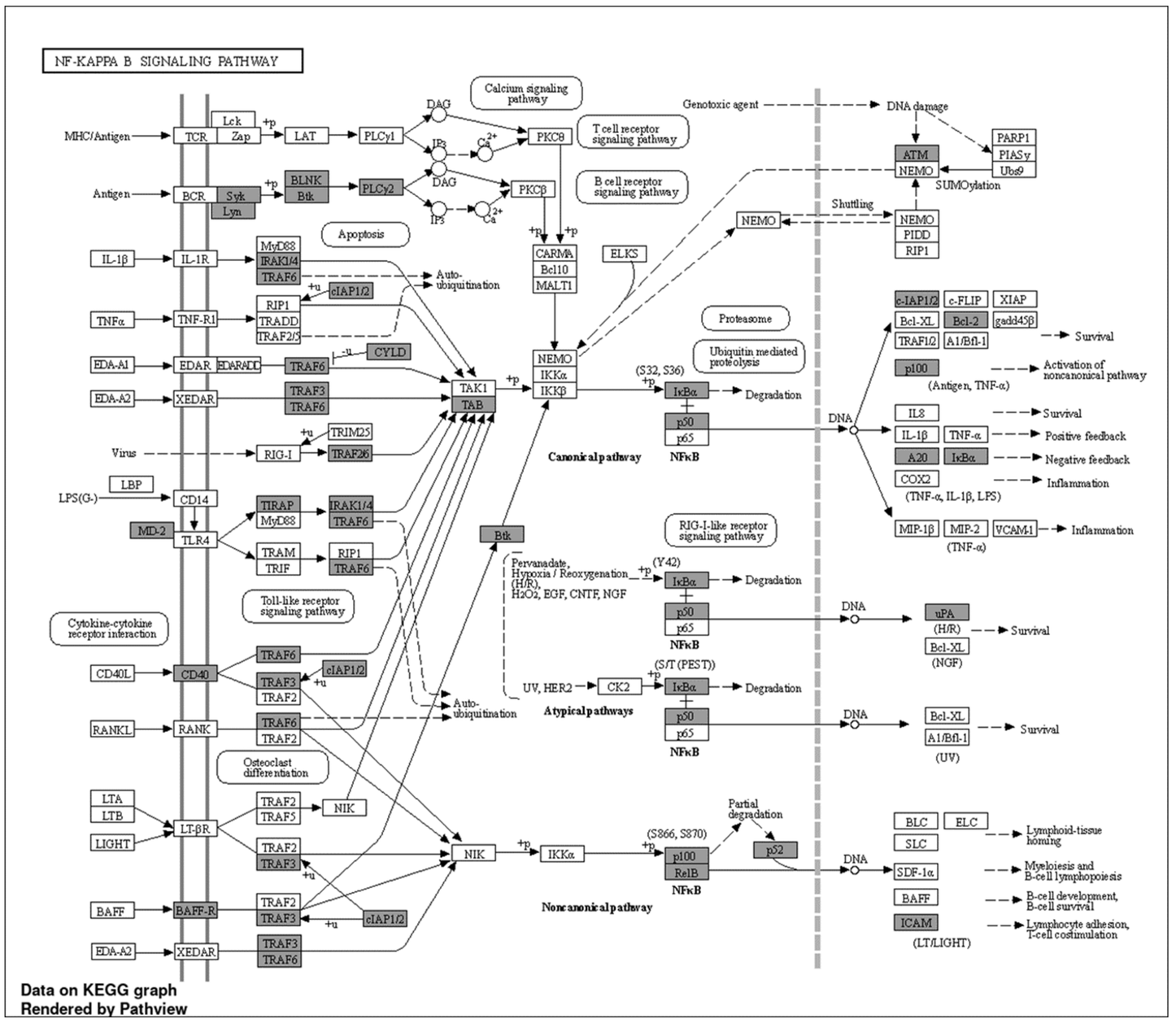

c Upregulated transcripts

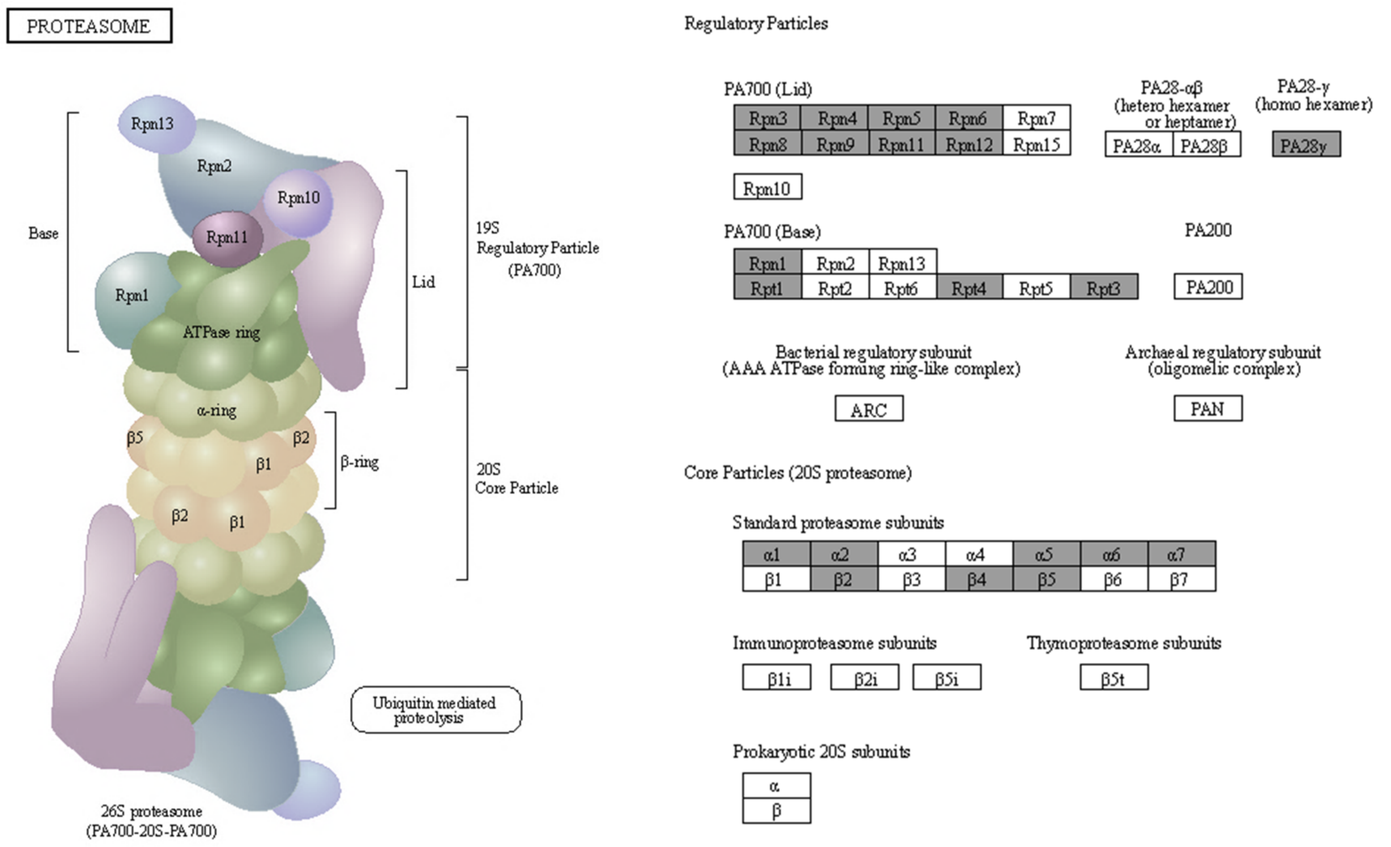

d All NFKB1 mutation carriers unstim. Naïve B cells vs WT

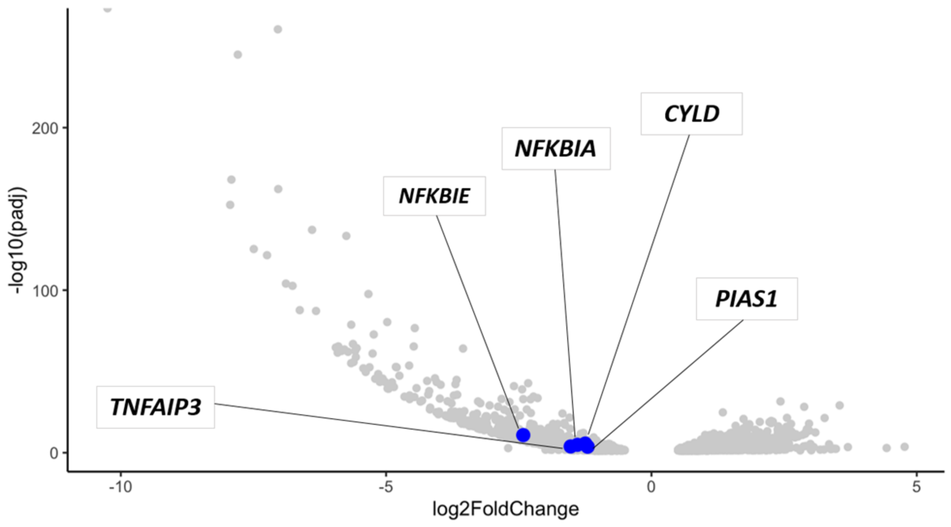

Affected NFKB1 mutation carriers stim. Naïve B cells vs WT

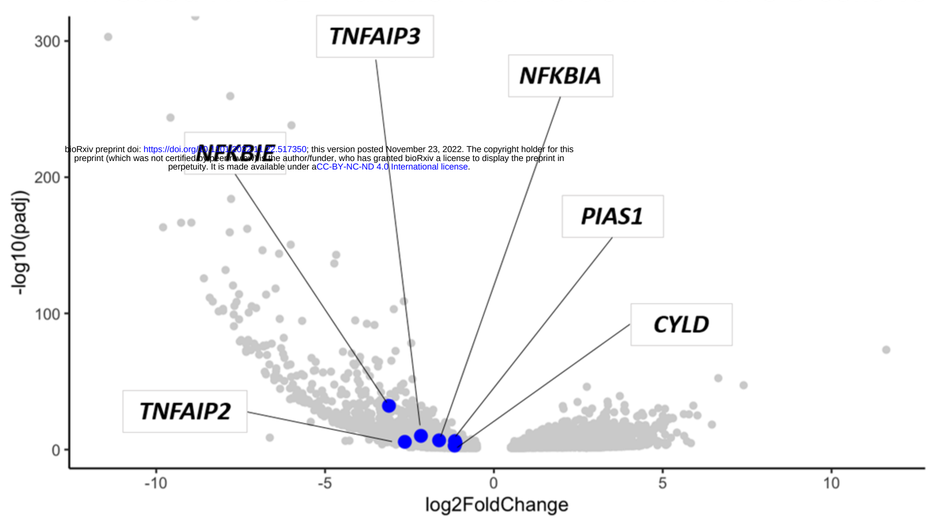

bioRxiv preprint doi: https://doi.org/10.1101/2022.11.23.517350; this version posted November 23, 2022. The copyright holder for this preprint (which was not certified by peer review) is the author/funder, who has granted bioRxiv a license to display the preprint in perpetuity. It is made available under aCC-BY-NC-ND 4.0 International license.

e Unstimulated naïve B cells vs WT

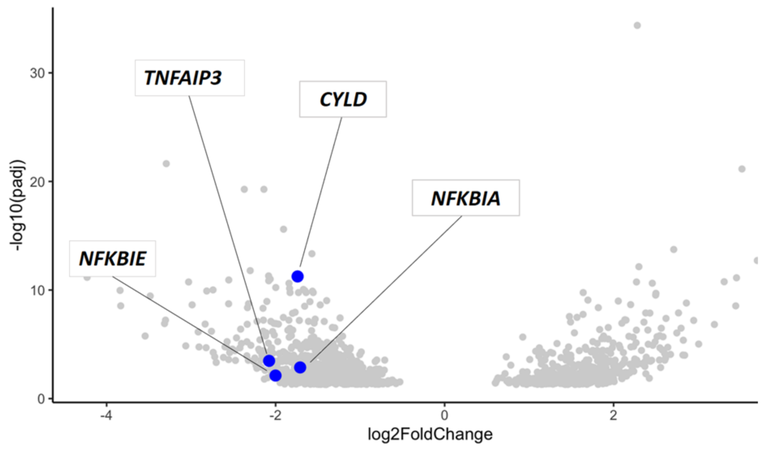

Unstimulated IgM memory B cells vs WT

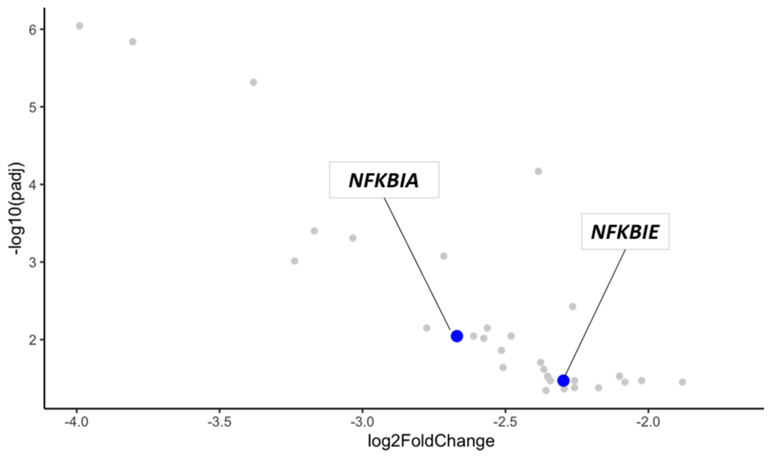

Unstimulated Switched memory B cells vs WT

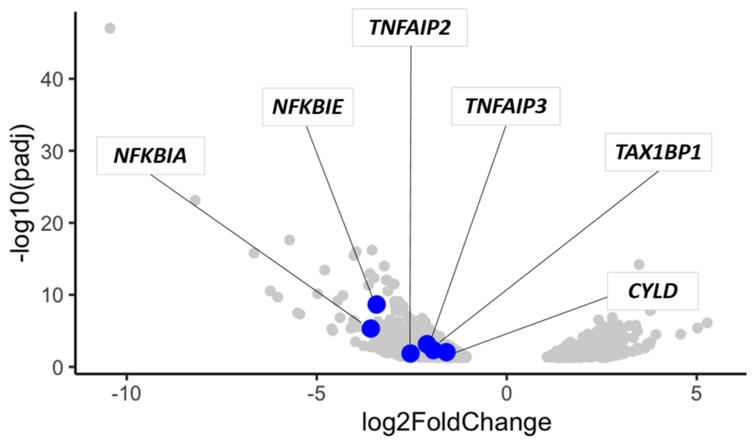

Unstimulated CD21 low B cells vs WT

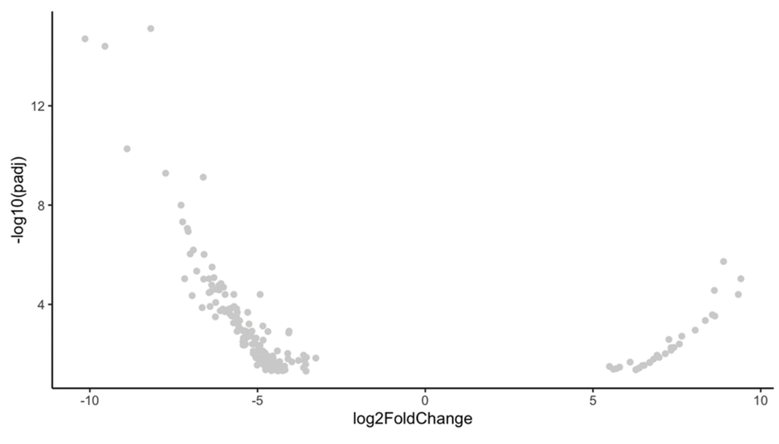

Unaffected NFKB1 mutation carriers stim. Naïve B cells vs WT

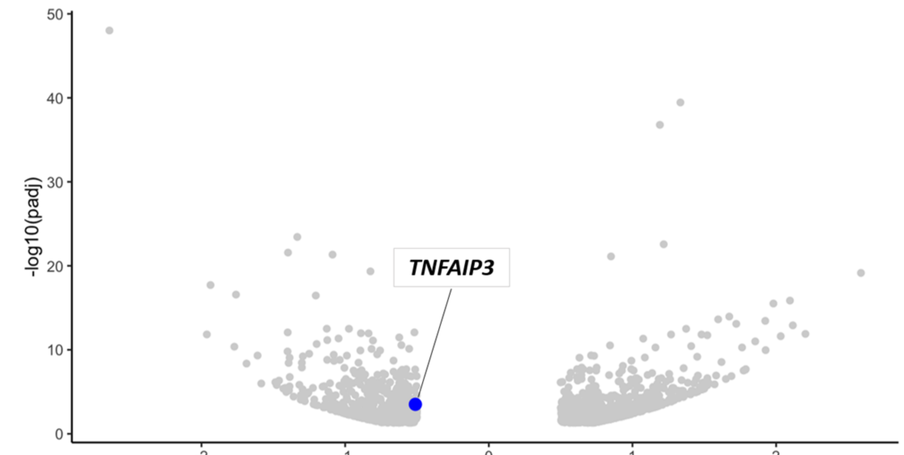

a

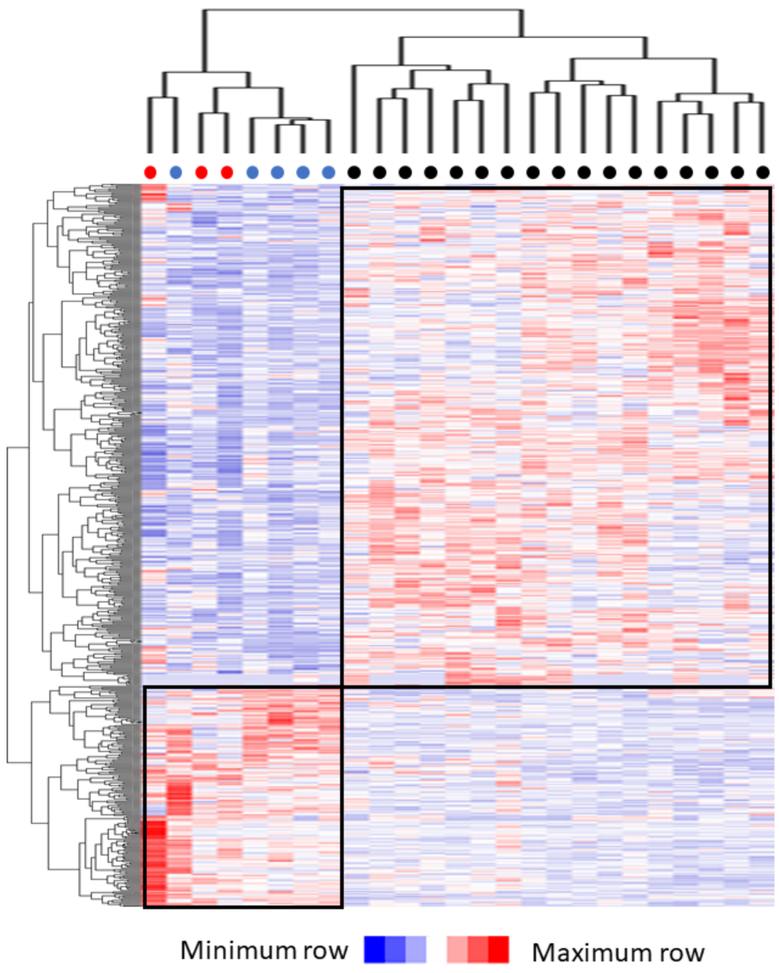

168 regions preferentially open in all NFKB1 mutation carriers

381 regions preferentially open in WT

b

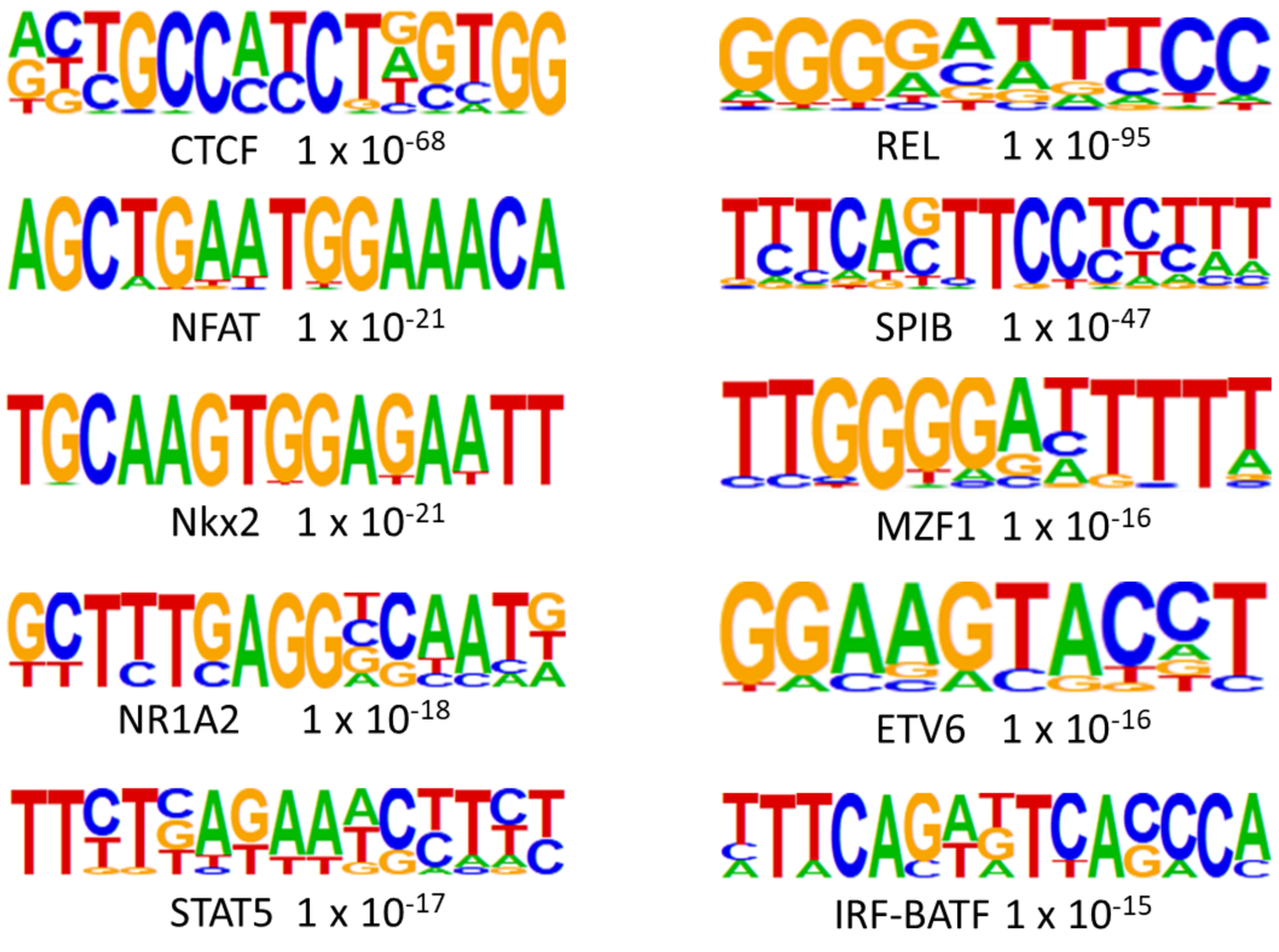

Enriched transcription factor binding motif in all NFKB1 mutation carriers

Enriched transcription factor binding motif in WT

c

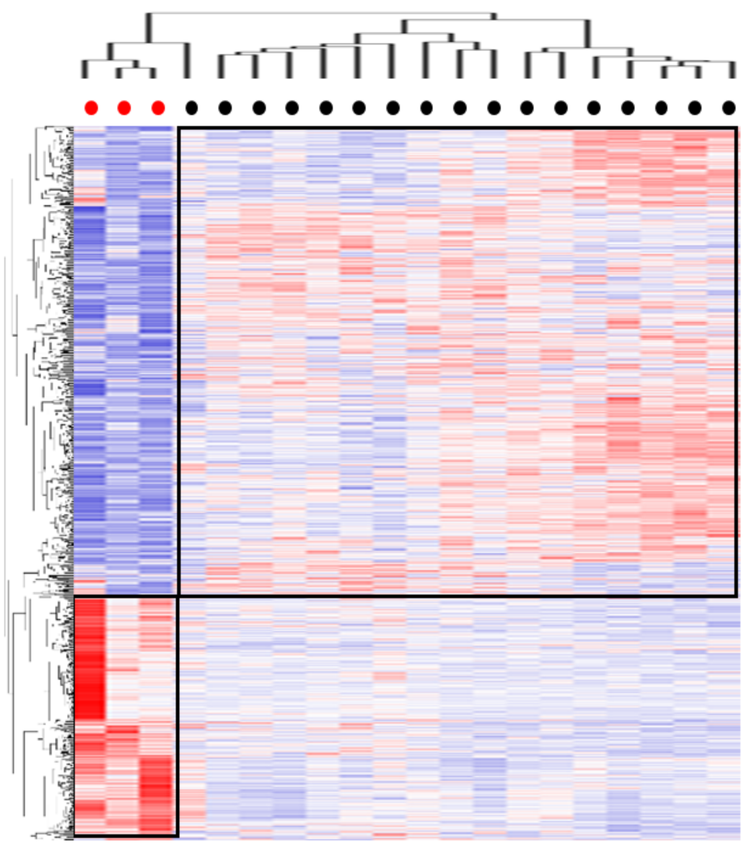

479 regions preferentially open in affected NFKB1 mutation carriers

917 regions preferentially open in WT

d

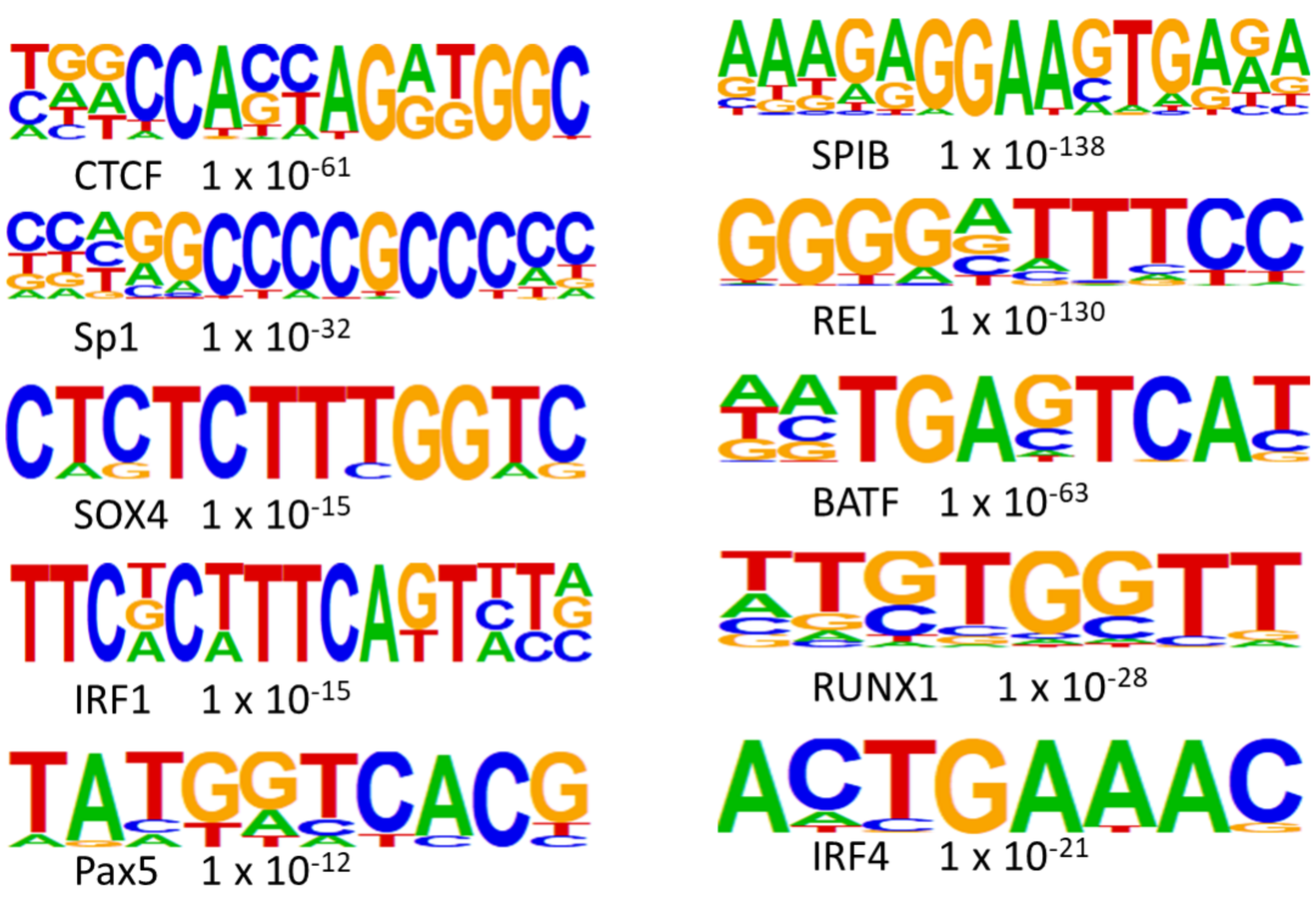

Enriched transcription factor binding motif in affected NFKB1 mutation carriers

Enriched transcription factor binding motif in WT

e

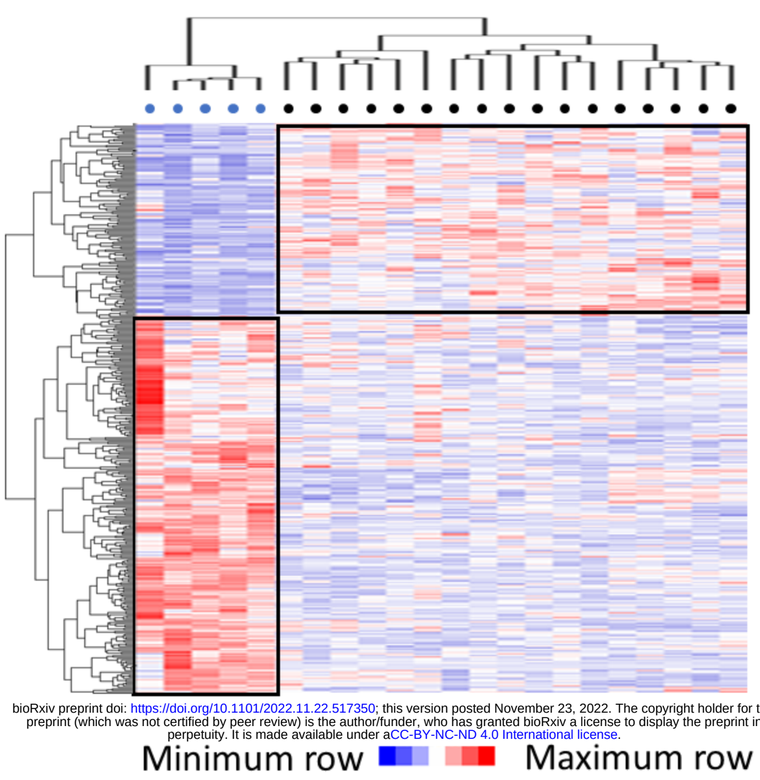

248 regions preferentially open in unaffected NFKB1 mutation carriers

129 regions preferentially open in WT

f

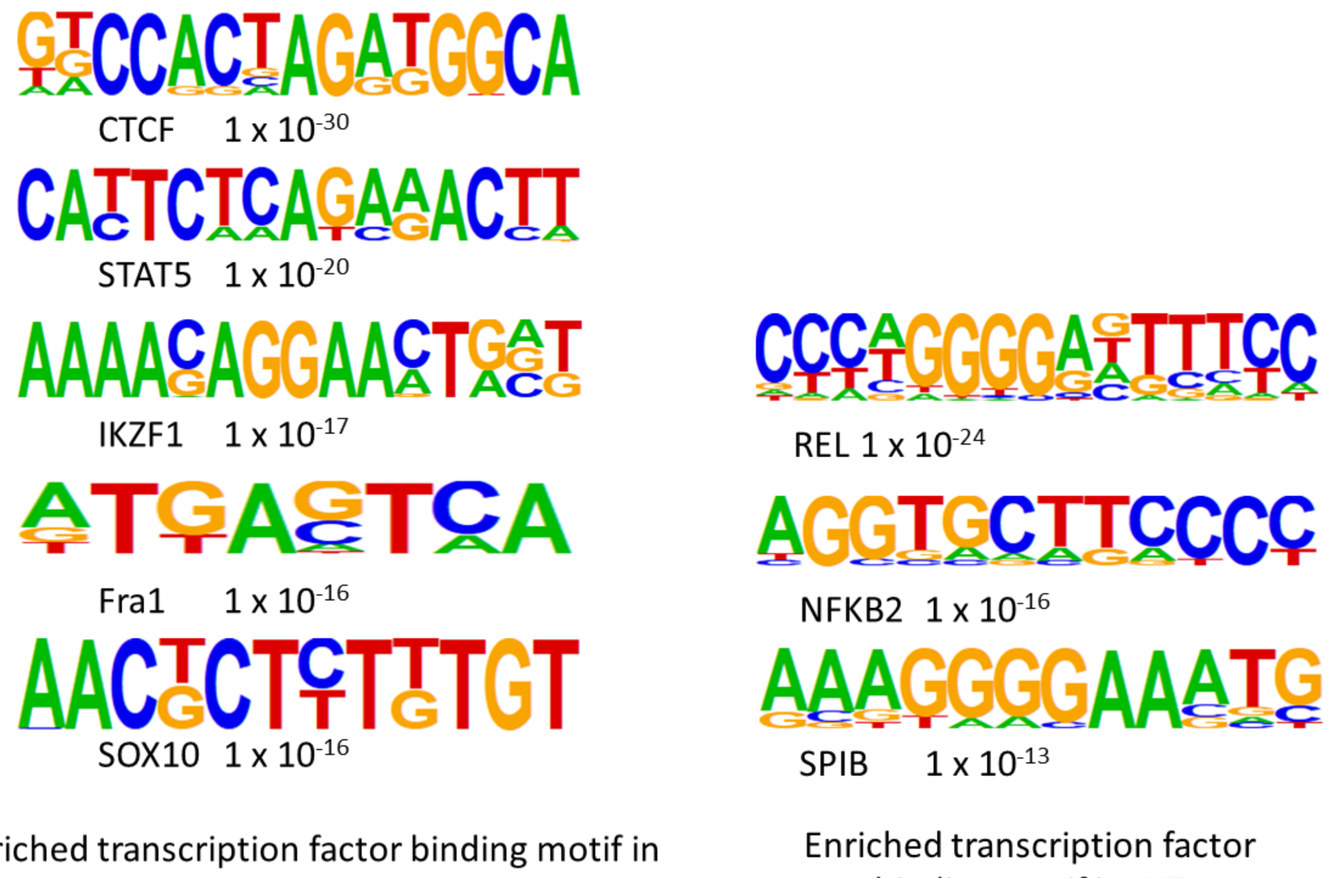

Enriched transcription factor binding motif in unaffected NFKB1 mutation carriers

Enriched transcription factor binding motif in WT

g

150 regions preferentially open in affected NFKB1 mutation carriers

242 regions preferentially open in unaffected NFKB1 mutation carriers

h

Enriched transcription factor binding motif in affected NFKB1 mutation carriers

Enriched transcription factor binding motif in unafffected NFKB1 mutation carriers

bioRxiv preprint doi: https://doi.org/10.1101/2022.11.22.517350; this version posted November 23, 2022. The copyright holder for this preprint (which was not certified by peer review) is the author/funder, who has granted bioRxiv a license to display the preprint in perpetuity. It is made available under aCC-BY-NC-ND 4.0 International license.

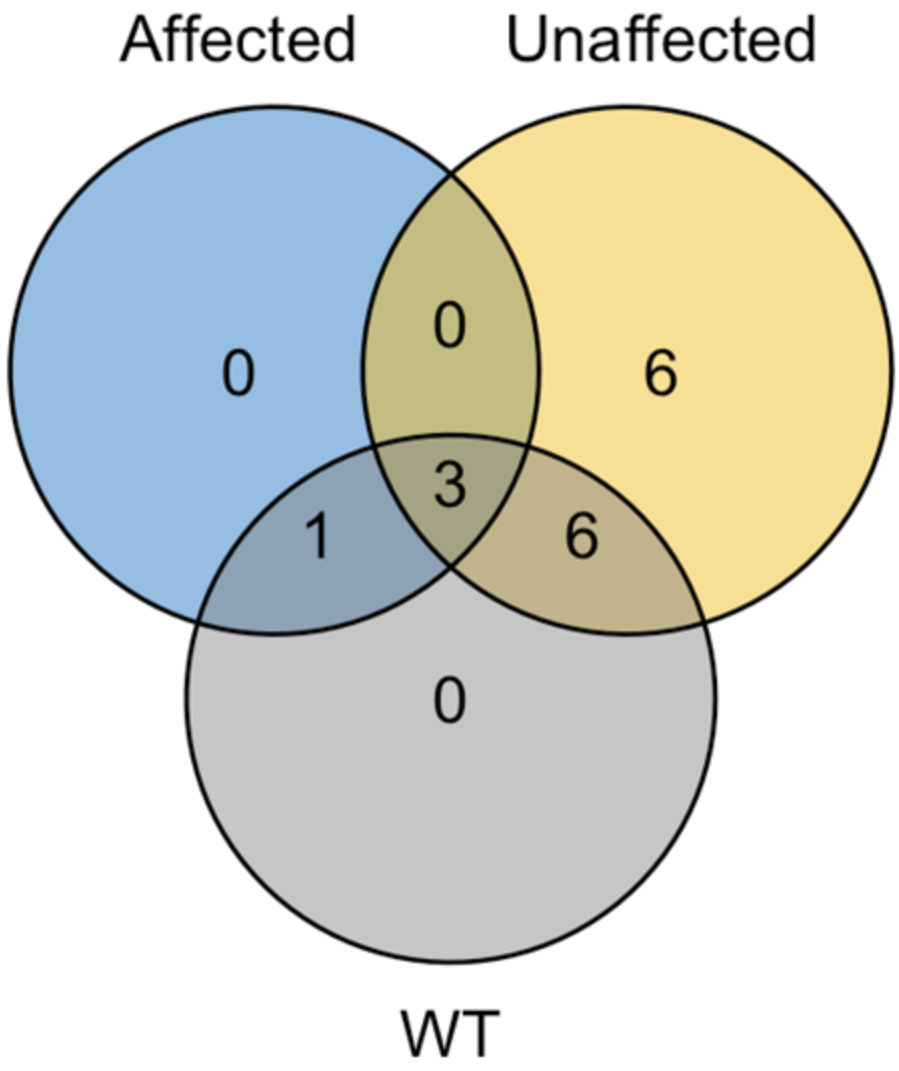

n=1
NFKBIA

n=3
FOSB
IRF1
NR4A2

n=6
BCL3
CCR7
CDKN1A
IKBKG
LYN
PRMT1

n=6
BCL2
CD83
IRF4
NFKBIZ
TNIP1
TRAF1

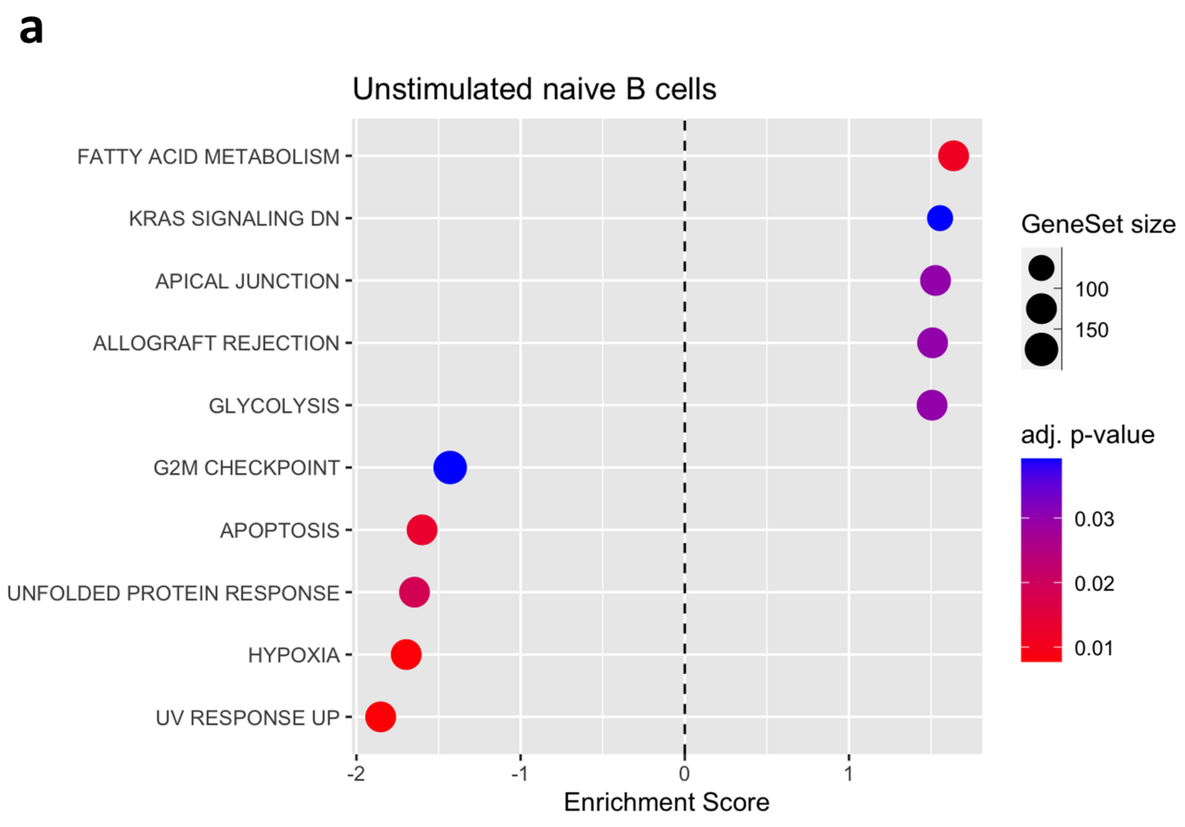

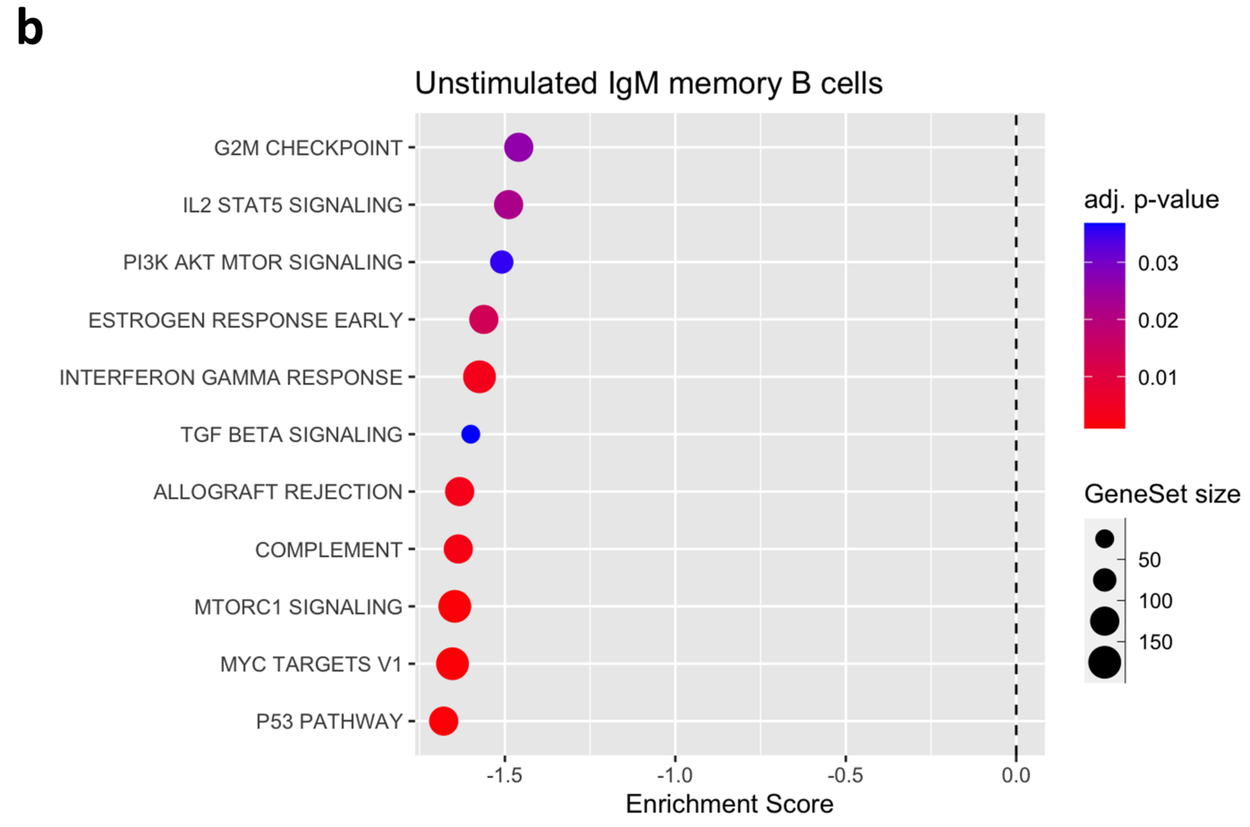

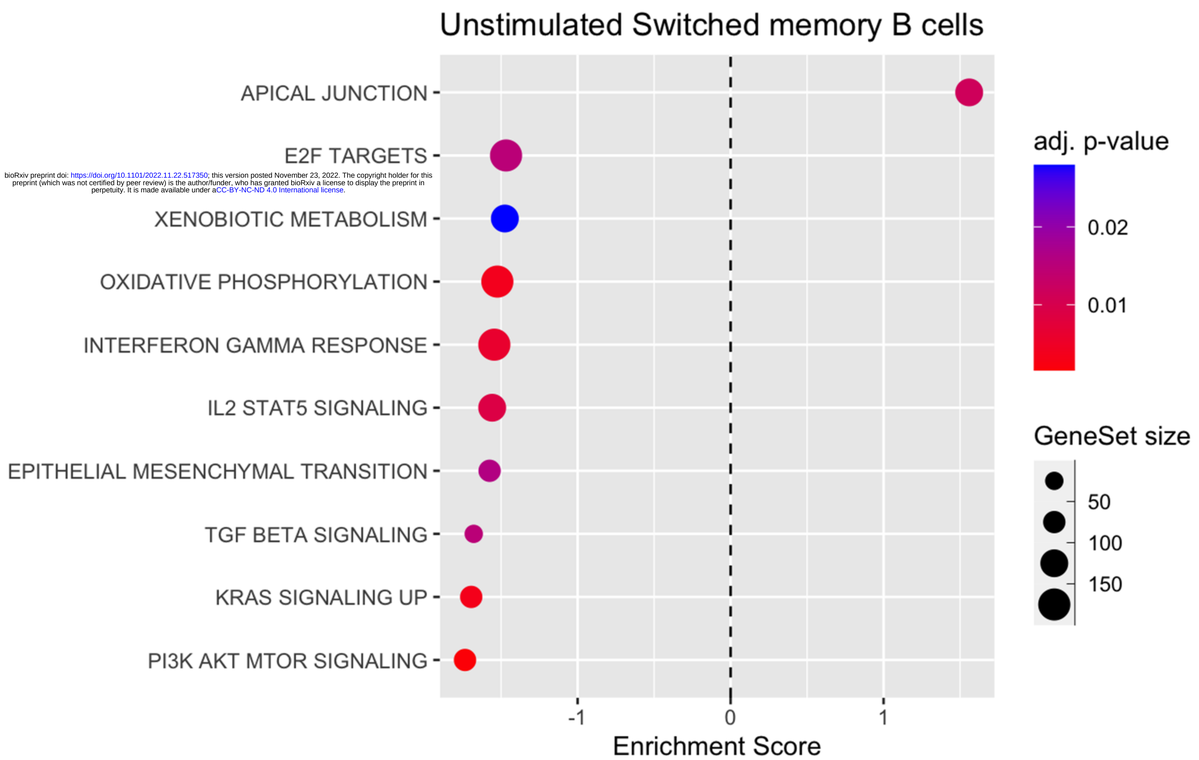

bioRxiv preprint doi: https://doi.org/10.1101/2022.11.22.517350; this version posted November 23, 2022. The copyright holder for this preprint (which was not certified by peer review) is the author/funder, who has granted bioRxiv a license to display the preprint in perpetuity. It is made available under aCC-BY-NC-ND 4.0 International license.

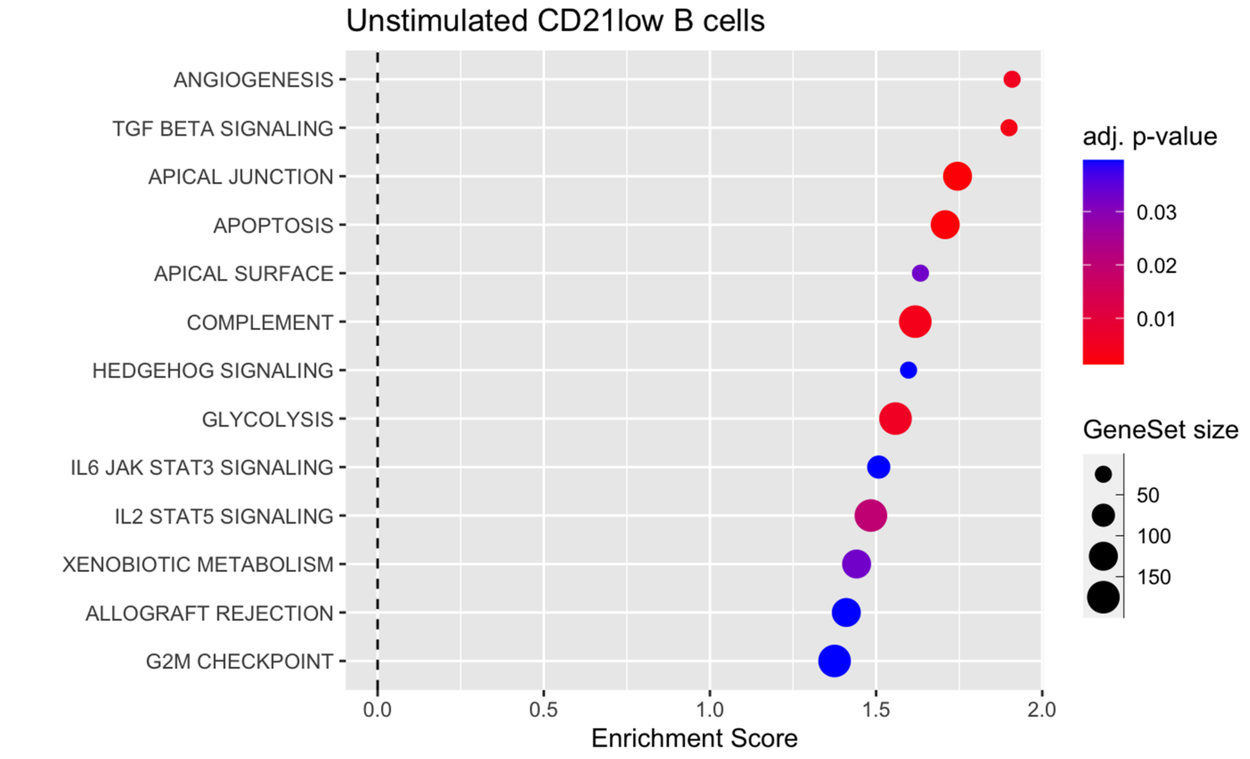

a

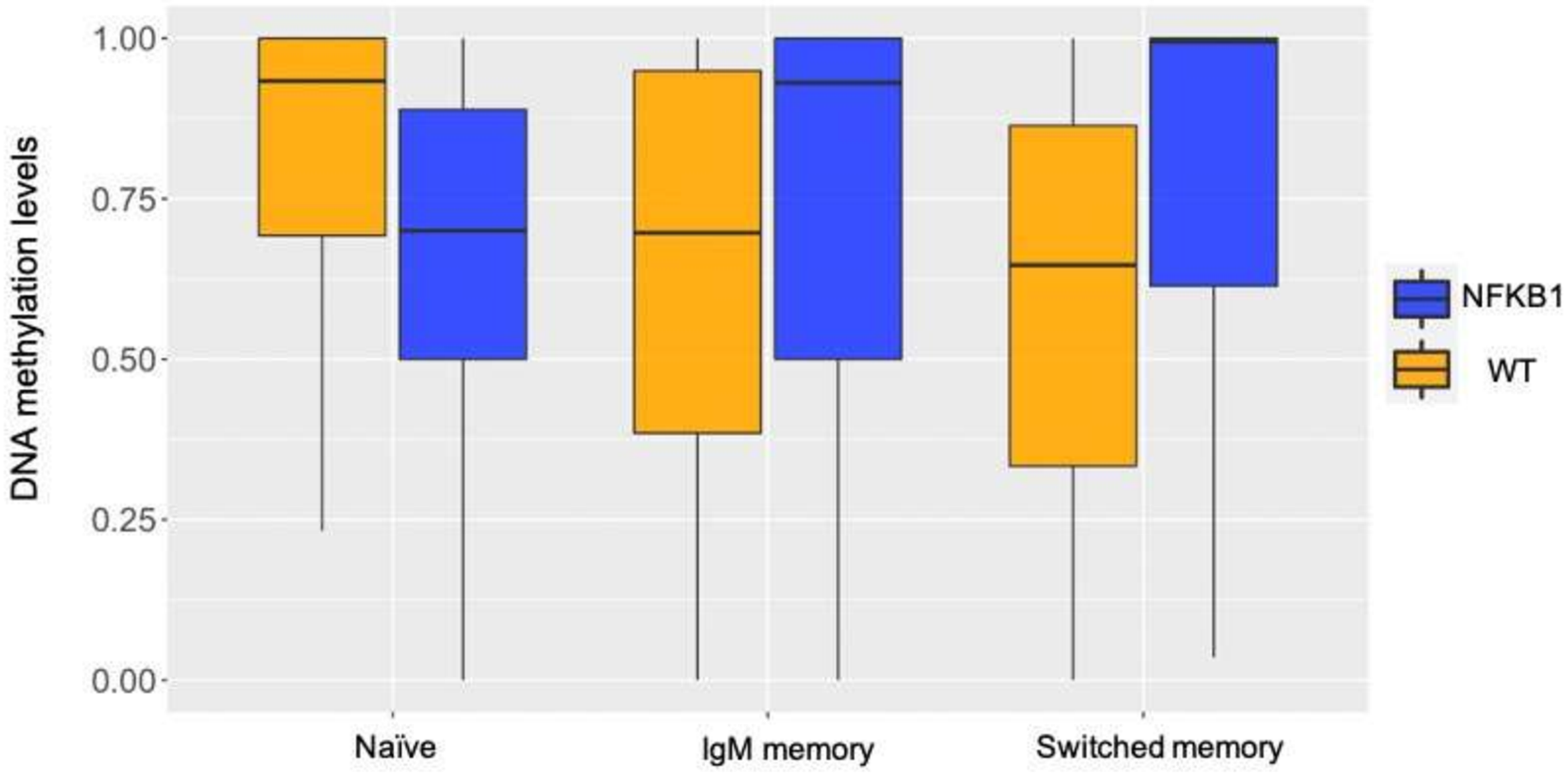

bioRxiv preprint doi: https://doi.org/10.1101/2022.11.22.517350; this version posted November 23, 2022. The copyright holder for this preprint (which was not certified by peer review) is the author/funder, who has granted bioRxiv a license to display the preprint in perpetuity. It is made available under aCC-BY-NC-ND 4.0 International license.

b

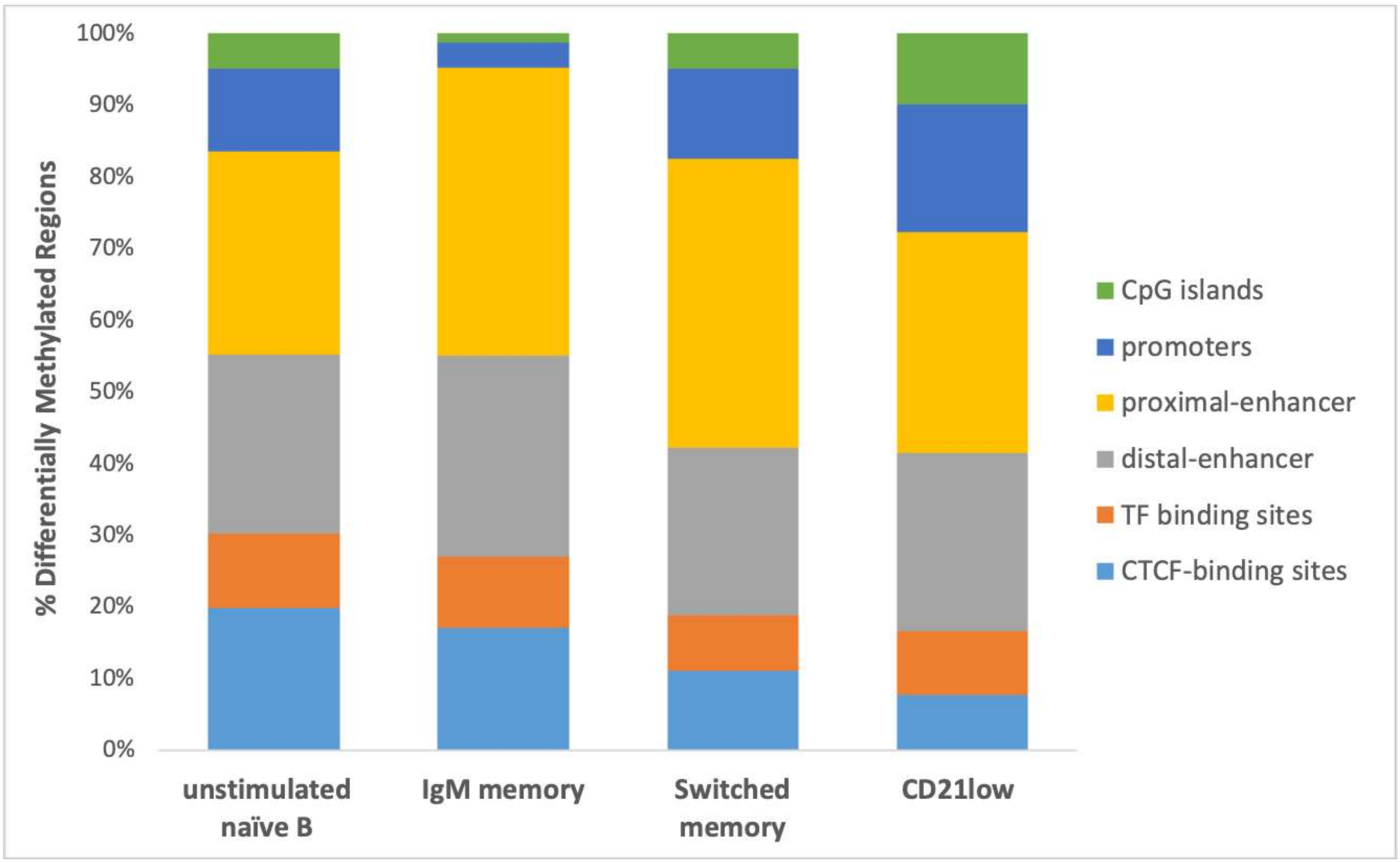

a

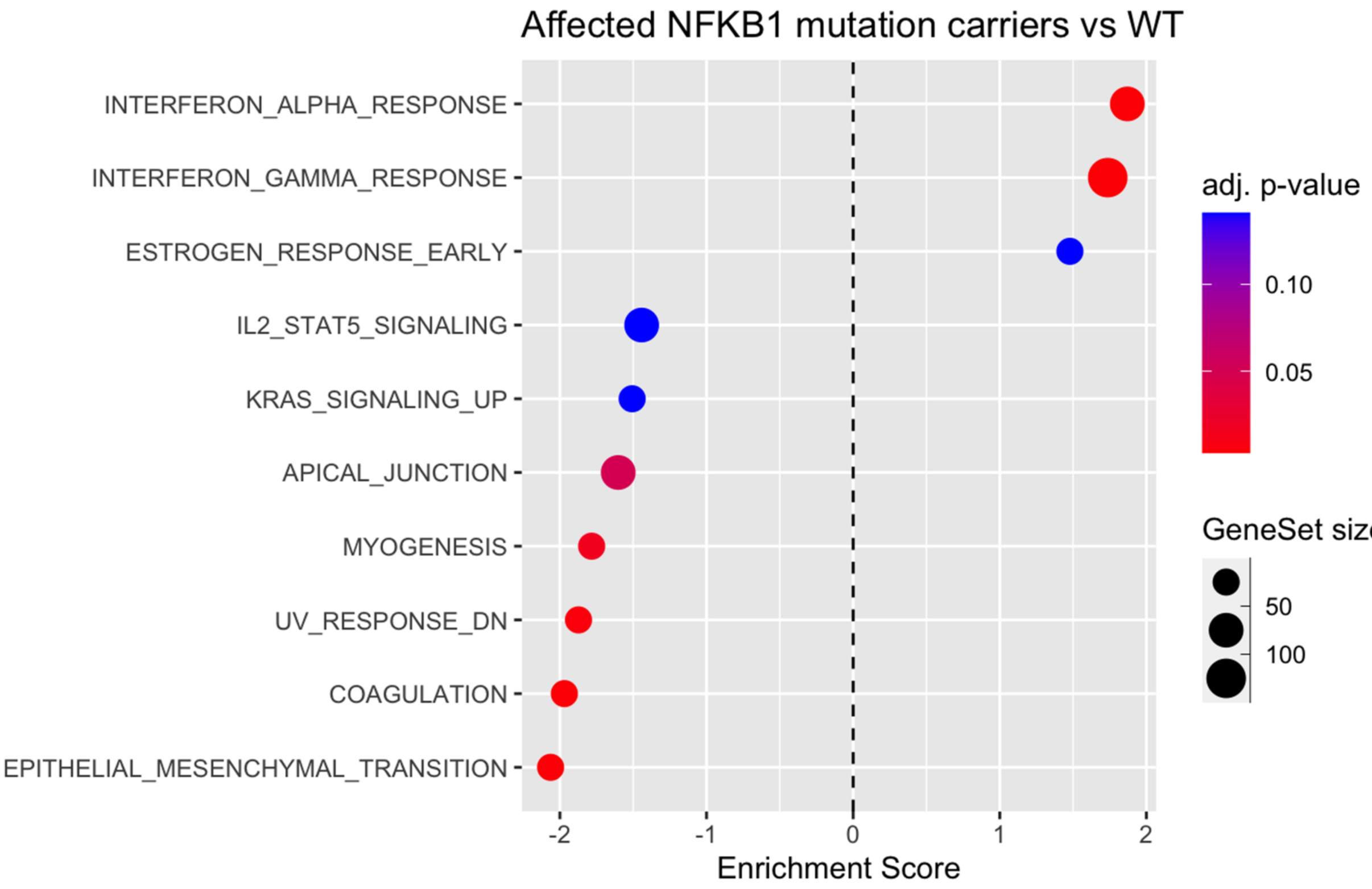

b

bioRxiv preprint doi: https://doi.org/10.1101/2022.11.22.517350; this version posted November 23, 2022. The copyright holder for this preprint (which was not certified by peer review) is the author/funder, who has granted bioRxiv a license to display the preprint in perpetuity. It is made available under aCC BY-NC-ND 4.0 International license.

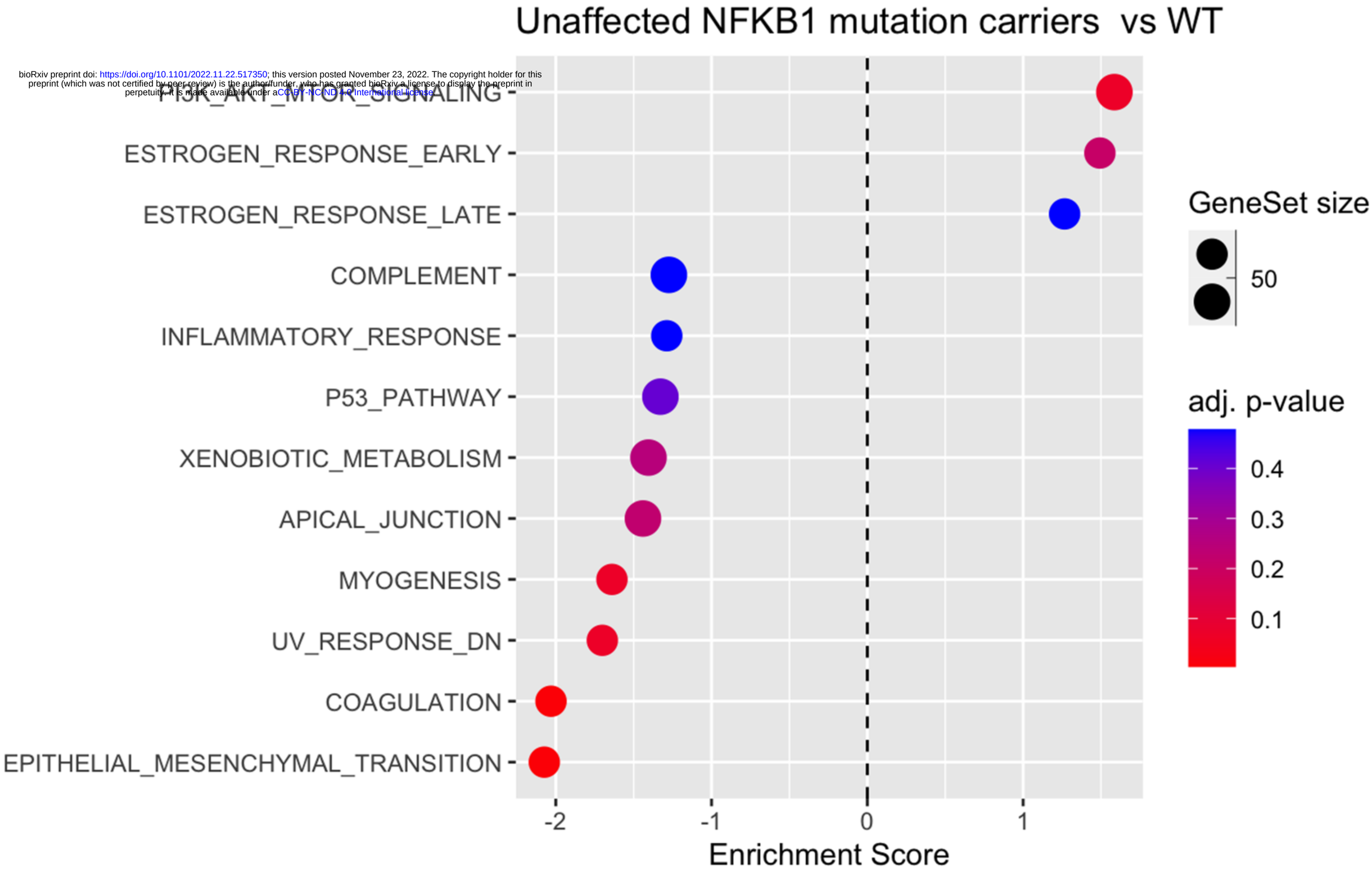

a

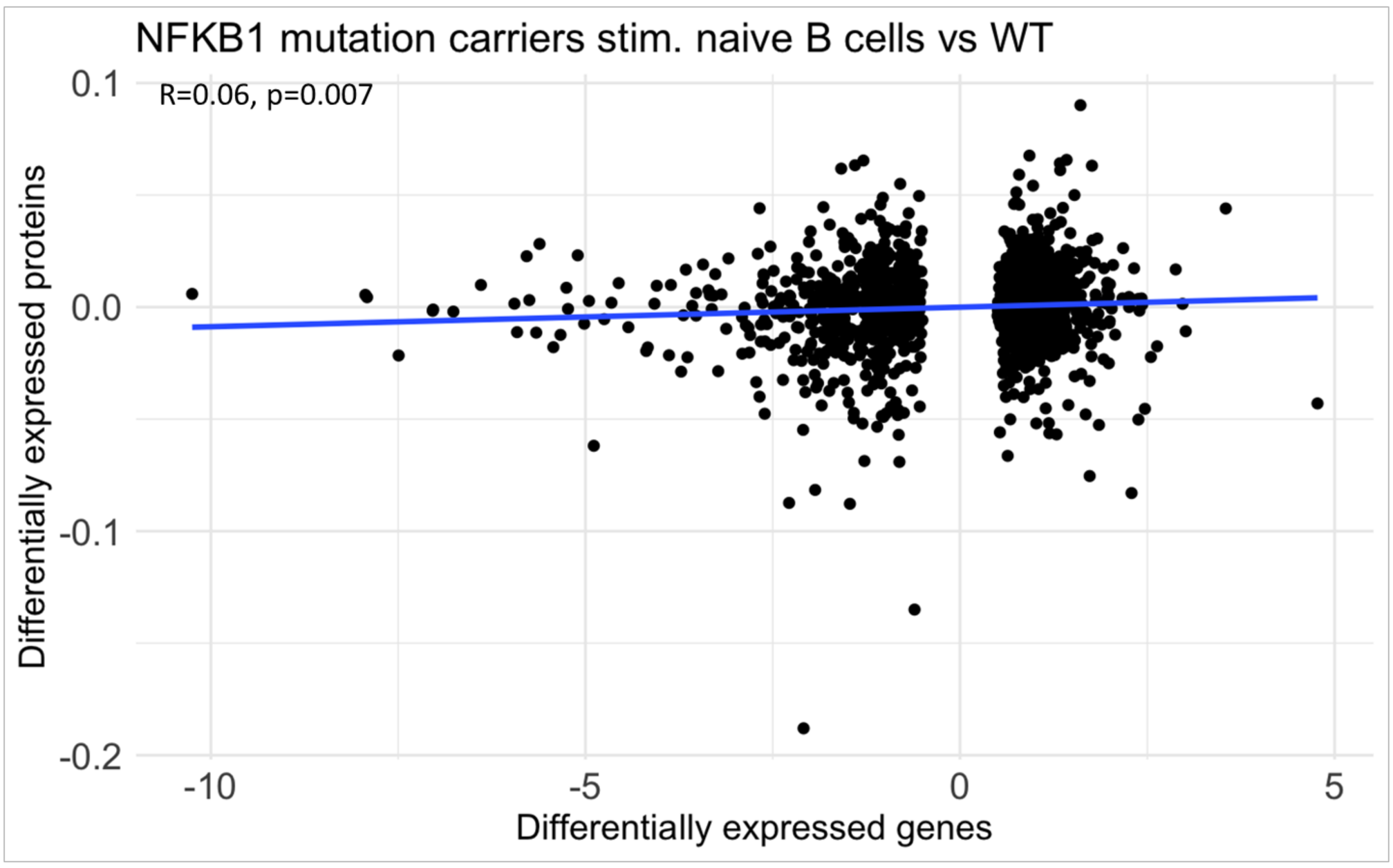

b

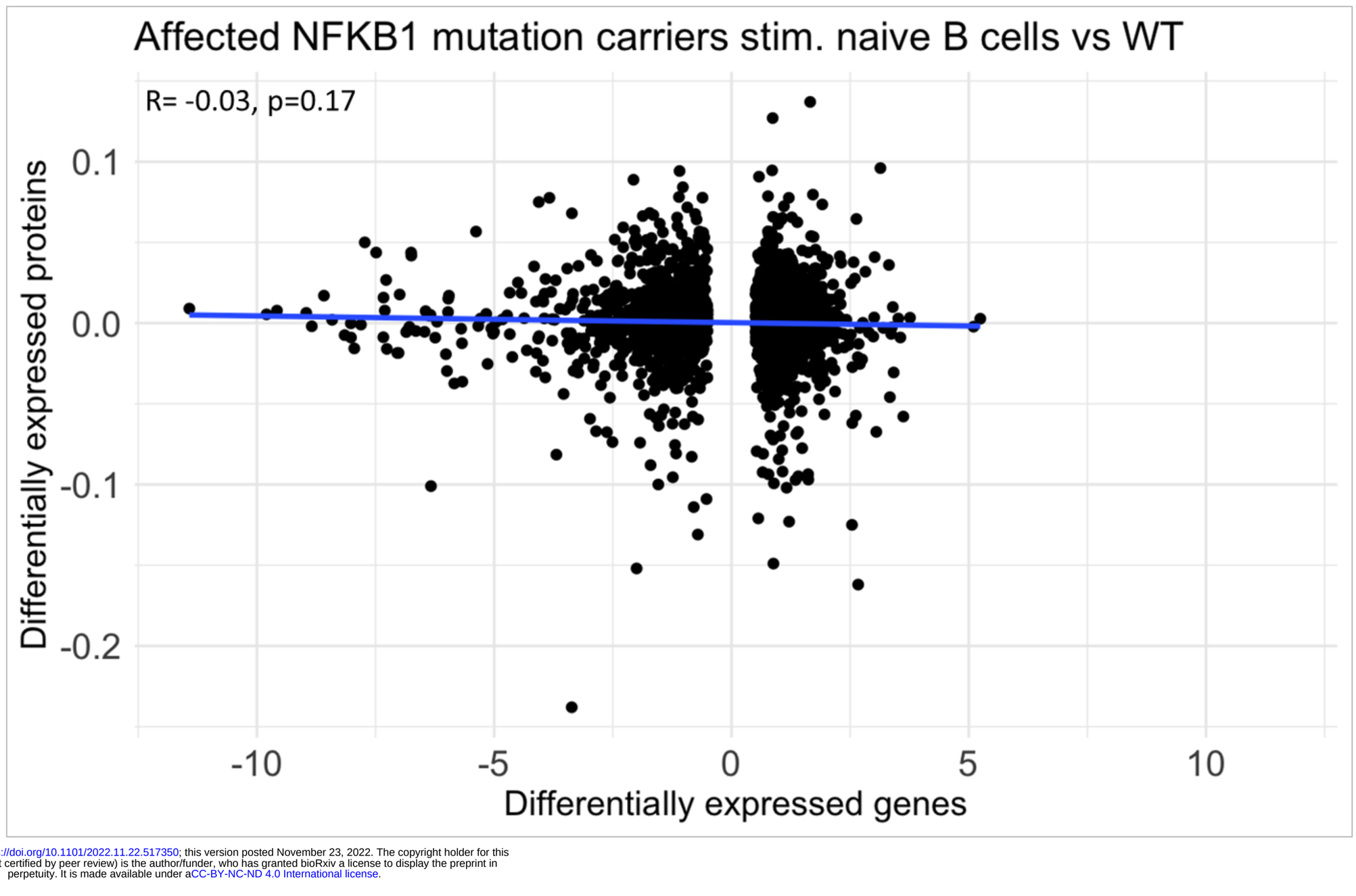

bioRxiv preprint doi: https://doi.org/10.1101/2022.11.22.517350; this version posted November 23, 2022. The copyright holder for this preprint (which was not certified by peer review) is the author/funder, who has granted bioRxiv a license to display the preprint in perpetuity. It is made available under aCC-BY-NC-ND 4.0 International license.

c

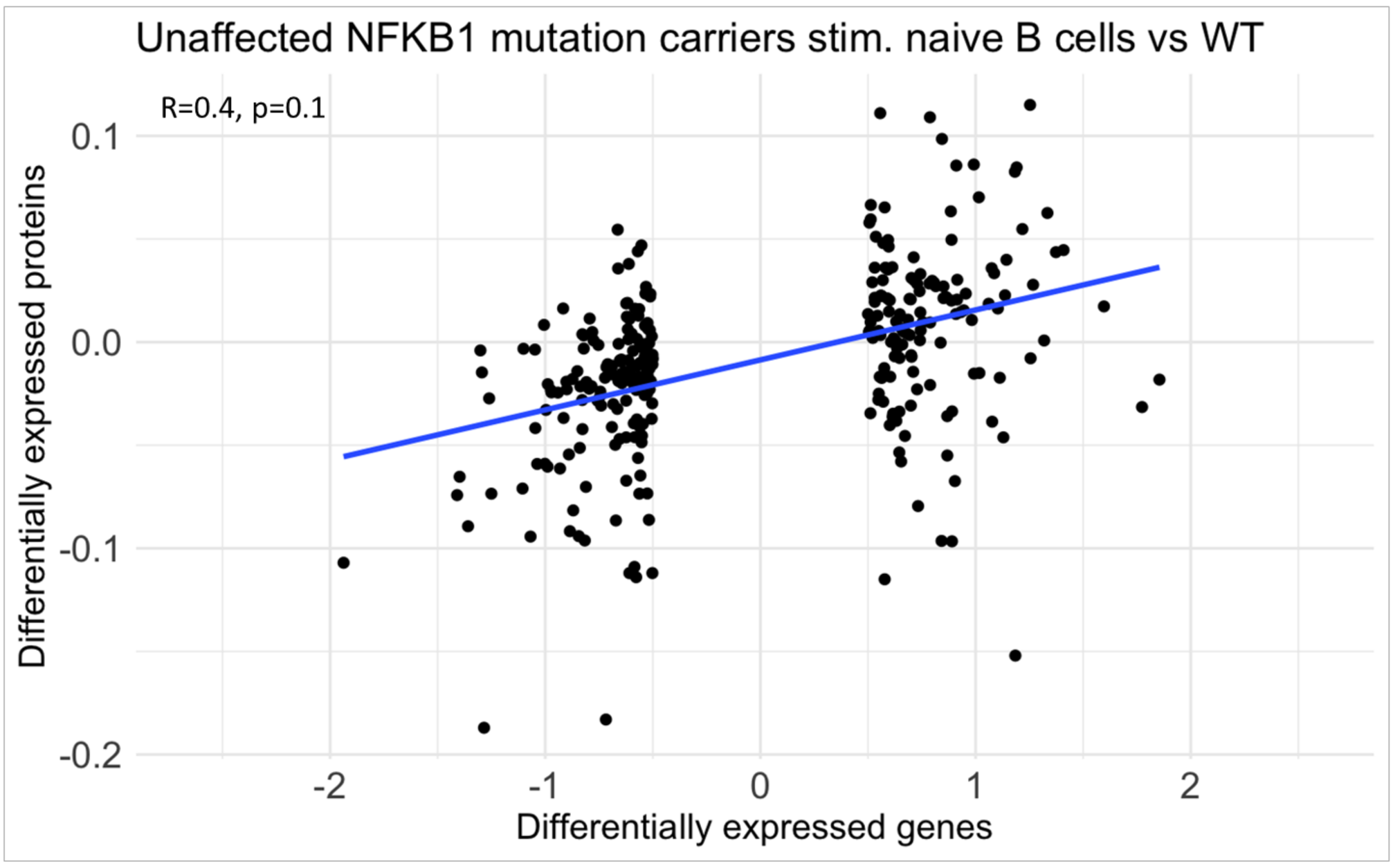

a Stimulated naïve B cells

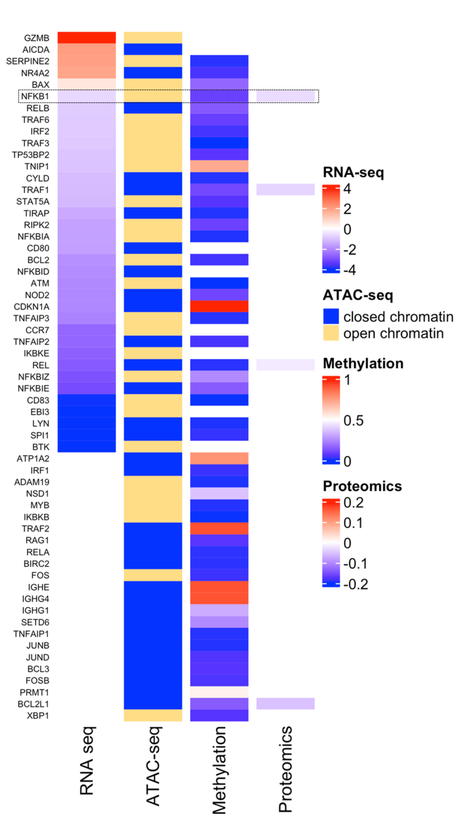

b Stimulated naïve B cells

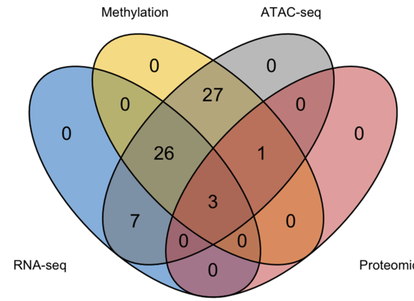

n=7
AICDA
BTK
CCR7
CD80
EBI3
GZMB
NFKBID

n=26
ATM
BAX
BCL2
CD83
CDKN1A
CYLD
IKBKE
IRF2
LYN
NFKBIA
NFKBIE
NFKBIZ
NOD2
NR4A2
RELB
RIPK2
SERPINE2
SPI1
STAT5A
TIRAP
TNFAIP2
TNFAIP3
TNIP1
TP53BP2
TRAF3
TRAF6

n=27
ADAM19
ATP1A2
BCL3
BIRC2
FOS
FOSB
IGHE
IGHG1
IGHG4
IKBKB
IRF1
ITCH
JUNB
JUND
MYB
NSD1
PRMT1
RAG1
RELA
SETD6
SOCS1
TAX1BP1
TNFAIP1
TRAF2
TWIST1
TWIST2

n=3
NFKB1
REL
TRAF1

n=1
BCL2L1

c Unstimulated naïve B cells

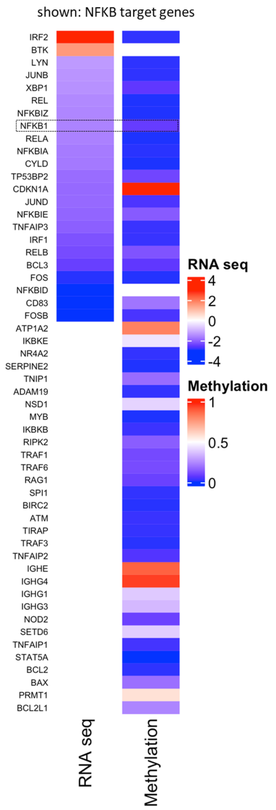

Unstimulated IgM memory B cells

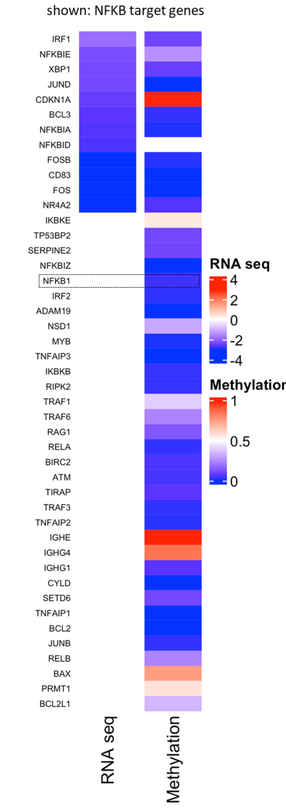

Unstimulated Switched memory B cells

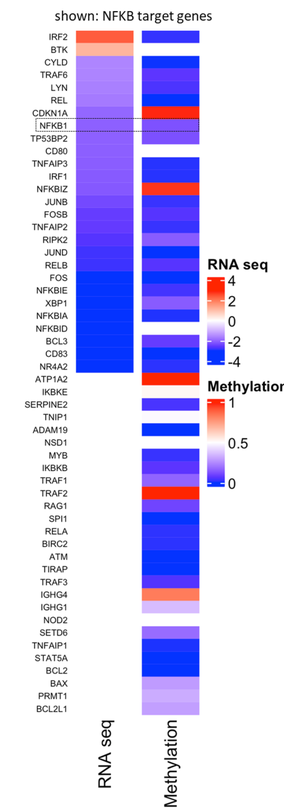

Unstimulated CD21-low B cells

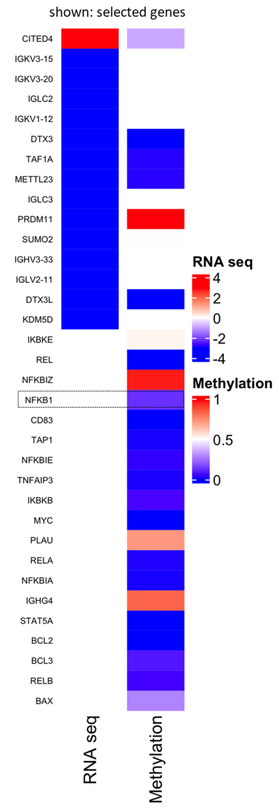

d Unstimulated naïve B cells

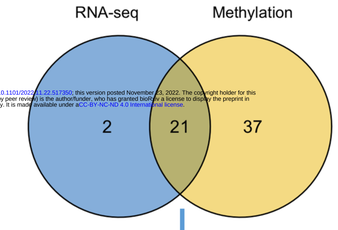

bioRxiv preprint doi: https://doi.org/10.1101/2022.11.22.517350; this version posted November 23, 2022. The copyright holder for this preprint (which was not certified by peer review) is the author/funder, who has granted bioRxiv a license to display the preprint in perpetuity. It is made available under aCC-BY-NC-ND 4.0 International license.

n=2
BTK
NFKBID

n=21
BCL3
CD83
CDKN1A
CYLD
FOS
FOSB
IRF1
IRF2
JUNB
JUND
LYN
NFKB1
NFKBIA
NFKBIE
NFKBIZ
REL
RELA
RELB
TNFAIP3
TP53BP2
XBP1

n=37	
ADAM19	*RAG1*
ATM	*RIPK2*
ATP1A2	*SERPINE2*
BAX	*SETD6*
BCL2	*SOCS1*
BCL2L1	*SPI1*
BIRC2	*STAT5A*
IGHE	*TAX1BP1*
IGHG1	*TIRAP*
IGHG3	*TNFAIP1*
IGHG4	*TNFAIP2*
IKBKB	*TNIP1*
IKBKE	*TNP2*
ITCH	*TRAF1*
MYB	*TRAF3*
NOD2	*TRAF6*
NR4A2	*TWIST1*
NSD1	*TWIST2*
PRMT1	

Unstimulated IgM memory B cells

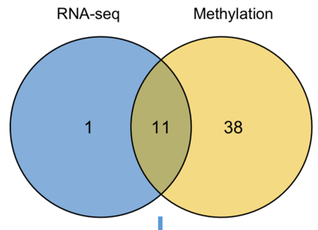

n=1
NFKBID

n=11
BCL3
CD83
CDKN1A
FOS
FOSB
IRF1
JUND
NFKBIA
NFKBIE
NR4A2
XBP1

n=38	
ADAM19	*PRMT1*
ATM	*RAG1*
BAX	*RELA*
BCL2	*RELB*
BCL2L1	*RIPK2*
BIRC2	*SERPINE2*
CYLD	*SETD6*
IGHE	*SOCS1*
IGHG1	*TAX1BP1*
IGHG4	*TIRAP*
IKBKB	*TNFAIP1*
IKBKE	*TNFAIP2*
IRF2	*TNFAIP3*
ITCH	*TP53BP2*
JUNB	*TRAF1*
MYB	*TRAF3*
NFKB1	*TRAF6*
NFKBIZ	*TWIST1*
NSD1	*TWIST2*

Unstimulated Switched memory B cells

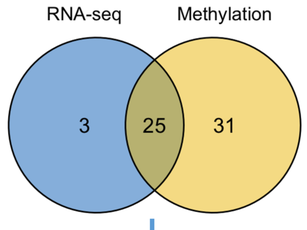

n=3
BTK
CD80
NFKBID

n=25	
BCL3	*NFKBIE*
CD83	*NFKBIZ*
CDKN1A	*NR4A2*
CYLD	*REL*
FOS	*RELB*
FOSB	*RIPK2*
IRF1	*TAX1BP1*
IRF2	*TNFAIP2*
JUNB	*TNFAIP3*
JUND	*TP53BP2*
LYN	*TRAF6*
NFKB1	*XBP1*
NFKBIA	

n=31	
ADAM19	*RELA*
ATM	*SERPINE2*
ATP1A2	*SETD6*
BAX	*SOCS1*
BCL2	*SPI1*
BCL2L1	*STAT5A*
BIRC2	*TIRAP*
IGHG1	*TNFAIP1*
IGHG4	*TNIP1*
IKBKB	*TNP2*
IKBKE	*TRAF1*
ITCH	*TRAF2*
MYB	*TRAF3*
NSD1	*TWIST1*
PRMT1	*TWIST2*
RAG1	

Unstimulated CD21-low B cells

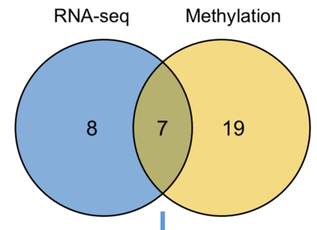

n=8
IGHV3-33
IGKV1-12
IGKV3-15
IGKV3-20
IGLC2
IGLC3
IGLV2-11
KDM5D

n=7
CITED4
DTX3
DTX3L
METTL23
PRDM11
SUMO2
TAF1A

n=19
IKBKE
REL
NFKBIZ
NFKB1
CD83
TAP1
NFKBIE
TNFAIP3
IKBKB
MYC
PLAU
RELA
NFKBIA
IGHG4
STAT5A
BCL2
BCL3
RELB
BAX